The host response of maize towards *Exserohilum turcicum* and its toxin, monocerin

by

Richard Gavin Kotze

Submitted in fulfilment of the requirements for the degree

Philosophiae Doctor: Plant Science

In the Faculty of Natural and Agricultural Sciences

Department of Plant and Soil Sciences

University of Pretoria

Pretoria

SUPERVISOR: DR. Q. KRITZINGER

CO-SUPERVISOR: DR. B.G. CRAMPTON

February 2020

Declaration

I, Richard Gavin Kotze declare that the thesis, which I hereby submit for the degree Philosophiae Doctor: Plant Science at the University of Pretoria, is my own work and has not previously been submitted by me for a degree at this or any other tertiary institution.

…….

Richard Gavin Kotze

11th February 2020

The host response of maize towards *Exserohilum turcicum* and its toxin, monocerin

by

Richard Gavin Kotze

Supervisor: **Dr. Q. Kritzinger**

Co-supervisor: **Dr. B.G. Crampton**

Department: **Plant Science and Soil Sciences**

Degree: **PhD Plant Science**

Summary

Northern leaf blight (NLB) is a devastating foliar disease of maize (*Zea mays* L.) throughout the maize growing regions of the world. The causal agent of NLB is the hemibiotrophic fungal pathogen, *Exserohilum turcicum*. *Exserohilum turcicum* produces a secondary metabolite, monocerin, which is phytotoxic and could aid the fungus in causing NLB in maize. This study was conceptualised to assess the infection strategy of *E. turcicum* in maize, as well as the host response of maize towards *E. turcicum* and its toxin monocerin.

The infection strategy of *E. turcicum* was evaluated through the use of high resolution light (LM), scanning (SEM) and transmission electron microscopy (TEM) to obtain a better understanding of the hemibiotrophic lifestyle of the fungus. During the biotrophic phase of fungal infection, the disease was characterised by chlorotic spots whereas cigar shaped lesions formed during the necrotrophic phase. Infection structures as well as conidiophores were observed for the first time through SEM. At 9 days post inoculation (9 dpi) the fungus was observed in the epidermal cells, visible in the xylem at 11 dpi, at 14 dpi the xylem was almost completely blocked, and at 18 dpi conidiophores formed through the stomata, and the fungus completed its life cycle. The results of this study provide updated insight into the infection strategy of the fungus in maize as well as supporting previous findings that *E. turcicum* is a hemibiotrophic pathogen.

Pathogenesis-related (PR) proteins are one of the many defence mechanisms plants use to protect themselves against fungal infection. Reverse transcription-quantitative PCR was applied to evaluate whether PR protein genes were upregulated in maize in response to *E. turcicum* infection and the presence of the *E. turcicum* toxin, monocerin. Expression of selected PR protein genes (*PR-1, PR-2, PR-3, PR10*) associated with fungal infection was induced in response to the fungus but only during the necrotrophic phase of the fungal growth. Monocerin did induce the gene expression of PR proteins but at a low level when compared to the fungus. *PR-10* (ribonuclease-like) was the only PR protein gene which was induced at a higher level by monocerin as compared to the fungus.

The phytotoxic effects of monocerin on the maize leaf cell ultrastructure were studied using LM and TEM. The cytoplasm as well as the vacuole and chloroplast were most affected by the phytotoxic nature of monocerin. The chloroplast was the most sensitive to the toxin due to disruption of the double-membrane, stroma and thylakoid membranes. As monocerin treatment caused an over accumulation of starch granules in the chloroplast, the gene expression of enzymes (*gwd, pwd, amy3*) involved in degradation of starch granules in the chloroplast was assessed following fungal infection and monocerin treatment. Expression of the all the starch degradation enzymes genes was inhibited during fungal infection but only *amy3* was inhibited by monocerin treatment.

Response of the maize host to *E. turcicum* infection and monocerin infiltration provided new understanding in the host-pathogen interaction which could be exploited in developing new control strategies against NLB in maize.

Acknowledgements

Dr Quenton Kritzinger, for his guidance, motivation, encouragement and input throughout this study. Thank you for all the support during this study especially during the challenging times.

Dr Bridget Crampton for your insight and guidance with the molecular work and always being there for me. Thank you for giving me the opportunity to work on maize, a crop that is close to my heart.

Without the funding of The Maize Trust and University of Pretoria this project would not have been possible. I gratefully acknowledge their contributions for this project.

Prof Dave Berger for always asking challenging questions as well as your wealth of knowledge.

Chris van der Merwe for your time and expertise on plant anatomy and microscopy and always willing to help out even in your retirement; without you I would not have finished this PhD.

Carel Oosthuizen for helping me with the statistics, editing of the thesis and friendship. Nicky Olivier for the technical support and numerous sport conversations. Brigette Langenhoven, for the numerous phone calls explaining and helping me with the gene expression studies. Eudri Venter for all your support as well as the preparations of numerous microscopy samples. Velushka Swart and Miekie Human for their overall support during this study. Renate Zipfel from the DNA Sequencing Facility, for walking the extra mile in helping me sequencing the genes. Molly Malefo and Tsholofelo Rampa for your continued support.

The personal of the Laboratory of Microscopy and Microanalysis, University of Pretoria for the assistance with the microscopy studies. Special thanks to Alan Hall, Erna van Wilpe and Chantelle Venter.

The lab members of the Cereal Foliar Pathogen Research (CFPR) and Molecular Plant-Pathogen Research (MPPI) groups for the invaluable advice they gave me and their support.

The staff of the H.G.W.J Schweickerdt Herbarium and Manie van der Schijff Botanical Garden for their continual kind, friendly and enthusiastic assistance, especially that of Jason Sampson, Magda Nel and Arnold Frisby who I share my love of plants with.

To my colleagues at Syngenta, Jack, Adri, Petrus and Buyani, you have helped me out immensely especially during the writing of this thesis with work related activities.

My family and friends for their support, encouragement and valuable advice during this study

My Sister, Vanessa Kotze and brother Jonathan Kotze for always being there for me.

My parents Ina and Gavin Kotze for always believing in me and encouraging me, in good and in difficult times of my study.

God for the guidance and support as well as always showing the path for me even when I did not know where to go.

Table of contents

List of tables

List of figures

List of abbreviations

°C	degree Celsius
µl	microlitre
µm	micrometre
µM	micromolar
ANOVA	analysis of variance
avr	avirulence
BLAST	Basic Local Alignment Search Tool
bp	base pair
cDNA	complementary DNA
cm	centimetre
CWDE	cell wall-degrading enzymes
DNA	deoxyribonucleic acid
DNase	deoxyribonuclease
DON	deoxynivalenol
dpi	days post-inoculation
ecp	extracellular proteins
FAOSTAT	Food and Agriculture Organization Corporate Statistical Database
FB_1	fumonisin B_1
gDNA	genomic DNA
GLS	grey leaf spot
h	hour
HMDS	hexamethyldisilazane
hpi	hours post infiltration
HST	host-selective toxin

JA	jasmonic acid
kDa	kilodalton
kV	kilovolt
LM	light microscopy
LR	London Resin
mM	millimolar
M	molar
mg	milligram
ml	millilitre
mm	millimetre
NCLS	Northern corn leaf spot
NE	necrotrophic effector
ng	nanogram
NHST	non-host selective toxin
NLB	Northern leaf blight
nm	nanometre
NMR	nuclear magnetic resonance
NRPS	non-ribosomal peptide
PCR	polymerase chain reaction
PR	pathogenesis-related
RH	relative humidity
RNA	ribonucleic acid
rRNA	ribosomal RNA
RT-qPCR	reverse transcription quantitative PCR
SA	salicylic acid
SAR	systemic acquired response

SC	solvent control
SCLB	Southern corn leaf blight
Sec	second
SEM	scanning electron microscope
SNP	single nucleotide polymorphisms
TEM	transmission electron microscope
T_m	melting temperature
V8	vegetable 8
WC	wounded control
YLS	yellow leaf spot

Chapter 1: General introduction

1.1. Background and motivation for this study

Maize (*Zea mays* L.) or corn as it is commonly known in the Americas, together with wheat (*Triticum aestivum* L.) and rice (*Oryza sativa* L.) are the most widely cultivated cereal crops worldwide (FAOSTAT, 2018). Maize is the biggest producer of the three, with recent annual production rates of above 1 billion tonnes throughout the world (FAOSTAT, 2018). In the developed world, maize is used as a source of food for human consumption, fodder for animals, as raw material for extractive/fermenting industries and as corn fructose sweetener (Gibson & Benson, 2002; Du Plessis, 2003). In developing countries, maize is mainly consumed directly and serves as an important staple diet for over 200 million people (Du Plessis, 2003; Koohafkan & Stewart, 2008; FAOSTAT, 2018).

Numerous pests and diseases affect the worldwide cultivation of maize for both subsistence and commercial farmers. These include bacterial, fungal and viral diseases, as well as insect and weed pests. Major fungal diseases that affect maize include *Fusarium* ear rot (Munkvold & Desjardins, 1997), grey leaf spot (GLS) (Latterell & Rossi, 1983) and northern leaf blight (NLB) (Leonard & Suggs, 1974). Northern leaf blight is a lethal foliar disease of maize caused by the hemibiotrophic fungal pathogen *Exserohilum turcicum* and is a serious threat to maize production worldwide (Leonard & Suggs, 1974; Klopper & Tweer, 2009). In addition to maize, sorghum (*Sorghum bicolor* (L.) Moench) and Johnson grass (*Sorghum halepense* (L.) Pers) also plays host to *E. turcicum* (Smith *et al.*, 2004; Agrios, 2005). Northern leaf blight is currently one of the most widespread maize diseases in South Africa especially in eastern parts of the country such as Mpumalanga and KwaZulu-Natal (Klopper & Tweer, 2009). Yield losses range from 15–30% but yield losses of up to 75% have been reported (Klopper & Tweer, 2009). The highest yield losses occur when NLB establishes before silking and spreads to the upper leaves during grain filling (Perkins & Pedersen, 1987; Klopper & Tweer, 2009). Yield losses can be attributed to the loss of photosynthetic leaf area due to the lesions that form on the leaves (Klopper & Tweer, 2009; Wise, 2011).

Optimal environmental conditions for *E. turcicum* establishment include heavy dew, frequent rain, high humidity (>90%), moderate temperatures (20–25°C) and prolonged leaf wetness (Leach *et al.*, 1977; Levy & Cohen, 1983). In the early stages of NLB, the disease can be characterised by small water-soaked spots, which appear on the lower leaves (Klopper & Tweer, 2009). The lesions (spots) then elongate becoming elliptical or cigar shaped and are tan

to grey-green in colour (Smith & Kinsey, 1980; Klopper & Tweer, 2009; Wise, 2011). As NLB progresses the lesions start to mature and become tan with distinct dark zones of sporulation (Klopper & Tweer, 2009; Wise, 2011). Multiple lesions can coalesce to form large irregular areas of dead tissue (Wise, 2011). Successful management of NLB can be achieved by implementing crop rotation, the use of resistant and tolerant cultivars, the management of crop residue and the effective use of fungicides (Klopper & Tweer, 2009; Wise, 2011).

The death of the cells that lead to the formation of the enlarged necrotic lesions could be due to toxic compounds produced by *E. turcicum* such as monocerin (Cuq *et al.*, 1993). Monocerin was first isolated from *Helminthosporium monoceras* (Aldridge & Turner, 1970) but has since also been isolated from *Curvularia ravenelii* (Scott *et al.*, 1984), *E. turcicum* (Robeson & Strobel, 1982), *Fusarium larvarum* (Grove & Pople, 1979) and *Microdochium bolleyi* (Sappapan *et al.*, 2008). Monocerin is a polyketide metabolite that exhibits antifungal, insecticidal and phytotoxic effects (Scott *et al.*, 1984; Cuq *et al.*, 1995; Axford *et al.*, 2004). It is a non-specific phytotoxin targeting species such as maize, Johnson grass, radish (*Raphanus sativus* L.), cucumber (*Cucumis sativus* L.) and tomato (*Solanum lycopersicum* L.) (Robeson & Strobel, 1982; Cuq *et al.*, 1993). Cuq *et al.* (1993) reported that necrotic lesions formed when a leaf puncture assay was done with monocerin on maize leaves.. Monocerin inhibited both the root and shoot elongation of Johnson grass and to a lesser extent cucumber (Robeson & Strobel, 1982).

The infection strategy of *E. turcicum* has previously been described but only light microscopy was used which, due to the poor reproductive quality of micrographs, makes interpretation of the findings difficult to interpret (Jennings & Ullstrup, 1957; Hilu & Hooker, 1964; Knox-Davies, 1974). Investigating the infection strategy of *E. turcicum* with electron microscopy will provide a better understanding of the infection process as well as the hemibiotrophic lifestyle of the fungus. Yield losses due to NLB can be reduced and prevented by a better understanding of the biology of the fungus as well as the host response against the fungus and toxin. As mentioned previously, it has been reported that monocerin does exhibit phytotoxic effects towards plants, but its possible involvement in the pathogenicity of *E. turcicum* infection in maize is not fully understood. Evaluating the phytotoxic effects of monocerin on maize will also provide a better understanding of the role that monocerin plays in NLB development.

Plants have numerous defence mechanisms that they utilise against abiotic and biotic stresses such as wounding, drought, and infection by viral, bacterial and fungal pathogens (Agrios, 2005). The production of pathogenesis-related (PR) proteins is one of these mechanisms that is induced in a response to fungal infections in plants (van Loon *et al.*, 2006). To date, 17 families of PR proteins have been characterised but not all of them are induced by fungal infections in plants (van Loon *et al.*, 2006). These proteins have various functions including being antifungal in nature, protease inhibitors, hydrolases and ribonuclease-like (Scherer *et al.*, 2005; van Loon *et al.*, 2006). Due to the increased resistance that fungal pathogens acquire against resistant maize lines as well as fungicides, alternative control methods need to be pursued. The induced expression of PR proteins could be a potential mechanism in controlling *E. turcicum* infection in maize.

1.2. Hypotheses, aim, objectives

1.2.1. Hypotheses

1. *Exserohilum turcicum* is a hemibiotrophic fungus that switches from a biotrophic to a necrotic lifestyle that leads to cell death.
2. Monocerin is a phytotoxic effector produced by *E. turcicum* and contributes to development of NLB disease
3. Pathogenesis-related protein gene expression is induced by *E. turcicum* infection and monocerin infiltration.
4. The expression of genes involved in starch degradation in the chloroplast is inhibited by *E. turcicum* infection and monocerin infiltration.

1.2.2. Aim

The primary aim of this study was to understand the role of *E. turcicum* infection and monocerin in the development of northern leaf blight in maize.

1.2.3. Objectives

The specific objectives of the study were to:

1. Determine the infection strategy of *E. turcicum* by using light microscopy (LM), transmission electron microscopy (TEM) and scanning electron microscopy (SEM).
2. Determine if pathogenesis-related (PR) protein genes are induced when monocerin and *E. turcicum* are applied to maize plants.
3. Determine the phototoxic effect of pure monocerin on the ultrastructure of maize leaf cells.
4. Determine whether starch gene expression in the chloroplast is inhibited by monocerin infiltration and *E. turcicum* infection.

1.3. Structure of thesis

This thesis is divided into six chapters as presented below.

Chapter 1: This chapter provides a brief background to and justification for the study, and states the aim, objectives and hypotheses.

Chapter 2: This chapter provides a concise review on foliar fungal pathogens and their phytotoxins of maize with an emphasis on northern leaf blight, the causal agent *E. turcicum* and the toxin it produces, monocerin.

Chapter 3: In this chapter the infection process of *E. turcicum* in maize leaves is characterised using light microscopy, scanning and transmission electron microscopy to provide an updated and detailed assessment on the infection strategy of the fungus in maize. In addition, this information is used to confirm whether the fungus follows a hemibiotrophic lifestyle.

Published as Kotze RG, van der Merwe CF, Crampton BG, Kritzinger Q, 2019. A histological assessment of the infection strategy of *Exserohilum turcicum* in maize. Plant Pathology **68**, 504-12 (DOI: 10.1111/ppa.12961).

Chapter 4: This chapter examines whether *E. turcicum* infection and pure monocerin infiltration induces a host response in maize leaves by inducing the expression of pathogenesis related (*PR*) protein genes.

Chapter 5: The phytotoxic effects of pure monocerin on the ultrastructure of maize leaf cells are investigated in this chapter. In addition, the effect of the toxin as well

as the fungus itself are examined to see whether the expression of genes coding for enzymes involved in degradation of starch granules in the chloroplast is inhibited.

Chapter 6: This chapter includes a general discussion, interpretation of the experimental results achieved, shortcomings of the study and suggestions for future research.

1.4. Conference contributions

Parts of this study were presented at the following conferences/symposia:

55th Annual Congress of the Microscopy Society of Southern Africa (MSSA), Sefako Makgatho Health Sciences University, 4–7 December 2017, Forever Resorts Warmbaths, Bela-Bela. The infection Strategy of *Exserohilum turcicum* in *Zea mays*. Kotze, R.G., Crampton, B.G., Kritzinger, Q. (Oral presentation).*

**Won the Wirsam Olympus Light Microscopy Prize for the best light microscopy oral presentation*

11th International Congress of Plant Pathology (ICPP), International Society for Plant Pathologist (ISPP) and The American Phytopathological Society (APS), 29 July – 3 August 2018, Boston, USA. The infection process of *Exserohilum turcicum*: A microscopy investigation. Kotze, R.G., Crampton, B.G., Kritzinger, Q. (Poster presentation).

51st Bi-annual Congress of South African Society for Plant Pathology (SASPP), University of Stellenbosch, 20–24 January 2019, Club Mykonos, Langebaan. Host response of maize against the foliar pathogen *Exserohilum turcicum*. Kotze, R.G., Kritzinger, Q., Crampton, B.G. (Oral presentation).

1.5. References

Agrios GN, 2005. *Plant Pathology*. San Diego, CA, USA: Elsevier Academic Press.

Aldridge DC, Turner WB, 1970. Metabolites of *Helminthosporium monoceras:* Structures of monocerin and related benzopyrans. *Journal of the Chemical Society C: Organic* **18**, 2598-600.

Axford LC, Simpson TJ, Willis CL, 2004. Synthesis and incorporation of the first polyketide synthase free intermediate in monocerin biosynthesis. *Angewandte Chemie International Edition* **43**, 727-30.

Cuq F, Brown SC, Petitprez M, Alibert G, 1995. Effects of monocerin on cell-cycle progression in maize root-meristems synchronized with aphidicolin. *Plant Cell Reports* **15**, 138-42.

Cuq F, Petitprez M, Herrmann-Gorline S, Klaebe A, Rossignol M, 1993. Monocerin in *Exserohilum turcicum* isolates from maize and a study of its phytotoxicity. *Phytochemistry* **34**, 1265-70.

Du Plessis J, 2003. *Maize production*. Pretoria, South Africa: Department of Agriculture.

FAOSTAT, 2018. FAO statistical database. In. Rome, Italy: Food and Agricultural Organization of the United Nations.

Gibson L, Benson G, 2002. Origin, history, and uses of corn (*Zea mays*). [http://agron-www.agron.iastate.edu/Courses/agron212/readings/corn_history.htm]. Accessed 31 May 2016.

Grove JF, Pople M, 1979. Metabolic products of *Fusarium larvarum* fuckel. The fusarentins and the absolute configuration of monocerin. *Journal of the Chemical Society, Perkin Transactions 1*, 2048-51.

Hilu HM, Hooker AL, 1964. Host-pathogen relationship of *Helminthosporium turcicum* in resistant and susceptible corn seedlings. *Phytopathology* **54**, 570-5.

Jennings P, Ullstrup A, 1957. A histological study of 3 *Helminthosporium* leaf blights of corn. *Phytopathology* **47**, 707-14.

Klopper R, Tweer S, 2009. Northern corn leaf blight fact sheet. [http://www.pannar.com/assets/disease_fact_sheets/Northern_Corn_Leaf_Blight.pdf]. Accessed 11 November 2019.

Knox-Davies P, 1974. Penetration of maize leaves by *Helminthosporium turcicum*. *Phytopathology* **64**, 1468-70.

Koohafkan P, Stewart BA, 2008. *Water and cereals in drylands*. The Food and Agriculture Organization of the United Nations and Earthscan.

Latterell FM, Rossi AE, 1983. Gray leaf spot of corn: a disease on the move. *Plant Disease* **67**, 842-7.

Leach CM, Fullerton RA, Young K, 1977. Northern leaf blight of maize in New Zealand: relationship of *Drechslera turcia* airspora to factors onfluencing sporulation, conidium development, and chlamydospore formation. *Phytopathology* **77**, 629.

Leonard K, Suggs EG, 1974. Setosphaeria prolata, the ascigerous state of Exserohilum prolatum. *Mycologia*, 281-97.

Levy Y, Cohen Y, 1983. Biotic and environmental factors affecting infection of sweet corn with *Exserohilum turcicum*. *Phytopathology* **73**, 722-5.

Munkvold GP, Desjardins AE, 1997. Fumonisins in maize: Can we reduce their occurrence? *Plant Disease* **81**, 556-65.

Perkins J, Pedersen W, 1987. Disease development and yield losses associated with Northern leaf blight on corn. *Plant Disease* **71**, 940-3.

Robeson DJ, Strobel GA, 1982. Monocerin, a phytotoxin from *Exserohilum turcicum* (= *Drechslera turcica*). *Agricultural and Biological Chemistry* **46**, 2681-3.

Sappapan R, Sommit D, Ngamrojanavanich N, *et al.*, 2008. 11-Hydroxymonocerin from the plant endophytic fungus *Exserohilum rostratum*. *Journal of natural products* **71**, 1657-9.

Scherer NM, Thompson CE, Freitas LB, Bonatto SL, Salzano FM, 2005. Patterns of molecular evolution in pathogenesis-related proteins. *Genetics and Molecular Biology* **28**, 645-53.

Scott FE, Simpson TJ, Trimble LA, Vederas JC, 1984. Biosynthesis of monocerin. Incorporation of 2H-, 13C-, and 18O-labelled acetates by *Drechslera ravenelii*. *Journal of the Chemical Society, Chemical Communications*, 756.

Smith CW, Betrán J, Runge ECA, 2004. *Corn : Origin, history, technology, and production*. Hoboken, N.J. :: John Wiley.

Smith D, Kinsey J, 1980. Further physiologic specialization in *Helminthosporium turcicum*. *Plant Disease* **64**, 779-81.

van Loon LC, Rep M, Pieterse CM, 2006. Significance of inducible defense-related proteins in infected plants. *Annual Review of Phytopathology* **44**, 135-62.

Wise K, 2011. *Diseases of Corn: Northern Corn Leaf Blight*. [https://www.extension.purdue.edu/extmedia/BP/BP-84-W.pdf]. 14 November 2019.

Chapter 2: Literature review – Foliar fungal pathogens of maize and their phytotoxins with emphasis on *Exserohilum turcicum* and monocerin

2.1. Introduction

Maize (*Zea mays* L.) or corn is an edible annual grain belonging to the grass family, Poaceae. This crop, together with wheat (*Triticum aestivum* L.) and rice (*Oryza sativa* L.) constitute the three most-produced cereal crops throughout the world (FAOSTAT, 2018). Since 2013, annual production levels have been in excess of one billion tonnes worldwide for maize (FAOSTAT, 2018). The world's three leading producers of maize are the United States of America (USA), China and Brazil with the Republic of South Africa (RSA) placed at 12th position (Table 2.1). For the last ten years, South Africa has produced annually on average 12.5 million tonnes of maize on 2.5 million ha land (Grain_SA, 2018). During the 2016/2017 season, South Africa had a record maize harvest with 16.74 million tonnes maize produced from 2.6 million ha land, which resulted in a yield of 6.02 t/ha (Grain_SA, 2018). The Free State, Mpumalanga and North West provinces are South Africa's main maize production centres, which in combination produce 81.5% of the total maize in South Africa (Grain_SA, 2018).

Maize is a primary staple food in Africa and Latin America with sub-Saharan Africa consuming more than 90% of the maize produced on the continent (Du Plessis, 2003; Awika, 2011). In developed countries such as the United States, maize is mainly used as fodder for animals, as fuel for ethanol production, as a high fructose corn sweetener and for second-cycle produce which includes meat, eggs and dairy products (Du Plessis, 2003; Koohafkan & Stewart, 2008; Awika, 2011). In developing countries, it is a significant source of food for humans as well as fodder for animals (Du Plessis, 2003; Koohafkan & Stewart, 2008).

Table 2.1. The top maize producing countries in the world between 2012 and 2016 (FAOSTAT, 2018). South Africa is 12th on the list of top producers.

#	Country	Tonnes
1	USA	343 163 928
2	China	219 357 219
3	Brazil	76 131 133
4	Argentina	32 002 722
5	Ukraine	26 361 968
6	Mexico	24 190 259
7	India	23 903 902
8	Indonesia	19 377 857
9	France	14 925 068
10	Canada	12 929 840
12	South Africa	11 182 951

The aim of this review is to provide a synopsis of the foliar fungal diseases associated with maize, and the phytotoxins they produce. A detailed description on northern leaf blight (NLB), *Exserohilum turcicum* and monocerin will be given since NLB is consistently one of the most damaging foliar diseases of maize.

2.2. Foliar fungal pathogens and their phytotoxins

The production of maize is severely hampered by a variety of pests and diseases, which are a significant problem for both commercial and subsistence farmers worldwide. These pests and diseases include fungal, bacterial and viral diseases, insect pests, and parasitic plants and weeds, which can affect all parts of the plant. Fungal diseases in maize usually become a major problem when ideal temperature and moisture conditions occur in the field (Munkvold & White, 2016). Commercially important fungal diseases of maize include grey leaf spot (GLS) (Latterell & Rossi, 1983), *Fusarium* ear rot (Munkvold & Desjardins, 1997) and northern leaf blight (NLB) (Leonard & Suggs, 1974).

2.2.1. Phytotoxins

Numerous plant pathogenic fungi have the ability to produce low molecular weight compounds or secondary metabolites which could play a key role in pathogenicity or virulence and the

primary infection process (fungal survival against the plant) (Yoder, 1980; Steyn, 1995; Mobius & Hertweck, 2009; Collemare & Lebrun, 2011). Any secondary metabolites produced by fungi that are toxic towards plants are known as phytotoxins (Bennett & Klich, 2003). Many of these phytotoxins play a role in causing or exacerbating plant diseases (Bennett & Klich, 2003). Phytotoxins, in general, can either be classified as a pathogenicity factor (qualitative), which is the ability to cause disease or as a virulence factor (quantitative), which refers to the extent or severity of the disease caused (Yoder, 1980). Phytotoxins which are classified as pathogenicity factor are required by the fungus to cause disease in plants. For example, with *Cercospora kikuchii* produces cercosporin, which is required by the fungus to cause Cercospora leaf blight in soya beans (*Glycine max* (L.) Merr.). Cercosporin deficient mutants of *C. kikuchii* failed to produced disease in soya beans (Upchurch *et al.*, 1991). Phytotoxins which are classified as virulence factors are not needed by the fungus to cause disease in plants, but their production results in an increase in disease severity. In contrast some phytotoxins are not needed for pathogenicity, as for example dothistromin deficient mutants of *Dothistroma septosporum* still have the ability to cause dothistroma needle blight of pines (Kabir *et al.*, 2015).

2.2.2. Host-selective and non-host selective phytotoxins

The phytotoxins that fungi produce can be classified as host-selective (HST) or non-host selective (NHST) depending on the number of species they affect. Host-selective phytotoxins are only biologically active towards the host plant species and sparingly or non-toxic towards non-host plant species (Scheffer & Livingston, 1984; Tsuge *et al.*, 2013). Host-selective toxins include: victorin (released by *Bipolaris victoriae,* Victoria blight of oats (*Avena sativa* L.)) (Scheffer & Livingston, 1984; Stergiopoulos *et al.*, 2013); HS-toxin (released by *Bipolaris sacchari*, eyespot disease of sugarcane (*Saccharum* spp.)) (Larkin & Scowcroft, 1981); and, PtrToxA and PtrToxB (*Pyrenophora tritici-repentis*, tan spot of wheat) (Ciuffetti *et al.*, 2010). Many of the necrotrophic fungal plant pathogens producing HST's have been grouped together in the order Pleosporales within the class Dothideomycetes (Friesen *et al.*, 2008). The same pair of alleles that controls resistance and susceptibility to fungi in plants also controls tolerance and sensitivity to their toxins, respectively (Scheffer & Livingston, 1984). In contrast to HST's, NHST's are produced by multiple species and biologically active towards numerous plant species regardless of whether or not they play host to the fungal pathogen (Scheffer & Livingston, 1984). Examples of NHST's include fumonisins (*Fusarium verticillioides,*

Fusarium proliferatum, *Alternaria alternata*) , AAL-toxins (*A. alternata*), dothistromin (*D. septosporum*, *Dothistroma pini*) and elsinochrome (*Elsinoë* spp.) (Stoessl *et al.*, 1990; Abbas & Boyette, 1992; Abbas *et al.*, 1995; Collemare & Lebrun, 2011; Stergiopoulos *et al.*, 2013).

2.2.3. Plant host target sites/ mode of action

Phytotoxins interact with a range of cellular targets of the plant cell, which include the chloroplast, mitochondrion, plasma membrane, nucleus, cellular and organelle membranes (Figure 2.1) (Scheffer & Livingston, 1984; Mobius & Hertweck, 2009; Collemare & Lebrun, 2011). Physiological effects of phytotoxins on plants include changes in respiration, cell permeability, protein synthesis, gene expression, carbon fixation, nutrient leakage and disruption of membrane integrity (Scheffer & Livingston, 1984; Mobius & Hertweck, 2009). Fumonisins and AAL-toxins are sphingosine analogue mycotoxins that target ceramide synthase and sphinganine–N-acetyltransferase which hamper lipid biosynthesis and increases membrane permeability (Figure 2.1) (Williams *et al.*, 2007). Tentotoxin is produced by several *Alternaria* species and targets ATP hydrolysis in the chloroplast which results in complete energy breakdown in the plant cell (Figure 2.1) (Mobius & Hertweck, 2009). Victorin produced by *B. victoriae* and trichothecenes such as deoxynivalenol (DON) produced by *Fusarium graminearum* are known inducers of apoptosis which is a major strategy of phytopathogenic fungi to obtain nutrients from plants (Mobius & Hertweck, 2009). The cytochalasan's family of phytotoxins, produced by a number of fungal species such as *Boeremia exigua* and *Penicillium expansum*, bind to actin filaments resulting in blocked cytokinesis as well as changing cellular morphology (Figure 2.1) (Berestetskiy *et al.*, 2008; Mobius & Hertweck, 2009). Iron is an essential nutrient required by fungal pathogens for their survival and is acquired from the plants through siderophore (iron chelators) such as ferricrocin (*Alternaria brassicicola*) (Mobius & Hertweck, 2009).

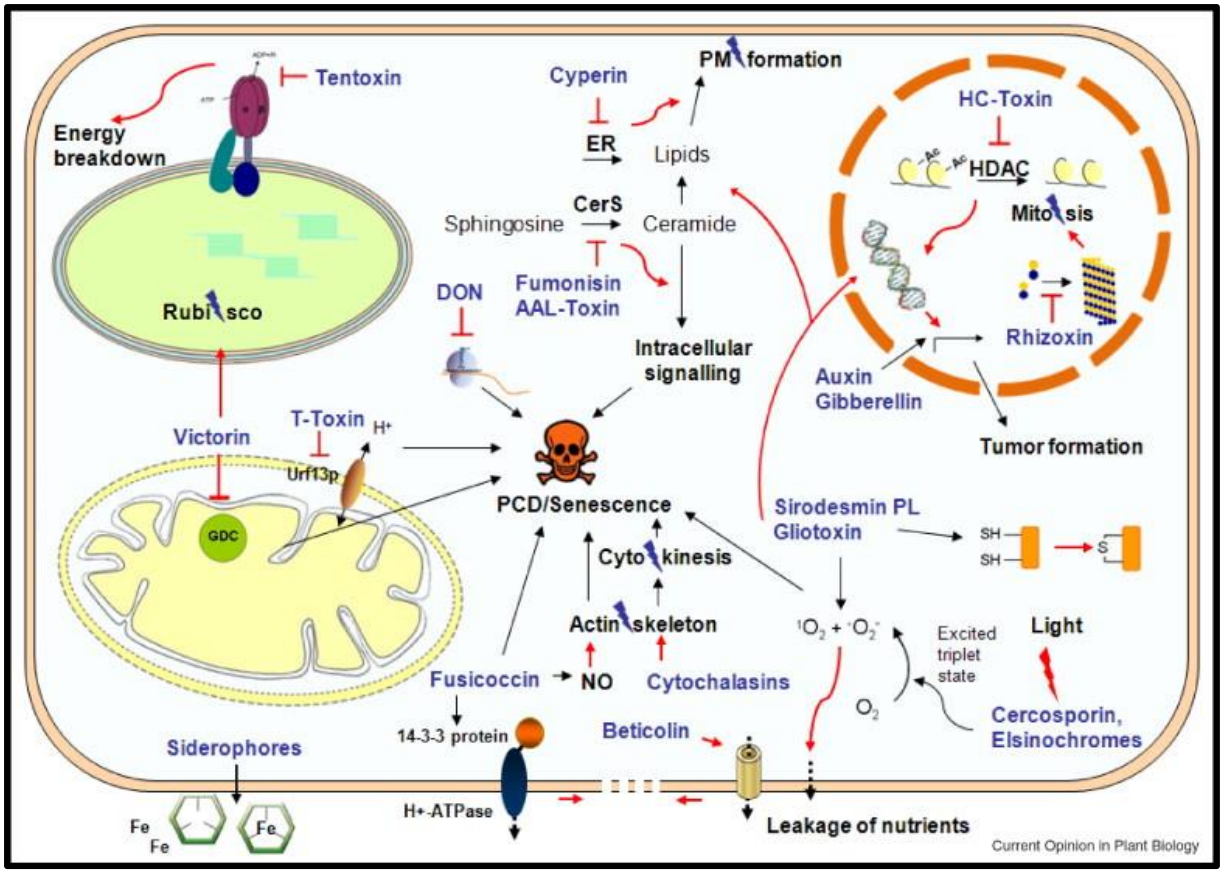

Figure 2.1. Graphic overview of the cellular targets and modes of action of fungal phytotoxins (Mobius & Hertweck, 2009).

2.2.4. Different maize foliar diseases and phytotoxins

Maize is susceptible to numerous foliar fungal pathogens that can cause diseases in the leaves, which ultimately lead to reduced yield or even death of the plants. Many of the pathogens follow a necrotrophic or hemibiotrophic lifestyle with some of these fungi often producing phytotoxins, which aid them in causing disease and completing their lifecycle (Table 2.2). The fungi listed in Table 2.2 and the diseases they cause have resulted in devastating epidemics and significant annual yield losses in maize in the past.

Table 2.2. Foliar fungal pathogens of maize and their respective phytotoxins they produce.

Pathogen	Other names	Disease	Phytotoxins	Cellular target	Chemical class	Host selectivity	References
Bipolaris maydis	*Cochliobolus heterostrophus, Helminthosporium maydis*	Southern corn leaf blight	T-toxin	T-urf13 protein	Polyketide	HST	(Scheffer & Livingston, 1984; Markham & Hille, 2001; Wolpert *et al.*, 2002)
			ophiobolin I		Sesterpenoid	Non-HST	(Sugawara *et al.*, 1987; Strobel *et al.*, 1988; Kim *et al.*, 1999; Au *et al.*, 2000)
			*Ch*ToxA		Protein	HST	(Lu *et al.*, 2015)
Bipolaris zeicola	*Cochliobolus carbonum, Helminthosporium zeicola*	Northern corn leaf spot	HC-toxin	Histone deacetyl-lyses (HDACs)	Cyclic tetrapeptide	HST	(Scheffer & Livingston, 1984; Brosch *et al.*, 1995; Ransom & Walton, 1997; Wolpert *et al.*, 2002; Walton, 2006; Munkvold & White, 2016)
Cercospora zeae-maydis, Cercospora zeina		Grey leaf spot	Cercosporin	Reactive oxygen species/ cell membrane	Polyketide	Non-HST	(Dunkle & Levy, 2000; Crous *et al.*, 2006; Meisel *et al.*, 2009)
Didymella maydis	*Phyllosticta maydis*	Yellow leaf blight	PM-toxin	T-urf13 protein	Polyketide	HST	(Comstock *et al.*, 1973; Yoder, 1980; Wolpert *et al.*, 2002)
Exserohilum turcicum	*Setosphaeria turcica, Helminthosporium turcicum*	Northern leaf blight	Monocerin		Polyketide	Non-HST	(Robeson & Strobel, 1982; Cuq *et al.*, 1993)
			E.t-toxin		Peptide		(Bashan & Levy, 1992; Bashan *et al.*, 1995)

2.2.4.1. Southern corn leaf blight

Southern corn leaf blight (SCLB) is caused by the necrotrophic fungus *Bipolaris maydis* (syn. *Cochliobolus heterostrophus*, *Helminthosporium maydis*) grouped in the order Pleosporales within the class Dothideomycetes (Table 2.2) (Manamgoda *et al.*, 2011; Condon *et al.*, 2013; Munkvold & White, 2016). The disease is found worldwide and is most severe in warm temperate and tropical areas (Munkvold & White, 2016). Southern corn leaf blight is characterised by lesions which are tan in colour, rectangular to oblong in shape and usually occur on the leaves (Figure 2.2) (Munkvold & White, 2016). The disease was responsible for a severe crop epidemic in the USA during the 1970 growth season (Ullstrup, 1972). Three races of *B. maydis* have been reported: race O, the most common race of the three; race T, which is virulent to maize plants with the Texas male-sterile cytoplasm (T-cms); and race C which is selectively virulent to maize plants with cytoplasm male-sterile C (C-cms) and has thus far been found only in China (Munkvold & White, 2016). Race T produces the phytotoxin T-toxin (Table 2.2), a linear polyketide metabolite HST, which is extremely toxic to the susceptible T-cms maize (Wolpert *et al.*, 2002; Munkvold & White, 2016). It was race T and the phytotoxin T-toxin, which was responsible for the maize epidemic of 1970 in the USA (Munkvold & White, 2016). This was due to race T becoming more prevalent as well as being virulent on maize lines with Texas male-sterile cytoplasm (T-cms). At the time of the epidemic, more than 80% of maize cultivars contained T-cms during the 1970's (Munkvold & White, 2016). The mode of action of T-toxin is that it targets the T-urf13 protein in the mitochondria of susceptible maize and results in conformational changes and pore formation of the mitochondrial membrane followed by mitochondrial swelling, ultimately leading to death of the cell (Figure 2.1) (Wolpert *et al.*, 2002; Mobius & Hertweck, 2009; Stergiopoulos *et al.*, 2013). In addition to the T-toxin, Lu *et al.* (2015) were the first to report that *B. maydis* produces a proteinaceous HST, *Ch*ToxA. *Ch*ToxA is a light-dependent HST that possesses necrosis inducing activity against maize (Lu *et al.*, 2015).

Figure 2.2. Typical lesions of Southern corn leaf blight (https://www.pioneer.com).

2.2.4.2. Northern corn leaf spot

Northern corn leaf spot (NCLS) is caused by the fungus *Bipolaris zeicola* (syn. *Cochliobolus carbonum*, *Helminthosporium carbonum*) (Manamgoda *et al.*, 2011). *Bipolaris zeicola* follows a necrotrophic lifestyle and is grouped within the order Pleosporales (Condon *et al.*, 2013). The disease is more prevalent on inbred lines as opposed to hybrids (Munkvold & White, 2016). The disease occurs wherever maize is grown throughout the world (Munkvold & White, 2016). *Bipolaris zeicola* causes spots on maize leaves which can be tan and oval to circular (race 1), can be oblong, and chocolate coloured (race 2) or can have narrow, long and light tan lesions (race 3) (Figure 2.3) (Manamgoda *et al.*, 2011; Munkvold & White, 2016). Five races of *B. zeicola* have been identified and include race 1, which occurs rarely; race 2, the most common race; race 3, race 4 and race 0, all of which have low pathogenicity (Munkvold & White, 2016). The host-selective toxin HC-toxin is produced by race 1 of *B. zeicola* and is extremely pathogenic to susceptible maize cultivars (Markham & Hille, 2001; Walton, 2006). HC-toxin is a cyclic-tetrapeptide metabolite which has a deleterious effect on susceptible maize lines that are homozygous recessive at the loci *Hm1* and *Hm2* (Walton, 2006). The *Hm* genes encode for HC-toxin reductase, and maize plants containing these genes can detoxify the HC-toxin, (Walton, 2006). Many of the effects of HC-toxin are the opposite of what those of the majority of other HST's since HC-toxin cannot kill the plant cells by itself (Walton, 2006; Petrov *et al.*,

2018). HC-toxin inhibits the enzyme histone deacetylases (HDAC's) (Figure 2.1) which results in hyperacetylation of histones and subsequent repression of gene expression in the plant (Mobius & Hertweck, 2009). The inhibition of HDAC's leads to hyperacetylated forms of nucleosomal histones H3 and H4 (Brosch *et al.*, 1995; Ransom & Walton, 1997). Histones are involved in the control of fundamental cellular processes such as cell cycle progression and gene expression (Brosch *et al.*, 1995). Rasmussen and Scheffer (1988) reported that HC-toxin could also inhibit chlorophyll synthesis.

Figure 2.3. Typical lesions of northern corn leaf spot (www.fieldcrops.cals.cornell.edu).

2.2.4.3. Grey leaf spot

Grey leaf spot (GLS) is a foliar fungal disease caused by either *Cercospora zeae-maydis* or by *Cercospora zeina* with both of these species belonging to the class Dothideomycetes (Crous *et al.*, 2006). *Cercospora zeina* is the causal agent for GLS in South Africa (Meisel *et al.*, 2009). The disease occurs worldwide where maize is grown, especially in the temperate to warm, humid areas of the world (Munkvold & White, 2016). Grey leaf spot is characterised by rectangular lesions on the leaves of susceptible plants, which turn grey as the fungus sporulates (Figure 2.4) (Klopper & Tweer, 2009a; Munkvold & White, 2016). The lesions are limited by

the veins resulting in lesions occurring parallel to the veins (Klopper & Tweer, 2009a). *Cercospora zeae-maydis* produces the non-host selective toxin cercosporin (Figure 2.1) whereas *C. zeina* cannot produce the toxin (Jenns, 1989; Swart *et al.*, 2017). Cercosporin is a photosensitising perylenequinone metabolite which is photoactivated by light (Daub & Ehrenshaft, 2000). Once cercosporin is photoactivated by light (Figure 2.1), it functions by producing reactive oxygen species (ROS) such as superoxide and hydrogen peroxide which induce oxidative lipid damage, thus causing damage to the cell membrane (Figure 2.1) (Daub & Ehrenshaft, 2000). As a result of the damage to the cell membrane, nutrients leak into the intracellular membrane, thus making them available to the fungus (Mobius & Hertweck, 2009).

Figure 2.4. Typical lesions of grey leaf spot (Photo: DK Berger)

2.2.4.4. Yellow leaf blight

Yellow leaf blight (YLB) is of minor importance when compared to the other diseases mentioned in this literature review (Table 2.2) (Munkvold & White, 2016). The causal agent of YLB is the fungal pathogen *Didymella maydis* (Syn. *Phyllosticta maydis*) grouped within the order Pleosporales within the class Dothideomycetes (Aveskamp *et al.*, 2010). The disease has been reported in northern and north-eastern USA, Argentina and Canada with similar

species also having been reported in Europe, Africa and Taiwan (Munkvold & White, 2016). The disease is characterised by necrotic lesions, which are yellow to tan in colour. Yellowing of the surrounding tissue of the leaf blade is also visible (Figure 2.5) (Arny & Nelson, 1971). The fungus produces a phytotoxin, PM-toxin, which is similar in activity and structure to the HST T-toxin produced by *B. maydis* and also promotes virulence in the fungus (Comstock *et al.*, 1973; Yoder, 1980). Maize with the Texas male-sterile cytoplasm (T-cms) is more susceptible to the disease compared to maize lines without (Comstock *et al.*, 1973). Phytotoxic effects induced by PM-toxin include reduced seedling root growth, leaf chlorosis, increased electrolyte leakage as well as irreversible swelling of the mitochondria and uncoupled oxidative phosphorylation (Comstock *et al.*, 1973).

Figure 2.5. Typical yellow leaf blight lesions (Munkvold & White, 2016).

2.3. Northern leaf blight

2.3.1. Importance and incidence of NLB

Northern leaf blight, also called northern corn leaf blight or turcicum blight, is a lethal foliar disease of maize and is a severe threat to maize production worldwide (Adipala *et al.*, 1993;

Dingerdissen *et al.*, 1996; Munkvold & White, 2016). It occurs when the fungal pathogen *Exserohilum turcicum* (Pass.) K.J. Leonard & Suggs (syn. *Setosphaeria turcica*, syn. *Helminthosporium turcicum*) infects maize leaves (Leonard & Suggs, 1974). Other host plant species for this pathogen include sorghum (*Sorghum bicolor* (L.) Moench) and Johnson grass (*Sorghum halepense* (L.) Pers) (Smith *et al.*, 2004; Agrios, 2005; Munkvold & White, 2016). The highest yield losses occur when NLB establishes itself during the reproduvtive stage of the maize growth cycle (Perkins & Pedersen, 1987; Carson, 1995b; Wise *et al.*, 2016). Yield losses normally range from 15–30% but yield losses of up to 75% have been reported (Perkins & Pedersen, 1987; Klopper & Tweer, 2009b). Yield losses can be attributed to the loss of photosynthetic leaf area due to the lesions (blighting) that form on the leaves (Wise, 2011; Munkvold & White, 2016). The disease is more prevalent in moist, warm and humid climates of midlatitude and highland areas of the tropics where maize is grown (Carson, 1995a; Borchardt *et al.*, 1998; Munkvold & White, 2016).

The first incidence of NLB was reported in Parma, Italy, in 1876 (Drechsler, 1923) but it is now found in the majority of maize producing countries. In South Africa, the first report of the disease was in 1956 (Bogyo, 1956). Areas in the world that are most affected include the Corn Belt of the USA, (Midwestern USA), Central and South America, sub-Saharan Africa, Mediterranean and China (Levy & Pataky, 1992; Adipala *et al.*, 1993; Borchardt *et al.*, 1998; Wise, 2011; Munkvold & White, 2016). The disease is more severe in the humid eastern parts of South Africa which include Mpumalanga and KwaZulu-Natal (Klopper & Tweer, 2009b).

2.3.2. NLB symptoms

Northern leaf blight is characterised by small water-soaked spots, which initially appear on the lower leaves after infection whereafter they enlarge, forming chlorotic spots (Figure 2.6, A) (Klopper & Tweer, 2009b; Wise *et al.*, 2016). The lesions (spots) then elongate becoming elliptical or cigar-shaped and are tan to grey-green (Figure 2.6, B) (Smith & Kinsey, 1980; Munkvold & White, 2016; Wise *et al.*, 2016). As NLB progresses the lesions start to mature and become tan with distinct dark zones of sporulation (Wise, 2011; Munkvold & White, 2016). The lesions are usually between 2.5 to 15 cm long (Vieira *et al.*, 2014; Munkvold & White, 2016). Multiple lesions can coalesce to form large irregular areas of dead tissue and thus blighting the leaves (Figure 2.6, B) (Wise, 2011).

Figure 2.6. Typical characteristic symptoms of NLB. A- multiple chlorotic spots; B- mature cigar shape lesions starting to coalesce, causing necrosis of large parts of the leaf (Photos: RG Kotze).

2.3.3. The causal agent of NLB, *Exerohilum turcicum*

Exserohilum turcicum is a filamentous hemibiotrophic fungus and member of the Dothideomycetes, a large fungal class that includes many important plant pathogens with high economic impact (Ohm *et al.*, 2012). The fungus initially lives as a biotroph off the living plant tissue, whereafter it switches to a necrotrophic stage, killing the infected cells and completing its life cycle (Chung *et al.*, 2010; Ohm *et al.*, 2012; Human, 2019). Morphologically the hyphae of the fungus are typically filiform, repeatedly branched, are brown or grey to black and are 3–12 µm in diameter (Figure 2.7, A) (Jennings & Ullstrup, 1957; Sivanesan, 1987). The conidia are between 73–137 µm in length and 18–23 µm in width, 3–8 septate, olive-brown in colour, spindle-shaped, slightly curved with a protruding hilum (Figure 2.7, B), and exhibit bipolar germination (Luttrell, 1964; Leonard & Suggs, 1974; Levy & Cohen, 1983b; Munkvold & White, 2016). The distinct protruding hilum is a characteristic feature of the genus *Exserohilum* (Figure 2.7, B) (Leonard & Suggs, 1974).

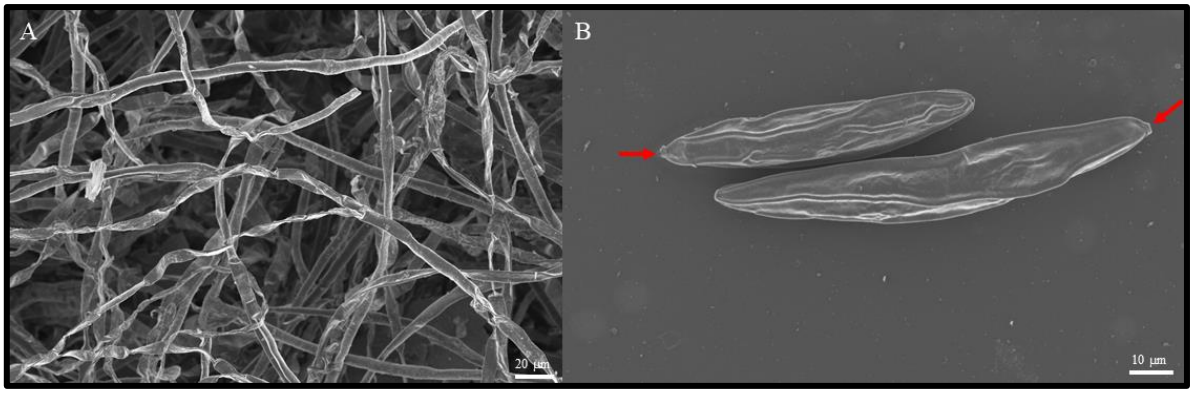

Figure 2.7. Scanning electron micrographs of A- hyphal growth of *E. turcicum*; B- conidia of *E. turcicum* with the protruding hilum indicated by red arrows (Micrographs: RG Kotze)

2.3.4. Disease cycle of NLB/*E. turcicum*

Exserohilum turcicum survives through winter as mycelia and conidia in and on leaf debris as well as in the soil (Robert & Findley, 1952; Munkvold & White, 2016). As the temperature starts to warm up during early spring, and moisture increases, new conidia are produced on the old residue (Robert & Findley, 1952; Klopper & Tweer, 2009b). Primary infection occurs when conidia spread to the lower leaves of young maize plants by wind or rain with secondary spread occurring within fields arising from conidia formed abundantly on infected leaves (Munkvold & White, 2016; Wise *et al.*, 2016). The fungus yet again overwinters in leaf debris and in the soil thus completing the life cycle. Conidia are the primary inoculum by which *E. turcicum* spreads from one leaf or plant to another and causes further infection (Munkvold & White, 2016; Wise *et al.*, 2016).

2.3.5. Disease development

Exserohilum turcicum infection mainly occurs during cool wet seasons. Disease development is favoured by heavy dew, frequent rain, high humidity (>90%), moderate temperatures (20–27°C), prolonged leaf wetness and photoperiod (Leach *et al.*, 1977; Levy & Cohen, 1983a; Levy & Cohen, 1983b; Munkvold & White, 2016). Therefore, symptoms are usually observed following periods of heavy dew, rain and overcast days during the growing seasons. Growth room studies indicated that NLB lesion progression was faster during the night than during the day (Levy & Cohen, 1984). Conidial germination and appressorium formation on maize leaves were favoured by prolonging dew conditions as well as short photoperiods and low light conditions (Levy & Cohen, 1983a; Levy & Cohen, 1983b). Warm nights and long periods of

high relative humidity are essential for the fungus to sporulate and complete its life cycle (Leach *et al.*, 1977). Disease progression is usually retarded by hot and dry weather conditions and thus the disease is more prevalent in the wetter areas of the world where maize is grown (Wise, 2011; Munkvold & White, 2016).

2.3.6. Infection strategy

Exserohilum turcicum typically causes yield loss by infecting and forming necrotic lesions, which leads to the loss of photosynthetic leaf area (Klopper & Tweer, 2009b). The infection process of maize leaves by *E. turcicum* starts when conidia on the maize leaf surface germinate, forming germination tubes whereafter it forms appressoria on the leaf epidermis cells (Knox-Davies, 1974). From the appressorium a fine infection hypha forms, which penetrates the outer epidermal cell wall, leading to thickening of the cell wall and invagination of the plasma membrane (Knox-Davies, 1974). Penetration is usually through the epidermal cell wall and rarely through the stomata (Jennings & Ullstrup, 1957). At the end of the infection hypha an intracellular vesicle forms, which subsequently gives rise to stout colonisation hyphae which extend into adjacent plant cells (Knox-Davies, 1974). As the disease progresses, intracellular growth is limited until the hyphae invade the vascular bundles and subsequently penetrate the xylem vessels and tracheids (Jennings & Ullstrup, 1957). After penetration of the vascular bundle, growth in the spongy mesophyll cells ceases (Jennings & Ullstrup, 1957). Growth throughout the vascular bundles is rapid as opposed to the initial dilatory growth of the hyphae in the spongy mesophyll cells. Wilted symptoms and necrosis of the bundle sheath and chlorenchyma cells follow extensive plugging of the xylem (Jennings & Ullstrup, 1957). In susceptible maize lines, the fungi thrive in the xylem tissue whereafter they invade the healthy bundle sheath and spongy mesophyll tissue (Hilu & Hooker, 1964). Rapid cell death follows and results in typical wilt like lesions (Hilu & Hooker, 1964). The death of healthy cells that causes the lesions could either be due to the presence of toxic fungal compounds (e.g. monocerin, E.t-toxin) (Table 2.2) or cell wall degrading enzymes (CWDE) produced by the fungus (Cuq *et al.*, 1993; Kubicek *et al.*, 2014).

2.3.7. Management of NLB in maize

The management of the disease can be achieved by the use of deep tillage and crop rotation practices, biological control, fungicides and resistant cultivars. The use of deep ploughing or

tilling practises will reduce the amount of primary inoculum carried over to the next season since plant residue is allowed to decompose (Wise *et al.*, 2016). Crop rotation with a non-host species of *E. turcicum* such as sunflower (*Helianthus annuus* L.) or soya beans will also reduce the inoculum load (Klopper & Tweer, 2009b). In maize fields with a history of NLB and where no or reduced tillage is practised, a two-year rotation with a non-host crop should be implemented (Wise, 2011).

Foliar fungicides are widely used by commercial farmers throughout the world to control NLB incidence in maize fields. The use of fungicides before 2002 was rare and only increased dramatically in 2007 (Wise & Mueller, 2011). This was due to several coinciding factors such as increased incidence of foliar pathogens such as NLB, the increased market price of maize, new fungicides being released, increased marketing of fungicides and tillage practices (Wise & Mueller, 2011). Strobilurins and triazoles are the two major classes of agricultural fungicides currently been used to prevent NLB (Bartlett *et al.*, 2002; Weems & Bradley, 2017). Brent and Hollomon (1998) reported that these chemical classes also run the risk of developing pathogen resistance and thus the fungicides cannot be used sustainably on their own over a long period.

Maize has two types of resistance against *E. turcicum*, namely polygenic and monogenic resistance. Polygenic or quantitative resistance is more durable than monogenic or qualitative resistance, is non-race-specific, more stable over time and is quantitatively expressed as a reduction in lesion number, lesion size and sporulation (Balint-Kurti & Johal, 2009; Munkvold & White, 2016). On the other hand, monogenic resistance is based on a single resistance gene called an *R*-gene, and provides race specific, high-level resistance against *E. turcicum* (Balint-Kurti & Johal, 2009). Maize plants with the appropriate *R*-gene can convey resistance towards a fungal pathogen by recognising the effectors secreted by these pathogens whereas plants are susceptible when they cannot recognise the effectors (Haasbroek, 2014). The four single dominant genes in maize which confer qualitative resistance are called *Ht1, Ht2, Ht3* and *HtN* (Hooker, 1961; Hooker, 1963a; Hooker, 1963b; Gevers, 1975; Hooker, 1977; Hooker, 1978; Hooker, 1981). The genes *Ht1, Ht2* and *Ht3* resistance phenotypes are characterised by chlorotic lesions and minimal sporulation events whereas *HtN* delays lesion development (Leonard *et al.*, 1989; Bentolila *et al.*, 1991; Simcox & Bennetzen, 1993). Martin *et al.* (2011) identified a putative *R*-gene on chromosome two, bin 2.06 of maize that conveys resistant against *E. turcicum* and could be the *Ht1* gene. The gene encodes a coiled-coil, nucleotide binding leucine rich repeat and was found to be uniquely expressed in resistant maize

genotypes (Martin *et al.*, 2011). A possible effector *AVRHt1* (avirulence) has been identified in *E. turcicum* which could possibly interact with the *Ht1* gene in maize (Mideros *et al.*, 2017).

Exserohilum turcicum races are based on their ability to overcome existing *Ht* resistance genes (*Ht1, Ht2, Ht3* and *HtN*) in maize (Leonard *et al.*, 1989). *Exserohilum turcicum* race 23N, carries *AVRHt1* but lacks *AVRHt2*, *AVRHt3* and *AVRHtN* and thus the isolate will only be able to cause disease in maize carrying any combination of *Ht2, Ht3* and *HtN* (Table 2.3). Maize lines with the *Ht1* gene will be resistant against an isolate that is race 23N. Race 123N describes an isolate that will be able to overcome all four resistance genes in maize and cause disease (Table 2.3). *Exserohilum turcicum* race 0 is ineffective (avirulent) against all the *Ht* genes and thus unable to cause disease in maize containing the resistance genes (Table 2.3).

Table 2.3. *Exserohilum turcicum* race typing against *Ht* resistance genes in maize. The races are based on their ability to overcome *Ht* resistance genes and cause disease in maize. Table adapted from Leonard *et al.* (1989).

***Exserohilum turcicum* Race**	**Maize disease reaction**			
	Ht1	*Ht2*	*Ht3*	*HtN*
0	R	R	R	R
1	S	R	R	R
2	R	S	R	R
12	S	S	R	R
23	R	S	S	R
23N	R	S	S	S
123N	S	S	S	S

R = Incompatible reaction between fungal race and *Ht* gene (host resistant).
S = Compatible reaction between fungal race and *Ht* gene (host susceptible).

Currently, the most effective way to manage the disease is an integrated approached using resistant maize cultivars, crop rotation with non-host species, sensible use of fungicides and deep tillage practices (Klopper & Tweer, 2009b; Wise, 2011).

2.3.8. E.t-toxin

Bashan and Levy (1992) isolated a water-soluble compound from different *E. turcicum* Race 0 (avirulent) (Table 2.3) isolates in Israel that exerted phytotoxic effects on susceptible sweet corn cultivars. The authors reported that water extracts made from the fungi inhibited

chlorophyll production in susceptible sweet corn cultivars (without *Ht* genes) but not in resistant cultivars (containing *Ht* genes). In a follow-up study, Bashan *et al.* (1995) isolated and structurally determined a water-soluble peptide (E.t toxin) consisting of three amino acids from extracts made from either fungal cultures or leaves infected with the fungus. Both synthetic and natural peptides inhibited chlorophyll levels in a susceptible sweet corn cultivar. The root growth of the susceptible sweet corn cultivar, Jubilee, was inhibited when treated with the synthetic peptide solution (Bashan *et al.*, 1995). Bashan *et al.* (1996) reported that non-pathogenic *E. turcicum* isolates from Johnson grass successfully infected susceptible maize lines (A619 and Jubilee) when the conidia were treated with the E.t toxin. Thus, this toxin could play an important role in *E. turcicum* infection of maize. Not much research has been done on E.t toxin since 1996 on E.t toxin and additional work should include whether the peptide is an HST or a NHST, determine its phytotoxic effects towards maize leaf ultrastructure as well as if it is toxic towards other organisms.

2.4. Monocerin

2.4.1. History

Monocerin is a lipophilic, dihydroisocoumarin and a polyketide metabolite that was first isolated in 1970 from *Exserohilum monoceras* (syn. *Helminthosporium monoceras*) (Aldridge & Turner, 1970; Axford *et al.*, 2004). Robeson and Strobel (1982) were the first authors to isolate monocerin from *E. turcicum* cultures and to report on its phytotoxicity towards plants. Monocerin and its related compounds have not only been isolated from *E. monoceras* and *E. turcicum* but have also been isolated from a variety of fungal pathogens (Table 2.4).

Table 2.4. Fungal pathogens from which monocerin has been isolated. Fungi marked with [a] fall within the class Sordariomycetes and fungi marked with [b] falls withing the class Dothideomycetes.

Fungus	Plant species isolated from	Reference
Colletotrichum sp.[a]	*Piper ornatum* N.E.Br.	(Tianpanich *et al.*, 2011)
Curvularia ravenelii[b]	unknown	(Scott *et al.*, 1984; Axford *et al.*, 2004)
Exserohilum monoceras[b]	*Echinochloa crus-galli* (L.) P.Beauv.	(Aldridge & Turner, 1970; Lim, 1999)
Exserohilum rostratum[b]	*Stemona* spp.	(Sappapan *et al.*, 2008)
Exserohilum turcicum[b]	*Sorghum halepense, Zea mays*	(Robeson & Strobel, 1982; Cuq *et al.*, 1993)
Microcera larvarum[a]	unknown	(Claydon *et al.*, 1979; Grove & Pople, 1979)
Microdochium bolleyi	*Fagonia cretica* L.	(Zhang *et al.*, 2008)
Readeriella mirabilis	unknown	(Turner & Aldridge, 1983)

2.4.2. Chemistry of monocerin

The structure of monocerin and its related compounds were first elucidated in 1970 by means of mass spectrometry and nuclear magnetic resonance (NMR) spectroscopy as (2S,3aR,9bR)-6-Hydroxy-7,8-dimethoxy-2-propyl-2,3,3a,9b-tetrahydro-5H-furo[3,2-c]isochromen-5-one (Figure 2.8) (Aldridge & Turner, 1970). In addition to monocerin, Aldridge and Turner (1970) also isolated three minor metabolites from *E. monoceras*, which included hydroxymonocerin, monocerene and monocerolide. It was initially reported that monocerin was of polyketide origin due to its structure, but due to the incorporation of C^{13}, H^{2} and O^{18} labelled acetates, it could possibly be of heptaketide origin (Scott *et al.*, 1984). Both the naturally occurring enantiomer and the racemate of monocerin were chemically synthesised the first time by Mori and Takaishi (1989). Monocerin can visually be described as a yellow oily substance that is readily dissolved in solvents such as methanol or chloroform (Cuq *et al.*, 1993; Axford *et al.*, 2004).

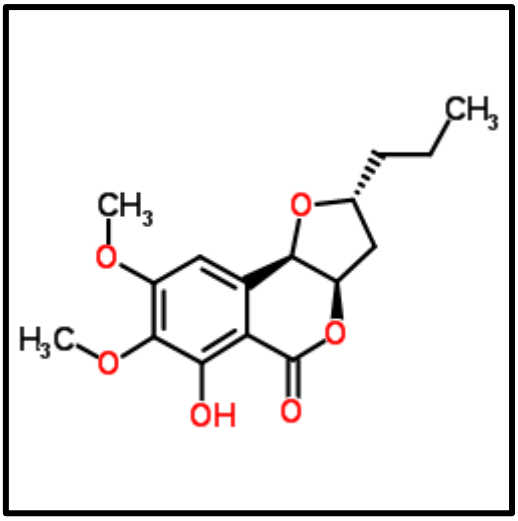

Figure 2.8. The chemical structure of monocerin (Mori & Takaishi, 1989).

2.4.3. Toxicity against other organisms

A few studies have reported on the toxicity of monocerin towards organisms which do not include plants. These studies have reported on the antifungal, antibacterial, antialgal, anti-insect and antiparasitic activities of monocerin, but no studies have reported on the effects it causes in humans and animals consuming diseased plant material. Aldridge and Turner (1970) were the first to report on the antifungal effects of crude monocerin extracts that were made from *E. monoceras* cultures. Additionally, the authors also mentioned that it can protect wheat against powdery mildew. Monocerin and one of its related compounds, fusarentin, have shown insecticidal activity against blowflies (*Calliphora vicina*) but did not cause any effects towards yellow fever mosquitos (*Aedes aegypti*) (Claydon *et al.*, 1979). Monocerin displayed antiparasitic activity against *Plasmodium falciparum* in a biological assay with an IC_{50} value of 0.68 µM monocerin concentration, whereas the positive control dihydroartemisinin had an IC_{50} value of 0.004 µM (Sappapan *et al.*, 2008). Monocerin has also shown good antifungal, antibacterial and antialgal activity against *Microbotryum violaceum* (anther smut fungus), *Escherichia coli* (Gram-negative bacterium), *Bacillus megaterium* (Gram-positive bacterium), and *Chlorella fusca*, respectively, at 3.24 mM monocerin (Zhang *et al.*, 2008).

2.4.4. Phytotoxicity of monocerin

Monocerin exerts phytotoxic effects on a wide range of agriculturally important taxa that include crops such as maize (Cuq *et al.*, 1993), radish (*Raphanus raphanistrum* L.) (Cuq *et al.*,

1993), cucumber (*Cucumis sativus* L.) (Robeson & Strobel, 1982), tomato (*Solanum lycopersicum* L.) (Robeson & Strobel, 1982; Lim, 1999), ryegrass (*Lolium multiflorum* Lam.) (Lim, 1999) and to a lesser extent rice (Lim, 1999) and weeds such as Johnson grass (Robeson & Strobel, 1982), creeping thistle (*Cirsium arvense* (L.) Scop.) (Robeson & Strobel, 1982), barnyardgrass (*Echinochloa crus-galli* (L.) P.Beauv.) (Lim, 1999) and bulrush (*Schoenoplectiella juncoides* (Roxb.) Lye) (Lim, 1999). The phytotoxic effects of monocerin include necrosis, chlorosis, reduced root development and cell death (Robeson & Strobel, 1982; Cuq *et al.*, 1993). Monocerin is considered a non-host selective toxin as it is phytotoxic to more than one plant species (Robeson & Strobel, 1982; Cuq *et al.*, 1993).

Robeson and Strobel (1982) were the first authors to report on the phytotoxicity of monocerin towards plants. The phytotoxic nature of monocerin was first observed when the authors performed a leaf dip assay where they applied monocerin at a concentration of 0.097 mM (0.3 mg/ml) to a punctured creeping thistle leaf. A necrotic spot of 7 mm in diameter together with necrotic spots along the main vein was observed 16 hours after incubation. After 40 hours of incubation, more than 50% of the leaf area was necrotic and the leaf was also brittle. The same was done for tomato leaves but at a concentration of 1 mM (0.33 mg/ml) monocerin (Robeson & Strobel, 1982). This caused the leaves to wilt within 16 hours but the leaves were not desiccated and no distinct areas of necrosis were apparent after 48 hours incubation. Robeson and Strobel (1982) additionally sprayed various concentrations of monocerin 0.32–3.24 mM (0.1-1.0 mg/ml) on cut leaves of Johnson grass. Chlorosis was observed after six days of incubation, and necrosis after eight days at all of the above-mentioned concentrations. Furthermore, the effect of monocerin on the root and shoot elongation of pre-germinated Johnson grass and cucumber seeds was also tested. At 3.24 mM (1 mg/ml) monocerin, root and shoot elongation was completely inhibited whereas at the lowest concentration of 0.1 mM (0.033 mg/ml) monocerin, the root and shoot elongation was inhibited by 50%. Pre-germinated seeds of cucumber were less sensitive to monocerin as compared to those of Johnson grass seedlings. In cucumber seedlings treated with 1 mg/ml monocerin root, and shoot elongation was inhibited by 33% when compared to the controls.

Cuq *et al.* (1993) purified and identified monocerin from crude chloroform extracts made from *E. turcicum* cultures isolated from maize in France. The authors further examined the phytotoxic effects of monocerin with the aid of various bioassays on the cells and protoplasts of maize. Brown necrotic lesions were observed on punctured leaves treated with a crude

extract containing monocerin. The authors reported that chloroform extracts inhibited radish, maize and tomato root elongation (Cuq *et al.*, 1993). The authors used pure monocerin in a detached leaf assay at different concentrations and temperatures. Monocerin was tested at a concentration range of 0.2–3 mM at both 24°C and 27°C. After 24 hours at 24°C, whitish necrosis developed along the veins whereas at 27°C the necrosis was brown and the area of the lesion was bigger (Cuq *et al.*, 1993). The minimum detection threshold was 0.4 mM with a plateau effect at 1 mM for both temperatures. No necrosis was seen in leaves treated with the 40% methanol control. The same range of monocerin concentrations was tested on the growth of pre-germinated radish seed. The maximal effect was reached at 2.5 mM but the ID_{50} value for both leaf and root bioassays were determined at 1 mM monocerin. Monocerin also reduced the viability of maize root cap cells as well as mesophyll protoplasts (Cuq *et al.*, 1993).

Root elongation was inhibited by over 91% in ryegrass, barnyardgrass and bulrush when treated with a monocerin solution of 0.32 mM (100 mg/L) made from *E. monoceras* (Lim, 1999). Root necrosis was also seen in the above-mentioned plants at a monocerin concentration of 0.32 mM (Lim, 1999). Monocerin did not have any effect on the root growth of tomato and lettuce even when 0.97 mM monocerin was applied to the plants (Lim, 1999). However, Cuq *et al.* (1993) reported that the growth of tomato roots was inhibited by 75% when the roots were treated with a crude extract made from *E. turcicum* when compared to the untreated control. Robeson and Strobel (1982) observed wilting effects on tomato leaves treated with 1 mM monocerin. Lim (1999) mentioned that monocerin plays a part in the expression of disease symptoms by *E. monoceras* but also in host selection (Lim, 1999). This is in contrast to Robeson and Strobel (1982) and Cuq *et al.* (1993) who reported that monocerin is a non-host selective toxin. Cuq *et al.* (1995) investigated the phytotoxic effects of monocerin on the cell cycle progression in maize root meristems. The authors reported that monocerin could interfere with the S and G2 stages of the cell division cycle where putative target molecules could be expressed.

It is interesting to note that in the first three studies (Robeson & Strobel, 1982; Cuq *et al.*, 1993; Lim, 1999) root inhibition assays were performed to test the phytotoxicity of monocerin whereas the last study investigated the effect of monocerin on the cell cycle progression of maize root cells (Cuq *et al.*, 1995). However, to date all the fungal pathogens from which moncerin has been isolated from, are known to be foliar pathogens and not soil pathogens.

Since monocerin not only exerts a phytotoxic effect towards leaf tissue but also the root tissue, it could potentially be used as a herbicide

2.5. Conclusion

The review provides a summary of the foliar pathogens of maize and the respective phytotoxins they produce, which could aid them in causing disease. It is evident that the fungal pathogens mentioned cannot cause disease without the host-selective phytotoxins they produce. It is apparent that if a race of a fungal pathogen, which produces phytotoxins, becomes prevalent in a season, as in the case of SCLB, it can lead to major maize yield losses, which in turn would lead to economic losses and food shortages. Additionally, this review also provides a detailed summary of NLB in maize as well as background on monocerin, with emphasis on its phytotoxicity. The infection process of *E. turcicum* has been studied before but only light microscopy was used, and the reproduction quality of the micrographs was poor in the past (Jennings & Ullstrup, 1957; Hilu & Hooker, 1964). This often makes the interpretation of the micrographs difficult especially examination of the infection and reproduction structures of the fungus. Due to an increase in resistance of the *E. turcicum* towards fungicides and resistant maize cultivars, alternative methods and strategies are needed to control NLB in maize. Monocerin is phytotoxic towards numerous plant species and could aid *E. turcicum* in causing disease in maize. Not much is known of the mode of action of the toxin as well as what part of the cell ultrastructure it exerts its toxic effects.

2.6. References

Abbas HK, Boyette C, 1992. Phytotoxicity of fumonisin B_1 on weed and crop species. *Weed Technology*, 548-52.

Abbas HK, Duke SO, Paul RN, Riley RT, Tanaka T, 1995. AAL-toxin, a potent natural herbicide which disrupts sphingolipid metabolism of plants. *Pesticide science* **43**, 181-7.

Adipala E, Lipps PE, Madden LV, 1993. Reaction of maize cultivars from Uganda to *Exserohilum turcicum*. *Phytopathology* **83**, 217-23.

Agrios GN, 2005. *Plant Pathology*. San Diego, CA, USA: Elsevier Academic Press.

Aldridge DC, Turner WB, 1970. Metabolites of *Helminthosporium monoceras:* Structures of monocerin and related benzopyrans. *Journal of the Chemical Society C: Organic* **18**, 2598-600.

Arny D, Nelson R, 1971. *Phyllosticta maydis* species nova, the incitant of yellow leaf blight of maize. *Phytopathology* **61**, 1170-2.

Au TK, Chick WSH, Leung PC, 2000. The biology of ophiobolins. *Life Sciences* **67**, 733-42.

Aveskamp MM, de Gruyter J, Woudenberg JH, Verkley GJ, Crous PW, 2010. Highlights of the Didymellaceae: A polyphasic approach to characterise *Phoma* and related pleosporalean genera. *Studies in Mycology* **65**, 1-60.

Awika JM, 2011. Major Cereal Grains Production and Use around the World. In: Awika JM, Piironen V, Bean S, eds. *Advances in Cereal Science: Implications to Food Processing and Health Promotion.* Wasgington, DC: ACS Publications, 1-13. (ACS Symposium Series; vol. 1089.)

Axford LC, Simpson TJ, Willis CL, 2004. Synthesis and incorporation of the first polyketide synthase free intermediate in monocerin biosynthesis. *Angewandte Chemie International Edition* **43**, 727-30.

Balint-Kurti PJ, Johal GS, 2009. Maize disease resistance. In. *Handbook of Maize: Its Biology.* 229-50.

Bartlett DW, Clough JM, Godwin JR, Hall AA, Hamer M, Parr-Dobrzanski B, 2002. The strobilurin fungicides. *Pest Management Science* **58**, 649-62.

Bashan B, Abadi R, Levy Y, 1996. Involvement of a phytotoxic peptide in the development of the Northern leaf blight of corn. *European Journal of Plant Pathology* **102**, 891-3.

Bashan B, Levy RS, Cojocaru M, Levy Y, 1995. Purification and structural determination of a phytotoxic substance from *Exserohilum turcicum*. *Physiological and Molecular Plant Pathology* **47**, 225-35.

Bashan B, Levy Y, 1992. Differential response of sweet corn cultivars to phytotoxic water-soluble compounds from culture filtrates of *Exserohilum turcicum*. *Plant Disease* **76**, 451-4.

Bennett JW, Klich M, 2003. Mycotoxins. *Clinical Microbiology Reviews* **16**, 497-516.

Bentolila S, Guitton C, Bouvet N, Sailland A, Nykaza S, Freyssinet G, 1991. Identification of an RFLP marker tightly linked to the *Ht1* gene in maize. *Theoretical and Applied Genetics* **82**, 393-8.

Berestetskiy A, Dmitriev A, Mitina G, Lisker I, Andolfi A, Evidente A, 2008. Nonenolides and cytochalasins with phytotoxic activity against *Cirsium arvense* and *Sonchus arvensis*: a structure-activity relationships study. *Phytochemistry* **69**, 953-60.

Bogyo TP, 1956. Maize varieties in Natal and East Griqualand. In. *Farming in S.A.*

Borchardt DS, Welz HG, Geiger HH, 1998. Genetic Structure of *Setosphaeria turcica* populations in tropical and temperate cimates. *Phytopathology* **88**, 322-9.

Brent KJ, Hollomon DW, 1998. *Fungicide resistance: the assessment of risk*. Global Crop Protection Federation Brussels.

Brosch G, Ransom R, Lechner T, Walton JD, Loidl P, 1995. Inhibition of maize histone deacetylases by HC toxin, the host-selective toxin of *Cochliobolus carbonum*. *Plant Cell* **7**, 1941-50.

Carson M, 1995a. A new gene in maize conferring the "chlorotic halo" reaction to infection by *Exserohilum turcicum*. *Plant Disease* **79**, 717-20.

Carson ML, 1995b. Inheritance of latent period length in maize Infected with *Exserohilum turcicum*. *Plant Disease* **79**.

Chung CL, Longfellow JM, Walsh EK, *et al.*, 2010. Resistance loci affecting distinct stages of fungal pathogenesis: use of introgression lines for QTL mapping and characterization in the maize - *Setosphaeria turcica* pathosystem. *BMC Plant Biology* **10**, 103.

Ciuffetti LM, Manning VA, Pandelova I, Betts MF, Martinez JP, 2010. Host-selective toxins, Ptr ToxA and Ptr ToxB, as necrotrophic effectors in the *Pyrenophora tritici-repentis*-wheat interaction. *New phytologist* **187**, 911-9.

Claydon N, Grove JF, Pople M, 1979. Insecticidal secondary metabolic products from the entomogenous fungus *Fusarium larvarum*. *Journal of Invertebrate Pathology* **33**, 364-7.

Collemare J, Lebrun MH, 2011. Fungal secondary metabolites: ancient toxins and novel effectors in plant–microbe interactions. In: Martin F, Kamoun S, eds. *In effectors in plant–microbe interactions.* Oxford, UK: Wiley-Blackwell, 377-400.

Comstock JC, Martinson CA, Gengenbach BG, 1973. Host specificity of a toxin from *Phyllosticta maydis* for Texas cytoplasmically male-sterile maize. *Phytopathology* **63**, 1357–61.

Condon BJ, Leng Y, Wu D, *et al.*, 2013. Comparative genome structure, secondary metabolite, and effector coding capacity across *Cochliobolus* pathogens. *PLOS Genetics* **9**, e1003233.

Crous PW, Groenewald JZ, Groenewald M, Caldwell P, Braun U, Harrington TC, 2006. Species of *Cercospora* associated with grey leaf spot of maize. *Studies in Mycology* **55**, 189-97.

Cuq F, Brown SC, Petitprez M, Alibert G, 1995. Effects of monocerin on cell-cycle progression in maize root-meristems synchronized with aphidicolin. *Plant Cell Reports* **15**, 138-42.

Cuq F, Petitprez M, Herrmann-Gorline S, Klaebe A, Rossignol M, 1993. Monocerin in *Exserohilum turcicum* isolates from maize and a study of its phytotoxicity. *Phytochemistry* **34**, 1265-70.

Daub ME, Ehrenshaft M, 2000. The photoactivated *Cercospora* toxin cercosporin: Contributions to plant disease and fundamental biology. *Annual Review of Phytopathology* **38**, 461-90.

Dingerdissen AL, Geiger HH, Lee M, Schechert A, Welz HG, 1996. Interval mapping of genes for quantitative resistance of maize to *Setosphaeria turcica*, cause of Northern leaf blight, in a tropical environment. *Molecular Breeding* **2**, 143-56.

Drechsler C, 1923. Some graminicolons species of *Helminthosporium*. *Journal of Agricultural Research* **24**, 641-739.

Du Plessis J, 2003. *Maize production*. Pretoria, South Africa: Department of Agriculture.

Dunkle LD, Levy M, 2000. Genetic relatedness of African and United States populations of *Cercospora zeae-maydis*. *Phytopathology* **90**, 486-90.

FAOSTAT, 2018. FAO statistical database. In. Rome, Italy: Food and Agricultural Organization of the United Nations.

Friesen TL, Faris JD, Solomon PS, Oliver RP, 2008. Host-specific toxins: effectors of necrotrophic pathogenicity. *Cell Microbiology* **10**, 1421-8.

Gevers H, 1975. A new major gene for resistance to *Helminthosporium turcicum* leaf blight of maize. *Plant Disease Reporter* **59**, 296-9.

Grain_SA, 2018. In. Pretoria, South Africa: Grain SA.

Grove JF, Pople M, 1979. Metabolic products of *Fusarium larvarum* fuckel. The fusarentins and the absolute configuration of monocerin. *Journal of the Chemical Society, Perkin Transactions 1*, 2048-51.

Haasbroek MP, 2014. *Characterization of Exserohilum turcicum isolates from South African maize production areas*. Pretoria, University of Pretoria, MSc dissertation.

Hilu HM, Hooker AL, 1964. Host-pathogen relationship of *Helminthosporium turcicum* in resistant and susceptible corn seedlings. *Phytopathology* **54**, 570-5.

Hooker AL, 1961. A new type of resistance in corn to *Helminthosporium turcicum*. *Plant Disease Reporter* **45**, 780-1.

Hooker AL, 1963a. Inheritance of chlorotic-lesion resistance to *Helminthosporium turcicum* in seedling corn. *Phytopathology* **53**, 660-2.

Hooker AL, 1963b. Monogenic resistance in *Zea mays* L. to *Helminthosporium turcicum*. *Crop science* **3**, 381-3.

Hooker AL, 1977. A second major gene locus in corn for chlorotic-lesion resistance to *Helminthosporium turicum*. *Crop science* **17**.

Hooker AL, 1978. Additional sources of monogenic resistance in corn to *Helminthosporium turcicum*. *Crop science* **18**.

Hooker AL, 1981. Resistance to *Helminthosporium turcicum* from *Tripsacum floridanum* incorporated into corn. *Maize Genetics Cooperation Newsletter* **55**, 87-8.

Human MP, 2019. *Effector identification from the susceptible Exserohilum turcicum – Zea mays interaction*. Pretoria, University of Pretoria, PhD Thesis.

Jennings P, Ullstrup A, 1957. A histological study of 3 *Helminthosporium* leaf blights of corn. *Phytopathology* **47**, 707-14.

Jenns AE, 1989. Regulation of cercosporin accumulation in culture by medium and temperature manipulation. *Phytopathology* **79**.

Kabir MS, Ganley RJ, Bradshaw RE, 2015. Dothistromin toxin is a virulence factor in dothistroma needle blight of pines. *Plant Pathology* **64**, 225-34.

Kim H-J, Kim J-C, Kim B-S, Kim H-G, Cho K-Y, 1999. Antibiotic and phytotoxic activities of ophiobolins from *Helminthosporium* species. *The Plant Pathology Journal* **15**, 14-20.

Klopper R, Tweer S, 2009a. Grey leaf spot fact sheet. [http://www.pannar.com/assets/disease_fact_sheets/Grey_Leaf_Spot.pdf]. Accessed 10 July 2018.

Klopper R, Tweer S, 2009b. Northern corn leaf blight fact sheet. [http://www.pannar.com/assets/disease_fact_sheets/Northern_Corn_Leaf_Blight.pdf]. Accessed 11 November 2019.

Knox-Davies P, 1974. Penetration of maize leaves by *Helminthosporium turcicum*. *Phytopathology* **64**, 1468-70.

Koohafkan P, Stewart BA, 2008. *Water and cereals in drylands*. The Food and Agriculture Organization of the United Nations and Earthscan.

Kubicek CP, Starr TL, Glass NL, 2014. Plant cell wall-degrading enzymes and their secretion in plant-pathogenic fungi. *Annual Review of Phytopathology* **52**, 427-51.

Larkin PJ, Scowcroft WR, 1981. Eyespot Disease of Sugarcane : Induction of host-specific toxin and its interaction with leaf cells. *Plant Physiology* **67**, 408-14.

Latterell FM, Rossi AE, 1983. Gray leaf spot of corn: a disease on the move. *Plant Disease* **67**, 842-7.

Leach CM, Fullerton RA, Young K, 1977. Northern leaf blight of maize in New Zealand: relationship of *Drechslera turcia* airspora to factors onfluencing sporulation, conidium development, and chlamydospore formation. *Phytopathology* **77**, 629.

Leonard KJ, Levy Y, Smith DR, 1989. Proposed nomenclature for pathogenic races of *Exserohilum turcicum* on corn. *Plant Disease* **73**, 776-7.

Leonard KJ, Suggs EG, 1974. *Setosphaeria prolata*, the ascigerous state of *Exserohilum prolatum*. *Mycologia* **66**, 281-97.

Levy Y, Cohen Y, 1983a. Biotic and environmental factors affecting infection of sweet corn with *Exserohilum turcicum*. *Phytopathology* **73**, 722-5.

Levy Y, Cohen Y, 1983b. Differential effect of light on spore germination of *Exserohilum turcicum* on corn leaves and corn leaf impressions. *Phytopathology* **73**, 249-52.

Levy Y, Cohen Y, 1984. A negative association between leaf sugar content and the development of northern leaf blight lesions in sweet corn. *Physiological Plant Pathology* **24**, 247-52.

Levy Y, Pataky JK, 1992. Epidemiology of Northern leaf blight on sweet corn. *Phytoparasitica* **20**, 53-66.

Lim C-H, 1999. Monocerin and ziganein: phytotoxins from pathogenic fungus *Exserohilum turcicum* Inu-1. *Agricultural Chemistry and Biotechnology* **42**, 45-7.

Lu S, Gillian Turgeon B, Edwards MC, 2015. A ToxA-like protein from *Cochliobolus heterostrophus* induces light-dependent leaf necrosis and acts as a virulence factor with host selectivity on maize. *Fungal Genetics and Biology* **81**, 12-24.

Luttrell E, 1964. Systematics of *Helminthosporium* and related genera. *Mycologia* **56**, 119-32.

Manamgoda DS, Cai L, Bahkali AH, Chukeatirote E, Hyde KD, 2011. *Cochliobolus*: an overview and current status of species. *Fungal Diversity* **51**, 3-42.

Markham JE, Hille J, 2001. Host-selective toxins as agents of cell death in plant-fungus interactions. *Molecular Plant Pathology* **2**, 229-39.

Martin T, Biruma M, Fridborg I, Okori P, Dixelius C, 2011. A highly conserved NB-LRR encoding gene cluster effective against *Setosphaeria turcica* in sorghum. *BMC Plant Biology* **11**, 151.

Meisel B, Korsman J, Kloppers FJ, Berger DK, 2009. *Cercospora zeina* is the causal agent of grey leaf spot disease of maize in southern Africa. *European Journal of Plant Pathology* **124**, 577-83.

Mideros SX, Chung C-L, Wiesner-Hanks T, *et al.*, 2017. Determinants of virulence and in vitro development colocalize on a genetic map of *Setosphaeria turcica*. *Phytopathology* **108**, 254-63.

Mobius N, Hertweck C, 2009. Fungal phytotoxins as mediators of virulence. *Current Opinion in Plant Biology* **12**, 390-8.

Mori K, Takaishi H, 1989. Synthesis of monocerin, an antifungal, insecticidal and phytotoxic heptaketide metabolite of *Exserohilum monoceras*. *Tetrahedron* **45**, 1639-46.

Munkvold GP, Desjardins AE, 1997. Fumonisins in maize: Can we reduce their occurrence? *Plant Disease* **81**, 556-65.

Munkvold GP, White DG, 2016. *Compendium of Corn Diseases*. APS press St. Paul, MN.

Ohm RA, Feau N, Henrissat B, *et al.*, 2012. Diverse lifestyles and strategies of plant pathogenesis encoded in the genomes of eighteen Dothideomycetes fungi. *PLOS Pathogens* **8**, e1003037.

Perkins J, Pedersen W, 1987. Disease development and yield losses associated with Northern leaf blight on corn. *Plant Disease* **71**, 940-3.

Petrov V, Qureshi MK, Hille J, Gechev T, 2018. Occurrence, biochemistry and biological effects of host-selective plant mycotoxins. *Food and Chemical Toxicology* **112**, 251-64.

Ransom RF, Walton JD, 1997. Histone hyperacetylation in maize in response to treatment with HC-toxin or infection by the filamentous fungus *Cochliobolus carbonum*. *Plant Physiology* **115**, 1021-7.

Rasmussen JB, Scheffer RP, 1988. Effects of selective toxin from *Helminthosporium carbonum* on chlorophyll synthesis in maize. *Physiological and Molecular Plant Pathology* **32**, 283-91.

Robert AL, Findley WR, 1952. Diseased corn leaves as a source of infection in artificial and natural epidemics of *Helminthosporium turcicum*. *Plant Disease Reporter* **36**, 9-10.

Robeson DJ, Strobel GA, 1982. Monocerin, a phytotoxin from *Exserohilum turcicum* (= *Drechslera turcica*). *Agricultural and Biological Chemistry* **46**, 2681-3.

Sappapan R, Sommit D, Ngamrojanavanich N, *et al.*, 2008. 11-Hydroxymonocerin from the plant endophytic fungus *Exserohilum rostratum*. *Journal of natural products* **71**, 1657-9.

Scheffer RP, Livingston RS, 1984. Host-selective toxins and their role in plant diseases. *Science* **223**, 17-21.

Scott FE, Simpson TJ, Trimble LA, Vederas JC, 1984. Biosynthesis of monocerin. Incorporation of 2H-, 13C-, and 18O-labelled acetates by *Drechslera ravenelii*. *Journal of the Chemical Society, Chemical Communications*, 756.

Simcox KD, Bennetzen JL, 1993. The use of molecular markers to study *Setosphaeria turcica* resistance in maize. *Phytopathology* **83**, 1326-30.

Sivanesan A, 1987. Graminicolous species of *Bipolaris, Curvularia, Drechslera, Exserohilum* and their teleomorphs. *Mycological Papers* **158**, 1-261.

Smith CW, Betrán J, Runge ECA, 2004. *Corn : Origin, history, technology, and production*. Hoboken, N.J. :: John Wiley.

Smith D, Kinsey J, 1980. Further physiologic specialization in *Helminthosporium turcicum*. *Plant Disease* **64**, 779-81.

Stergiopoulos I, Collemare J, Mehrabi R, De Wit PJ, 2013. Phytotoxic secondary metabolites and peptides produced by plant pathogenic Dothideomycete fungi. *FEMS Microbiology Reviews* **37**, 67-93.

Steyn PS, 1995. Mycotoxins, general view, chemistry and structure. *Toxicology Letters* **82-83**, 843-51.

Stoessl A, Abramowski Z, Lester HH, Rock GL, Towers GHN, 1990. Further toxic properties of the fungal metabolite dothistromin. *Mycopathologia* **112**, 179-86.

Strobel G, Kenfield D, Sugawara F, 1988. The incredible fungal genus —*Drechslera* — and its phytotoxic ophiobolins. *Phytoparasitica* **16**, 145-52.

Sugawara F, Strobel G, Strange RN, Siedow JN, Van Duyne GD, Clardy J, 1987. Phytotoxins from the pathogenic fungi *Drechslera maydis* and *Drechslera sorghicola*. *Proceedings of the National Academy of Sciences* **84**, 3081-5.

Swart V, Crampton BG, Ridenour JB, *et al.*, 2017. Complementation of *CTB7* in the Maize Pathogen *Cercospora zeina* Overcomes the Lack of In Vitro Cercosporin Production. *Molecular Plant-Microbe Interactions* **30**, 710-24.

Tianpanich K, Prachya S, Wiyakrutta S, Mahidol C, Ruchirawat S, Kittakoop P, 2011. Radical scavenging and antioxidant activities of isocoumarins and a phthalide from the endophytic fungus *Colletotrichum* sp. *Journal of natural products* **74**, 79-81.

Tsuge T, Harimoto Y, Akimitsu K, *et al.*, 2013. Host-selective toxins produced by the plant pathogenic fungus Alternaria alternata. *FEMS Microbiology Reviews* **37**, 44-66.

Turner W, Aldridge D, 1983. Fungal metabolites, vol II. *Paris: Academic*, 257-9.

Ullstrup AJ, 1972. The impacts of the Southern corn leaf blight epidemics of 1970-1971. *Annual Review of Phytopathology* **10**, 37-50.

Upchurch RG, Walker DC, Rollins JA, Ehrenshaft M, Daub ME, 1991. Mutants of *Cercospora kikuchii* altered in cercosporin synthesis and pathogenicity. *Applied and Environmental Microbiology* **57**, 2940-5.

Vieira RA, Mesquini RM, Silva CN, Hata FT, Tessmann DJ, Scapim CA, 2014. A new diagrammatic scale for the assessment of Northern corn leaf blight. *Crop Protection* **56**, 55-7.

Walton JD, 2006. HC-toxin. *Phytochemistry* **67**, 1406-13.

Weems JD, Bradley CA, 2017. Sensitivity of *Exserohilum turcicum* to demethylation inhibitor fungicides. *Crop Protection* **99**, 85-92.

Williams LD, Glenn AE, Zimeri AM, Bacon CW, Smith MA, Riley RT, 2007. Fumonisin disruption of ceramide biosynthesis in maize roots and the effects on plant development and *Fusarium verticillioides*-induced seedling disease. *Journal of agricultural and food chemistry* **55**, 2937-46.

Wise K, 2011. *Diseases of Corn: Northern Corn Leaf Blight*. [https://www.extension.purdue.edu/extmedia/BP/BP-84-W.pdf]. 14 November 2019.

Wise K, Mueller D, 2011. Are fungicides no longer just for fungi? An analysis of foliar fungicide use in corn. *APSnet Features*, -.

Wise K, Mueller D, Sisson A, Smith D, Bradley C, Robertson A, 2016. *A Farmer's Guide to Corn Diseases*. St. Paul, Minnesota: APS Press.

Wolpert TJ, Dunkle LD, Ciuffetti LM, 2002. Host-selective toxins and avirulence determinants: what's in a name? *Annual Review of Phytopathology* **40**, 251-85.

Yoder OC, 1980. Toxins in pathogenesis. *Annual Review of Phytopathology* **18**, 103-29.

Zhang W, Krohn K, Draeger S, Schulz B, 2008. Bioactive isocoumarins isolated from the endophytic fungus *Microdochium bolleyi*. *Journal of natural products* **71**, 1078-81.

Chapter 3: A histological assessment of the infection strategy of *Exserohilum turcicum* in maize

This chapter has been published as: Kotze, R.G., van der Merwe, C.F., Crampton, B.G., Kritzinger, Q., 2018. A histological assessment of the infection strategy of *Exserohilum turcicum* in maize. Plant Pathology (DOI: 10.1111/ppa.12961).

Abstract

Northern leaf blight is a lethal foliar disease of maize caused by the fungus *Exserohilum turcicum*. The aim of this study was to elucidate the infection strategy of the fungus in maize leaves using modern microscopy techniques and to understand better the hemibiotrophic lifestyle of *E. turcicum*. Leaf samples were collected from inoculated B73 maize plants at 1, 4, 9, 11, 14 and 18 days post-inoculation (dpi). Samples were prepared according to standard microscopy procedures and analysed using light microscopy as well as scanning (SEM) and transmission electron microscopy (TEM). Microscopic observations were preceded by macroscopic observations for each time point. The fungus penetrated the leaf epidermal cells at 1 dpi and the disease was characterized by chlorotic leaf flecks. At 4 dpi the chlorotic flecks enlarged to form spots, and at 9 dpi hyphae were seen in the epidermal cells surrounding the infection site. At 11 dpi lesions started to form on the leaves and SEM revealed the presence of hyphae in the vascular bundles. At 14 dpi the xylem was almost completely blocked by hyphal growth. Hyphae spread into the adjacent bundle sheath cells causing cellular damage, characterized by plasmolysis, at 18 dpi and conidiophores formed through the stomata. Morphologically, lesions started to enlarge and coalesce leading to wilting of leaves. This study provides an updated, detailed view of the infection strategy of *E. turcicum* in maize and supports previous findings that *E. turcicum* follows a hemibiotrophic lifestyle.

Keywords: electron microscopy, *Exserohilum turcicum*, fungal infection, hemibiotroph, light microscopy, northern leaf blight

3.1. Introduction

Northern leaf blight (NLB) is a devastating foliar disease of maize (*Zea mays* L.) and is a serious threat to its production worldwide. In addition to maize, the disease can affect other crops including sorghum (*Sorghum bicolor* (L.) Moench) and grass species (White, 1999; Agrios, 2005). Currently, NLB is one of the most widespread diseases of maize in South Africa, especially in the wetter eastern parts of the country (Klopper & Tweer, 2009) and causes significant yield losses in both quality and quantity of the grain. Typical yield losses range from 15% to 30% but can be as high as 75% during optimal disease conditions (Klopper & Tweer, 2009). The disease is the most severe if infection happens before silking and spreads to the upper leaves during grain filling (Perkins & Pedersen, 1987; Carson, 1995; Klopper & Tweer, 2009). Yield losses can be predominantly ascribed to the loss of photosynthetic leaf area due to the blighting of the leaves (Klopper & Tweer, 2009; Wise, 2011). Disease development is favoured by dew periods of at least 4 h, 90–100% relative humidity (RH), prolonged leaf wetness, and moderate temperatures ranging from 17 to 27°C (Levy & Cohen, 1983a; Bentolila *et al.*, 1991; White, 1999; Klopper & Tweer, 2009; Wise, 2011).

Initial symptoms of NLB can be characterized by minute chlorotic flecks, which appear on leaves after infection (White, 1999; Klopper & Tweer, 2009). Mature symptoms of NLB are characterized by grey-green coloured elliptical or cigar-shaped lesions that are 2.5–17.5 cm in length (White, 1999; Wise, 2011). As the disease progresses, the lesions start to mature and become tan coloured with distinct dark zones that are associated with fungal sporulation (White, 1999; Klopper & Tweer, 2009; Wise, 2011). In the advanced stages of the disease, multiple lesions can coalesce forming large irregular areas of dead tissue on the leaves (Wise, 2011). In severe infection, almost all of the leaves may be infected and can be entirely blighted, resembling frost or drought injury (White, 1999).

The causal agent of NLB is *Exserohilum turcicum* (sexual stage *Setosphaeria turcica*, syn. *Helminthosporium turcicum*), which is a filamentous hemibiotrophic fungus from the class Dothideomycetes (Leonard & Suggs, 1974). The hyphae are brown or grey to black in colour and are 3–12 µm in diameter (Jennings & Ullstrup, 1957; Sivanesan, 1987). Conidia are the primary inoculum by which the disease spreads from one plant to another. They are 73–137 µm in length and 18–23 µm in width, 3–8 septate, olive-brown in colour, spindle shaped with

a protruding hilum and exhibit bipolar germination (Luttrell, 1964; Levy & Cohen, 1983b; White, 1999).

The infection strategy of *E. turcicum* has been previously described by Jennings and Ullstrup (1957), Hilu and Hooker (1964); Hilu and Hooker (1965) and Knox-Davies (1974). Chung *et al.* (2010) and Ohm *et al.* (2012) described *E. turcicum* as a hemibiotrophic fungus, which initially lives as a biotroph, feeding off living host tissue; subsequently it switches to a necrotrophic lifestyle, killing the infected cells of the host. In the first histological study on NLB, carried out by Jennings and Ullstrup (1957), the authors used light microscopy (LM) to determine whether there were any histological differences between resistant and susceptible inbred lines of maize for three different *Helminthosporium* leaf blights, including NLB. In addition, they compared the host–parasite relationship of these three blights with maize. Similarly, Hilu and Hooker (1964) performed a histopathological study on *E. turcicum* in resistant and susceptible maize types. Their study was expanded to include observations of the cellular host response to fungal invasion and cytological changes associated with necrosis. Additionally, Hilu and Hooker (1965) studied the localized infection as well as the histology of virulent and avirulent isolates of *E. turcicum* in susceptible maize seedlings. Knox-Davies (1974) observed fine infection hyphae (penetration pegs) that developed from the appressoria of *E. turcicum* during the penetration of the epidermal cells of maize leaves. Although the above-mentioned studies gave insight into the histopathology following infection by *E. turcicum*, only light microscopy was used. In addition, it is often difficult to interpret some micrographs from these studies due to their poor reproduction quality.

Other microscopy techniques that can be used to examine host–pathogen interactions include scanning electron microscopy (SEM), transmission electron microscopy (TEM) and confocal microscopy. Transmission electron microscopy is useful in visualizing the ultrastructure of cells whereas, with SEM, the topography of the leaf surface and subsequent infection sites can be observed. Confocal microscopy is a valuable tool to study the initial infection phase of a fungus when it is difficult to detect the fungal infection structures in the leaf.

The present study was originated to characterize the infection process of *E. turcicum* in maize in order to correlate cytological processes with on-going molecular host–pathogen interaction studies in the laboratory (M. Human, University of Pretoria, Pretoria, South Africa, personal communication). Thus, the aims of this study were, first, to use light and electron microscopy

to provide further insight into the infection process of *E. turcicum* in maize and, secondly, to use this information to confirm the existence of a hemibiotrophic lifestyle of *E. turcicum* during maize infection. This study provides a basis for further studies involving the characterization of the host defence response in maize towards the fungus.

3.2. Materials and methods

3.2.1. Fungal strain, culture conditions and preparation of inoculum

South African *Exserohilum turcicum* isolate 2 was obtained from NLB lesions on maize leaves collected in the Reitz region, Free State, during February 2007 (Haasbroek *et al.*, 2014). Identification of isolate 2 was confirmed by means of a single multiplex PCR assay described by Haasbroek *et al.* (2014), which specifically determines the mating type of *E. turcicum* isolates. Pure cultures were grown and routinely maintained on V8 juice agar (Beckman & Payne, 1982) and incubated at room temperature. Conidia were harvested by flooding Petri dishes with 2 ml sterile distilled water containing 0.1% Tween 20 followed by lightly scraping the agar surface with a sterile surgical blade to dislodge the conidia. The conidial suspension was filtered through muslin cloth to remove mycelial debris; the concentration was determined using a Neubauer haemocytometer and adjusted to 5×10^4 spores/ml.

3.2.2. Maize cultivation and infection trial

Maize plants of the inbred line B73 (susceptible to NLB; (Craven & Fourie, 2011)) were grown in 20 cm pots containing a soil mixture consisting of one part potting soil (Culterra, Nietgedacht, South Africa) and one part silica sand (Rolfes Silica, Brits, South Africa). The plants were maintained in a growth room with the temperature ranging from 20 to 25°C and with a relative humidity (RH) of between 50% and 100% during the night and day, with a photoperiod of 16 h. The plants were watered every second day until run-off and supplemented with Lawn and Leaf fertilizer (7:1:3; Wonder) twice during the infection period. Maize plants (approximately 36 days old) at the V9 growth stage (9th leaf stage, which represents older plants; (Lee, 2011)) were inoculated by adding 2 ml of a conidial suspension into the whorl of each plant. The inoculated plants, eight biological replicates per experiment, were then incubated for 12 h at 20°C with 100% RH in the dark, after which they were maintained as before the infection. Leaf samples were harvested at 1, 4, 9, 11, 14 and 18 days post-inoculation

(dpi). Control samples were harvested at 0 dpi before the infection process took place. The experiment was repeated twice.

3.2.3. Microscopy

For LM and TEM, control and infected maize leaf samples with symptoms, which included either chlorotic spots or necrotic lesions, were cut transversely into 1 mm^2 sections and fixed by vacuum infiltration with 2.5% glutaraldehyde in 0.075 M phosphate buffer (pH 7.4). After fixation, samples were washed three times with 0.075 M phosphate buffer followed by post fixation in 1% aqueous osmium tetroxide (OsO_4; SPI-Chem) for 1 h. Subsequently, the samples were rinsed three times in 0.075 M phosphate buffer. Finally, the samples were dehydrated in a graded ethanol series using distilled water (50%, 70%, 90%, 100%, 100%, 100%).

The samples were infiltrated with increasing concentrations of LR white resin (SPI-Chem, West Chester, PA) at 30%, 50%, 70%, 90%, 100% for 1 h in each concentration at room temperature. Finally, the samples were embedded in 100% LR white resin at 60°C for 39 h. For LM, the samples were cut into 500 nm sections with a glass knife on an Ultracut E ultramicrotome (Reichert) and stained with toluidine blue, after which samples were viewed with an AXIO Imager.M2 (Zeiss). For TEM, the samples were cut into 100 nm sections with a diamond knife on an Ultracut E ultramicrotome and sections were contrasted with 4% aqueous uranyl acetate and lead citrate for viewing with a JEM2100F TEM (JEOL).

For SEM, maize leaf samples were cut into either 10 × 10 mm or 10 × 3 mm sections. Samples were prepared and fixed as described for LM and TEM but were dried with hexamethyldisilazane (HMDS; reagent grade, ≥99%; Merck) after the ethanol-dehydration step. The samples were mounted on aluminium stubs and coated with either carbon or ruthenium tetroxide (RuO_4) vapour (Van der Merwe & Peacock, 1999). Subsequently, samples were viewed with an Ultra Plus SEM (Zeiss) and micrographs taken at 3 kV accelerating voltage.

3.3. Results

The effect of *E. turcicum* infection on maize leaf morphology, anatomy, cell ultrastructure and integrity was examined during the progression of NLB disease in maize. The life cycle of *E. turcicum in planta* was usually completed within 18 days after inoculation of maize leaves in the growth room. A 100% infection rate was observed for all maize plants.

Throughout the study, the control noninfected maize plants exhibited no visible NLB infection and the leaves were healthy and intact (Figure 3.1, a). Additionally, the light and scanning electron micrographs of the control tissue showed intact cells with clearly defined chloroplasts and nuclei in the spongy mesophyll and bundle sheath cells (Figure 3.2, a & Figure 3.3, a). Intact vascular bundles were also observed.

Penetration of the maize leaf by *E. turcicum* typically elicited localized host responses, which resulted in very small visible chlorotic flecks seen at 1 dpi (Figure 3.1, b). These flecks occurred where the fungus had penetrated the leaf epidermis. Penetration of the leaf epidermal cells occurred between 12 and 18 h post-inoculation. Scanning electron micrographs (Figure 3.3, b) revealed that conidial germination and penetration of the leaf epidermis occurred within 1 dpi. Germinated conidia produced germ tubes, which grew towards leaf epidermal cell walls and subsequently formed appressoria (Figure 3.3, b). In this study conidia were on average 70–105 µm in length (Appendix, Figure 7.1), germ tubes were 35–300 µm long and appressoria were 12–22 µm in width. Penetration of the leaf epidermis was direct and occurred at the juncture between epidermal cell walls; it was not observed to occur through the stomata or leaf trichomes even when in close contact with both these structures (Figure 3.3, c).

Morphologically, at 4 dpi chlorotic flecks had enlarged to form chlorotic spots on infected maize leaves (Figure 3.1, c) but microscopically the fungus was not observed in the leaf tissue. Light micrographs of paradermal sections of infected maize leaves harvested at 9 dpi revealed that the tissue in the necrotic spots had collapsed compared to the surrounding healthy tissue (Figure 7.2, a); complete tissue degradation was evident and cells were necrotic (Figure 7.2, b). A hypha of *E. turcicum* was observed in an epidermal cell in close proximity to one of these spots (Figure 3.2, b). At a macroscopic level, the necrotic spots stayed the same size from 4 dpi until 11 dpi.

At 11 dpi, the necrotic spots started to expand and small lesions started to form on infected leaves (Figure 3.1, d). Additionally, the hyphae penetrated the xylem vessels and tracheids of the vascular bundle (Figure 3.2, c & Figure 3.3, d, e), at which point the lesions became necrotic and enlarged. After penetration of the vascular bundle, abundant hyphae were visible throughout the xylem tracheids and vessels, in contrast to the limited number of hyphae seen in the epidermal and mesophyll cells previously. Necrotic lesions appeared concurrently with plugging of the xylem by hyphae. At this time point, cells within the maize leaf were still intact with well-defined cell walls and visible organelles (Figure 3.2, c).

By 14 dpi, necrotic lesions on the maize leaves had started to enlarge and elongate to form the distinct cigar-shaped lesions that are characteristic of NLB infection in maize leaves (Figure 3.1, e). Plugging of the xylem vessels and tracheids by the hyphae was more extensive at 14 dpi than at 11 dpi (Figure 3.2, d & Figure 3.3, f). The xylem in the smaller vascular bundles was almost filled with hyphae whereas the xylem in the major veins was approximately 75% blocked with hyphae. Additionally, shrinking and collapse of the spongy mesophyll cells were observed in close proximity to one of the major veins (Figure 3.2, d). The collapse of spongy mesophyll cells between parasitized vascular bundles was associated with the extensive plugging of major veins and complete blocking of minor veins. When an entire lesion was visualized by examination of a number of microscopy sections, it was observed that some of the cells in the lesion had died without any direct contact with the fungus. Chloroplasts in both the spongy mesophyll and bundle sheath cells within a lesion had started to disintegrate. As the cells became more plasmolysed, the nuclei also degraded and this was followed by collapse of the cells. Hyphae only grew out of the xylem into the bundle sheath cells after the tissue became necrotic (Figure 3.3, f). Colonization from one vein to another was accomplished by hyphal growth through cross veins found throughout the maize leaf (Figure 3.2, e).

Morphologically, at 18 dpi, the cigar-shaped lesions had started to coalesce, killing large parts of the leaf (Figure 3.1, f). At a cellular level, complete tissue collapse was observed, with the exception of the vascular bundles and epidermal cells, in contrast to the control tissue (Figure 3.2, a, f & Figure 3.3, a). Although the xylem vessels and tracheids were still intact in the infected plants, the phloem tissue was completely disintegrated and granulation of the protoplasm was visible within bundle sheath cells (Figure 3.2, f). The hyphae grew out of the xylem into the bundle sheath cells (Figure 3.2, f & Figure 3.3, g), the intercellular airspaces and the area that was once occupied by the spongy mesophyll cells. The mycelium accumulated

in the substomatal cavity and conidiophores were produced from the mycelium through the stomata when adequate moisture was present on the leaf surface (Figure 3.2, f & Figure 3.3, h). Conidiophores bore numerous conidia. Additionally, hyphal growth could also be seen in the sclerenchyma cells and the epidermis, which were intact but deformed (Figure 3.2, f). The phloem tissue and spongy mesophyll cells completely collapsed and disintegrated, and chloroplasts were also completely broken down (Figure 3.2, f). The fungus only colonized the phloem after complete collapse of this tissue. TEM revealed that the hyphae had grown into a bundle sheath cell (Figure 3.4). The septal pore between two adjacent fungal cells was also visible. Contraction of the protoplasm and accumulation of starch granules is indicative of cell degradation (Van Asch, 1990).

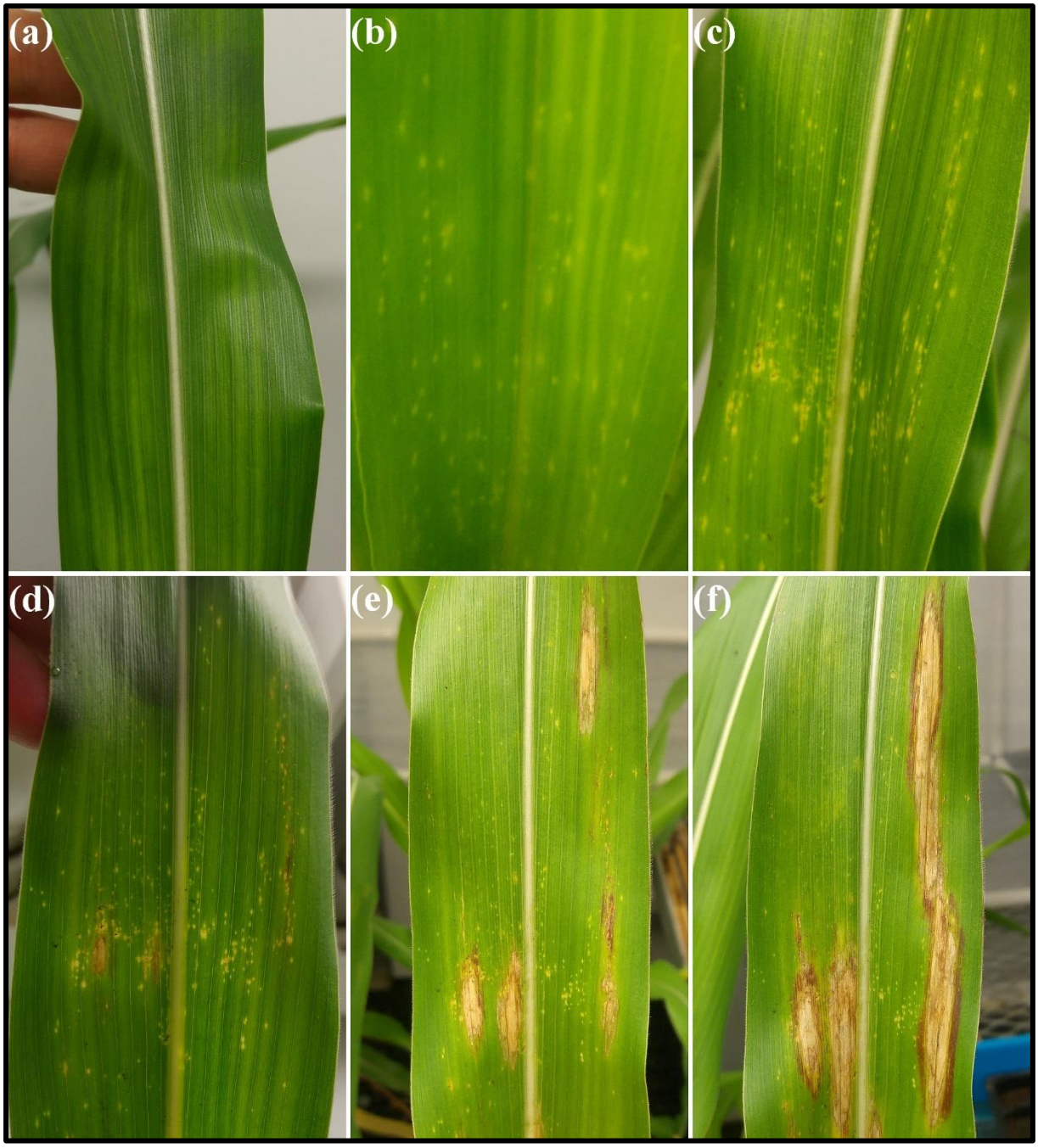

Figure 3.1. Visual progression of northern leaf blight caused by *Exserohilum turcicum* on B73 maize leaves. (a) Uninoculated leaf; (b) chlorotic flecks present (1 day post-inoculation, dpi); (c) chlorotic flecks start to enlarge (4 dpi); (d) lesions start to form (11 dpi); (e) lesions start to enlarge, forming distinct cigar-shaped lesions (14 dpi); (f) cigar-shaped lesions start to coalesce, killing large parts of leaf (18 dpi).

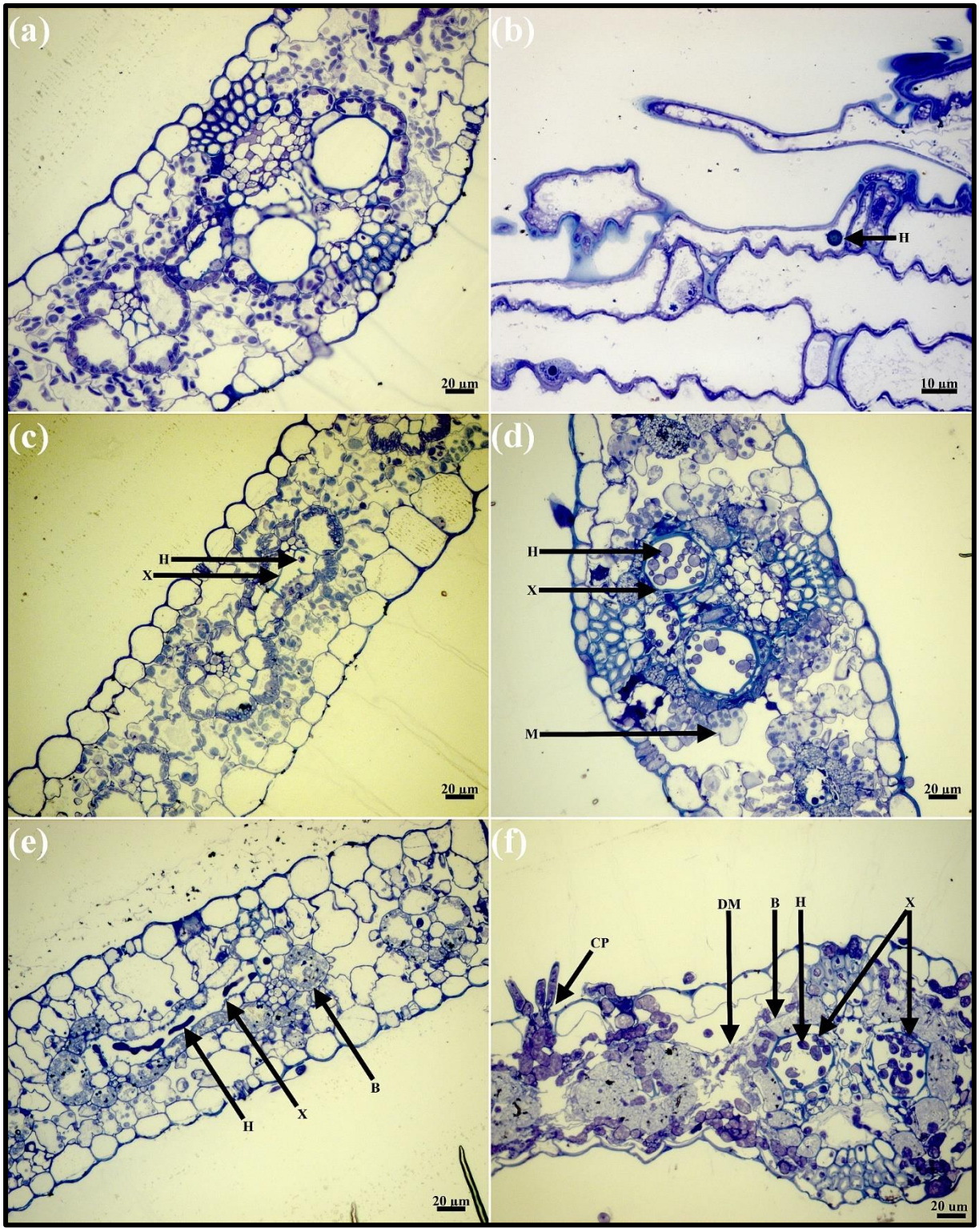

Figure 3.2. Light microscopy of B73 maize leaves during *Exserohilum turcicum* infection. (a) Uninoculated maize leaf showing a major vein with a minor vein in close proximity, intact spongy mesophyll cells, epidermis and bundle sheath cells are visible; (b) hyphal growth present in an epidermal cell (9 days post-inoculation, dpi); (c) hyphal growth present in a xylem vessel of one of the minor veins (11 dpi); (d) abundant hyphae present in the xylem vessel in

major and minor veins and shrinking and collapsing of spongy mesophyll cells is seen in close proximity of the major vein (14 dpi); (e) hypha present in a cross vein (14 dpi); (f) sporulating lesion stage showing complete tissue collapse with fungal growth in xylem, epidermis, bundles sheath cells and disintegrated spongy mesophyll cells (18 dpi). Hyphae have accumulated in the substomatal cavity from where conidiophores have formed through the stomata. (a, c–f) transverse sections; (b) paradermal section. B, bundle sheath cells; H, hypha; E, epidermal cell; X, xylem; M, spongy mesophyll cells; CP, conidiophores; DM, disintegrated spongy mesophyll cells.

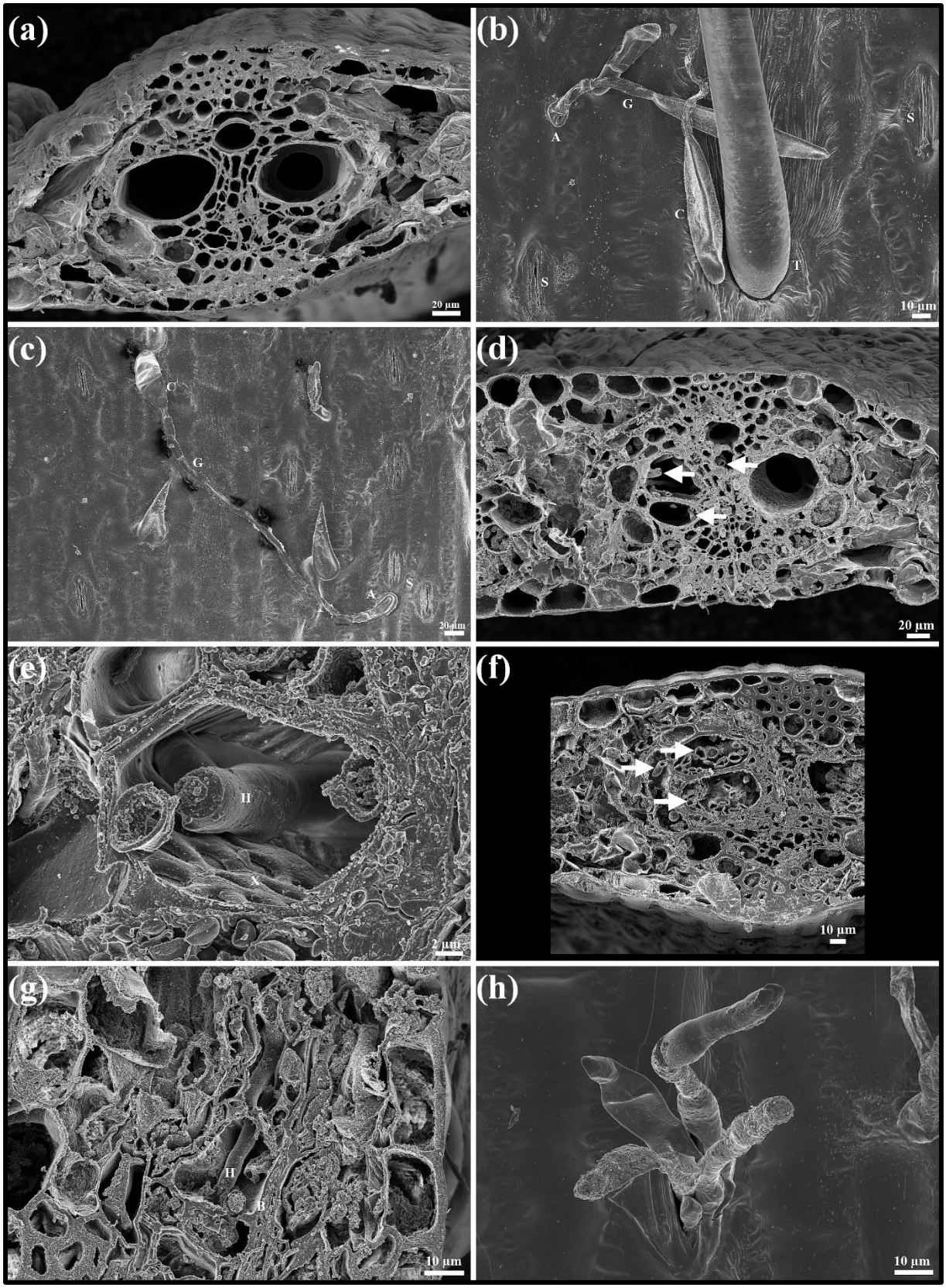

Figure 3.3. Scanning electron microscopy of B73 maize leaves during infection by *Exserohilum turcicum*. (a) Uninoculated maize leaf, transverse section of a major vein with intact cells; (b, c) a germinating conidium (C) with a germination tube (G) and appressorium

(A) in close proximity to a stomata (S) and a trichome (T) at 1 dpi; (d) hyphal growth (arrowed) in the xylem (11 dpi); (e) a single hypha growing through a xylem vessel (X), the lignified secondary cell wall is also present; (f) extensive plugging of the xylem with hyphae (arrowed; 14 dpi); (g) hyphal growth through two adjacent bundle sheath cells (B); (h) conidiophores emerging through a stomata.

Figure 3.4. Transmission electron micrograph of bundle sheath cell of a B73 maize leaf infected by *Exserohilum turcicum*. Hyphae (H) are present in the bundle sheath cell and the septum is intact with a septal pore (SP). Contraction of the protoplasm and the accumulation of starch granules (SG) indicate that the bundle sheath cell is degrading.

3.4. Discussion

In the present study, high-resolution SEM and TEM as well as LM microscopy were used to study the infection strategy of *E. turcicum* in maize. Studying the host–pathogen relationship between maize and *E. turcicum* contributes to knowledge of the pathogenicity of the fungus and may also assist in developing improved ways to prevent the disease in maize. In general, the histological observations made during this study are in agreement with those made by Jennings and Ullstrup (1957), Hilu and Hooker (1964), Hilu and Hooker (1965) and Knox-Davies (1974). However, this study employed technological advancements in microscopy techniques that allowed the researchers to improve observations and advance scientific understanding of the interaction between the host and pathogen. To the best of the researchers'

knowledge this work presents the first description of the infection process of *E. turcicum* with the use of electron microscopy.

Typical NLB disease progression was observed in this study. The lesions started to coalesce and mature, and distinct dark zones were seen that are associated with fungal sporulation (Klopper & Tweer, 2009). Hilu and Hooker (1964) reported that lesions developed during the first 6 days and greatly enlarged within 8 dpi, whereas, in the present study, lesions were not detected until 11 dpi. However, Jennings and Ullstrup (1957) noted only wilted areas after approximately 14 dpi.

Successful germination of conidia, germ tube growth and appressorium formation were observed on the infected maize leaves. This was in agreement with what has been described by Hilu and Hooker (1964), Jennings and Ullstrup (1957) and Knox-Davies (1974), with a few exceptions. Germ tubes of up to 300 µm in length were noted in this study, which is 150 µm longer than germ tube lengths reported by Hilu and Hooker (1964). Appressoria on average measured 12 × 22 µm in width, which is more than double the size of the 4 × 6 µm measurement recorded by Jennings and Ullstrup (1957). Because SEM was used to study the topography and fungal growth on the maize leaf surface, it is possible that more accurate measurements were achieved due to the larger surface areas studied than is possible with LM and TEM. Both Knox-Davies (1974) and Jennings and Ullstrup (1957) observed that the fungus could penetrate through stomata but preferentially entered the plant directly through the epidermal cells; however, in the present study, fungal penetration was only observed through the epidermis. Similarly, species of *Cochliobolus*, a closely related genus to *Exserohilum*, penetrate through the epidermal cell walls rather than through the stomata, although entrance through the stomata has been observed (Jennings & Ullstrup, 1957; Ohm *et al.*, 2012).

During the penetration stage, Knox-Davies (1974) noted the formation of an intracellular vesicle after the penetration peg penetrated the cuticle and epidermal cell wall. Vesicle formation in the epidermal cell was also seen by Hilu and Hooker (1964). The intracellular vesicle gave rise to a stout colonization hypha that extended into adjacent cells and resulted in intracellular growth (Knox-Davies, 1974). In the current study, fine infection hyphae were not observed in the epidermal cells but normal hyphae, which could also have been stout colonization hyphae (Knox-Davies, 1974), appeared to be visible in the epidermal cells at 9 dpi.

Both Jennings and Ullstrup (1957) and Hilu and Hooker (1964) reported that after the initial infection stage of the epidermal cells, hyphae grew intracellularly into spongy mesophyll cells towards the vascular bundle, penetrating the xylem vessels and tracheids. This is in contrast to the present study, where initial intracellular growth through the spongy mesophyll cells was not seen. This difference may have been because mature maize plants were infected in the current study as opposed to the seedlings used in previous investigations; thus, the fungus was able to grow intercellularly between the spongy mesophyll cells towards the vascular bundles because mature plants have more intercellular airspaces than seedlings. Hilu and Hooker (1964) observed that the hyphae entered the xylem at 2–3 dpi in susceptible lines and could grow throughout the xylem for 6–8 days without causing any deleterious effects on the cells. In the present study, hyphal growth was only seen in the xylem for the first time at 11 dpi when visible necrotic lesions started to form on the leaf.

Disease progression observed after 14 dpi in the current study was similar to reports by Jennings and Ullstrup (1957). In both studies it was observed that the xylem of minor veins was completely blocked and that major veins were 80–90% blocked. Both Jennings and Ullstrup (1957) and Hilu and Hooker (1964) reported that the width of the hyphae in the xylem tissue was 6–15 µm but in this study the width was found to be between 3–11 µm. This difference in width could be ascribed to the different isolates used as well as to the different maize varieties. Enlargement of the lesions was also observed at this time point and was probably due to the hyphae spreading through the cross veins, thus colonizing other parts of the leaf. Additionally, this could have contributed to the typical cigar-shaped lesions that characterize NLB. The collapsing and death of spongy mesophyll cells can be attributed to localized wilting and/or toxic compounds and/or cell wall-degrading enzymes (CWDE). The first cause of cell death could be due to mechanical plugging of the xylem with hyphae. Jennings and Ullstrup (1957) described NLB as a localized wilt disease because hyphae moved out of the xylem into moribund chlorenchyma tissue only after lesions formed. Hilu and Hooker (1964) agreed with these findings except that hyphae were observed to leave the xylem and grow into normal bundle sheath and mesophyll cells. In the present study, growth out of the xylem into living bundle sheath cells was also observed but no growth into living mesophyll cells was seen. Initially, the mesophyll cells showed no sign of injury but, after 24–48 h, cell death occurred and resulted in a wilt-type lesion (Hilu & Hooker, 1964).

The sudden death of cells can possibly be attributed to toxic compounds being released by the fungus. Cuq *et al.* (1993) reported that *E. turcicum* produces a phytotoxin, monocerin, that produced necrotic lesions (characteristic symptom of NLB) on maize leaves treated with the toxin. With *Cochliobolus carbonum* (*Helminthosporium carbonum*) and *Cochliobolus heterostrophus* (*Helminthosporium maydis*), host necrosis was seen with the invading hyphae in the mesophyll cells as opposed to *E. turcicum* where necrosis of the mesophyll cells was only seen after 11 dpi (Jennings & Ullstrup, 1957).

In the later stages of *E. turcicum* infection, and once mature lesions had formed on maize leaves, Hilu and Hooker (1964) observed complete collapse of all tissues with the exception of the epidermal cell layer. This is in contrast to observations in the present study where collapse of mesophyll cells, parenchyma cells of the vascular bundles and the phloem tissue was observed, but xylem tissue, bundle sheath cells and sclerenchyma cells remained intact despite being colonized with hyphae. Epidermal cells were also still intact and colonized but were deformed.

Overall, the anatomical and morphological differences that were seen between the current study and those of Jennings and Ullstrup (1957) and Hilu and Hooker (1964) can be attributed to differences in the virulence of the isolates that were used, the susceptibility of the maize line to the disease, the growth stage of plants and the environmental conditions that the plants were grown in.

A number of authors have suggested that *E. turcicum* exhibits a hemibiotrophic interaction with maize (Lim *et al.*, 1974; Leonard *et al.*, 1989; Chung *et al.*, 2010; Ohm *et al.*, 2012; Wu & Turgeon, 2013). This is based on observations of only limited damage in the host tissue during the early phase of infection and an extended incubation period with no visible symptoms before the development of necrotic lesions on the leaves in the later phases of infection. The results of this study further support the hemibiotrophic lifestyle of *E. turcicum*. This foliar pathogen of maize initially spends the first part of its lifestyle as a biotroph in the sense that it does not kill the host tissue. Initially, it grows as an epiphyte on the leaf surface, after which it penetrates the leaf epidermal cells and grows inter- and intracellularly towards the vascular bundles without killing cells, causing limited damage in the plant. It then switches to a necrotrophic lifestyle once it colonises the xylem tracheids and vessels, which leads to extensive plugging of the xylem, gradual death of the spongy mesophyll cells and the formation

of conidiophores through the stomata. Host tissue damage and necrosis are only seen during this phase and the fungus also exhibits accelerated growth. The death of cells during the necrotrophic phase of *E. turcicum* may be caused by a combination of localized wilt, toxins and CWDE; thus, additional studies need to be conducted to investigate whether or not toxins such as monocerin and CWDE are expressed and, if so, when they are expressed, as well as the interaction between localized wilting and toxin or CWDE.

The use of modern light and electron microscopy has enabled the authors to provide an updated assessment of the infection strategy of *E. turcicum* on maize. SEM revealed a number of newly observed features of fungal development, which included infection structures as well as the formation of conidiophores through the stomata. LM provided a detailed picture of how the fungus colonized the leaf once it penetrated the xylem tissue and also how it completed its life cycle in maize. TEM enabled visualization of the death of living cells at an ultrastructural level. Lastly, this study supports previous microscopic and macroscopic observations that *E. turcicum* follows a hemibiotrophic lifestyle and provides a good foundation for further research to characterize the host defence response to this foliar pathogen of maize.

3.5. Acknowledgements

The authors are extremely grateful to the Laboratory for Microscopy and Microanalysis of the University of Pretoria for the use of their equipment. The authors also want to thank A. Hall and Dr E. Venter for their valuable advice and help. The authors declare they have no conflicts of interest.

3.6. References

Agrios GN, 2005. *Plant Pathology*. San Diego, CA, USA: Elsevier Academic Press.

Beckman PM, Payne GA, 1982. External growth, penetration, and development of *Cercospora zeae-maydis* in corn leaves. *Phytopathology* **72**, 810-5.

Bentolila S, Guitton C, Bouvet N, Sailland A, Nykaza S, Freyssinet G, 1991. Identification of an RFLP marker tightly linked to the *Ht1* gene in maize. *Theoretical and Applied Genetics* **82**, 393-8.

Carson M, 1995. A new gene in maize conferring the "chlorotic halo" reaction to infection by *Exserohilum turcicum*. *Plant Disease* **79**, 717-20.

Chung CL, Longfellow JM, Walsh EK, *et al.*, 2010. Resistance loci affecting distinct stages of fungal pathogenesis: use of introgression lines for QTL mapping and characterization in the maize - *Setosphaeria turcica* pathosystem. *BMC Plant Biology* **10**, 103.

Craven M, Fourie AP, 2011. Field evaluation of maize inbred lines for resistance to *Exserohilum turcicum*. *South African Journal of Plant and Soil* **28**, 69-74.

Cuq F, Petitprez M, Herrmann-Gorline S, Klaebe A, Rossignol M, 1993. Monocerin in *Exserohilum turcicum* isolates from maize and a study of its phytotoxicity. *Phytochemistry* **34**, 1265-70.

Haasbroek MP, Craven M, Barnes I, Crampton BG, 2014. Microsatellite and mating type primers for the maize and sorghum pathogen, *Exserohilum turcicum*. *Australasian Plant Pathology* **43**, 577-81.

Hilu HM, Hooker AL, 1964. Host-pathogen relationship of *Helminthosporium turcicum* in resistant and susceptible corn seedlings. *Phytopathology* **54**, 570-5.

Hilu HM, Hooker AL, 1965. Localized infection by *Helminthosporium turcicum* on corn leaves. *Phytopathology* **55**, 189-92.

Jennings P, Ullstrup A, 1957. A histological study of 3 *Helminthosporium* leaf blights of corn. *Phytopathology* **47**, 707-14.

Klopper R, Tweer S, 2009. Northern corn leaf blight fact sheet. [http://www.pannar.com/assets/disease_fact_sheets/Northern_Corn_Leaf_Blight.pdf]. Accessed 11 November 2019.

Knox-Davies P, 1974. Penetration of maize leaves by *Helminthosporium turcicum*. *Phytopathology* **64**, 1468-70.

Lee C, 2011. Corn growth stages and growing degree days: A quick reference guide. [http://www2.ca.uky.edu/agcomm/pubs/agr/agr202/agr202.pdf]. Accessed 18 June 2018.

Leonard KJ, Levy Y, Smith DR, 1989. Proposed nomenclature for pathogenic races of *Exserohilum turcicum* on corn. *Plant Disease* **73**, 776-7.

Leonard KJ, Suggs EG, 1974. *Setosphaeria prolata*, the ascigerous state of *Exserohilum prolatum*. *Mycologia* **66**, 281-97.

Levy Y, Cohen Y, 1983a. Biotic and environmental factors affecting infection of sweet corn with *Exserohilum turcicum*. *Phytopathology* **73**, 722-5.

Levy Y, Cohen Y, 1983b. Differential effect of light on spore germination of *Exserohilum turcicum* on corn leaves and corn leaf impressions. *Phytopathology* **73**, 249-52.

Lim SM, Kinsey JG, Hooker AL, 1974. Inheritance of virulence in *Helminthosporium turcicum* to monogenic resistant corn. *Phytopathology* **64**, 1150-1.

Luttrell E, 1964. Systematics of *Helminthosporium* and related genera. *Mycologia* **56**, 119-32.

Ohm RA, Feau N, Henrissat B, *et al.*, 2012. Diverse lifestyles and strategies of plant pathogenesis encoded in the genomes of eighteen Dothideomycetes fungi. *PLOS Pathogens* **8**, e1003037.

Perkins J, Pedersen W, 1987. Disease development and yield losses associated with northern leaf blight on corn. *Plant Disease* **71**, 940-3.

Sivanesan A, 1987. Graminicolous species of *Bipolaris, Curvularia, Drechslera, Exserohilum* and their teleomorphs. *Mycological Papers* **158**, 1-261.

Van Asch MAJ, 1990. *Studies on the resistance of wheat and maize to fungal patogenesis*. Pietermaritzburg, University of Natal, PhD thesis.

Van der Merwe C, Peacock J, 1999. Enhancing conductivity of biological material for SEM. *Microscopy Society of Southern Africa Proceedings* **29**, 44.

White DG, 1999. *Compendium of corn diseases*. APS press St. Paul, MN.

Wise K, 2011. *Diseases of Corn: Northern Corn Leaf Blight*. [https://www.extension.purdue.edu/extmedia/BP/BP-84-W.pdf]. 14 November 2019.

Wu D, Turgeon BG, 2013. *Setosphaeria rostrata*: Insights from the sequenced genome of *Setosphaeria turcica*. *Fungal Genetics and Biology* **61**, 158-63.

Chapter 4: Expression analysis of pathogenesis-related protein genes in maize in response to *Exserohilum turcicum* infection and monocerin infiltration

Abstract

Pathogenesis-related (PR) proteins are one of the defence mechanisms plants use in response to fungal infections such as *Exserohilum turcicum*, which is the causal agent of northern leaf blight (NLB) in maize. *Exserohilum turcicum* produces monocerin, a phytotoxic secondary metabolite, which could aid the fungus in causing disease. The aim of this study was to elucidate whether expression of PR protein genes is induced upon infection with *E. turcicum* infection as well in response to monocerin infiltration. Fungus infected maize leaf material was harvested at 0, 4, 9, and 14 days post-inoculation (dpi) and monocerin infiltrated material at 0, 24 and 48 hours post-infiltration (hpi). Expression analysis of PR protein genes were examined using maize leaf cDNA. *PR-1* (antifungal), *PR-2* (β-1,3-glucanase), *PR-3* (chitinase) gene expression were highly induced by the fungus whereas *PR-10* (ribonuclease-like) was only induced at a very low level. Expression of three PR protein genes was induced by monocerin after 24 hpi except for *PR-1*, the expression of which was not significantly different from its control. The expression of all four PR protein genes was lower after 48 hpi than at 24 hpi but was also induced by the solvent control (SC) and wounded control (WC) indicating that these controls do have an effect on the expression of PR protein genes. The expression of the PR protein genes was higher in the fungal infected tissue compared to the monocerin treated tissue indicating that monocerin probably affects other defence genes or exerts its toxicity at some other cellular level. The results of this study yield additional insights into the host response of maize to *E. turcicum* and suggest that its toxin, monocerin, did elicit a defence response in maize by inducing PR protein gene expression albeit at a lower level than the fungus.

Keywords: *Exserohilum turcicum*, gene expression, maize, monocerin, northern leaf blight, pathogenesis-related proteins, RT-qPCR

4.1. Introduction

Northern leaf blight (NLB) is an economically important foliar disease of maize throughout the world. The disease has been associated with yield losses of between 15–30% but can be as high as 75% in ideal conditions (Klopper & Tweer, 2009). The causal agent of NLB is the hemibiotrophic fungus *Exserohilum turcicum* (sexual stage *Setosphaeria turcica*, syn. *Helminthosporium turcicum*) (Leonard & Suggs, 1974). *Exserohilum turcicum* produces a secondary metabolite, monocerin, a phytotoxic polyketide metabolite, which possibly aids the fungus in causing disease in maize (Aldridge & Turner, 1970; Robeson & Strobel, 1982; Cuq *et al.*, 1993). Numerous methods to control the disease including deep ploughing, crop rotation, resistant maize cultivars and applying fungicides, exist. Unfortunately, the fungus has the ability to form new races that can overcome existing resistance in maize lines as well as to become resistant to fungicides (Klopper & Tweer, 2009; Wise, 2011). There is thus a continuous drive to develop new strategies in controlling this disease in maize. These include developing new fungicides and breeding new maize lines involving the plant's natural defences against pathogens such as the upregulation of pathogenesis-related (PR) proteins.

Pathogenesis-related proteins are one of many mechanisms that plants use to protect themselves in response to various abiotic and biotic threats such as wounding, drought, cold and pathogen invasion, which includes bacterial, viral and fungal attacks (Bowles, 1990; Agrios, 2005). The production of PR proteins occurs in both healthy and infected cells as opposed to phytoalexins, which are only produced in healthy cells surrounding localised damaged and necrotic cells (van Loon *et al.*, 2006; Ebrahim *et al.*, 2011). The production of PR proteins in healthy cells can prevent the affected plant from further infection (Ebrahim *et al.*, 2011). Pathogenesis-related proteins can either inhibit pathogens with their antimicrobial properties or by regulating expression of genes involved in the host defence, or both (Majumdar *et al.*, 2017). Pathogenesis-related proteins have various functions including hydrolases, protease inhibitors and transcription factors (Scherer *et al.*, 2005). Overall, PR proteins are low molecular weight molecules of between 6–43 kDa, stable at low pH, thermostable and resistant to proteases, which enable them to survive the harsh environment they occur in such as the vacuoles, cell wall or intracellular spaces (Niki *et al.*, 1998; Ebrahim *et al.*, 2011). The majority of PR proteins are induced through signalling compounds such as salicylic acid (SA), jasmonic acid (JA) and ethylene (van Loon & van Strien, 1999; Miyamoto *et al.*, 2012; Manghwar *et al.*, 2018). Salicylic acid is involved in inducing the expression of *PR-1, PR-2* and *PR-5* genes

whereas JA has been reported to induce chitinases (*PR-3, PR-4, PR-8 and PR-11*) and *PR-13* (Uknes *et al.*, 1992; Morris *et al.*, 1998; Sels *et al.*, 2008; Miyamoto *et al.*, 2012; Manghwar *et al.*, 2018).

To date, 17 PR protein families have been identified according to their function and properties, and include an antifungal protein (PR-1), β–1,3–glucanase (PR-2), chitinases (PR-3, PR-4, PR-8, PR-11), thaumatin-like proteins (PR-5), proteinases (PR-6, PR-7), peroxidase (PR-9), RNase (PR-10), defensin (PR-12), thionin (PR-13), lipid-transfer protein (PR-14) oxalate-oxidases (PR-15, PR-16), while the function of PR-17 is still unknown (van Loon & van Strien, 1999; van Loon *et al.*, 2006). Pathogenesis-related proteins which have been associated with fungal infection and/or mycotoxin production include PR-1, PR-2, PR-3, PR-5 and PR-10 (Jondle *et al.*, 1989; Stone *et al.*, 2000; Sekhon *et al.*, 2006; Chen *et al.*, 2010; Galeana-Sánchez *et al.*, 2017; Manghwar *et al.*, 2018). The role of the PR-1 family is still poorly understood but it is one of the PR proteins that is most abundantly produced during a fungal attack (Breen *et al.*, 2017). It is known that PR-1 has antifungal properties and recent reports have indicated that it has sterol binding activity, harbours a defence signalling peptide and is targeted by plant pathogens during infection (Breen *et al.*, 2017). The PR-2 family consists of the β-1,3-glucanases, which catalyse the hydrolytic cleavage of β-1,3-glucosidic linkages in β-1,3-glucans (Xie *et al.*, 2015). PR-3 is responsible for the hydrolytic breakdown of chitin. Both chitin and β-1,3-glucanase are important structural components of fungal cell walls of many pathogenic fungi (Li *et al.*, 2001). PR10 has been reported to have ribonuclease activity and its gene expression has been reported to be induced by fungal infection (Bantignies *et al.*, 2000; Chen *et al.*, 2010).

Numerous phytotoxins produced by phytopathogenic fungi have been reported to induce PR proteins directly or affect pathways such as SA or JA pathways, which in turn induce PR proteins. Fumonisin B_1, a programmed cell death eliciting mycotoxin, produced by various *Fusarium* species such as *Fusarium verticillioides*, is capable of inducing the expression of *PR-1*, *PR-2* and *PR-5* genes in *Arabidopsis* plants (Stone *et al.*, 2000). Additionally, the activity of β-1,3-glucanase (*PR-2*) in germinating maize embryos is also inhibited by fumonisin B_1 (Galeana-Sánchez *et al.*, 2017). *Fusarium verticillioides* and moniliformin, the phytotoxin it produces, elicit a host response by inducing the expression of *PR-4* (chitinases) in germinating maize embryos (Bravo *et al.*, 2003). The well-known mycotoxin family, the trichothecenes, which include deoxynivalenol and T-2 toxin, induced the expression of *PR-1* in *Arabidopsis*

leaves. Thus, the expression of PR protein genes is not only induced by fungal pathogens, but often also by their respective phytotoxins (Nishiuchi *et al.*, 2006). This study was designed to evaluate whether or not *E. turcicum* infection and monocerin infiltration elicit a defence response in maize, particularly the expression of PR protein genes. It was hypothesised that the expression PR protein genes are induced in maize in response to *E. turcicum* infection and monocerin infiltration. These results will contribute to our understanding of the response of maize to *E. turcicum* and monocerin as well as whether monocerin could aid the fungus in causing disease.

4.2. Materials and methods

4.2.1. Materials

All the reagents used in this study were purchased from Merck (Modderfontein, South Africa) unless otherwise stated. Primers were synthesised by Integrated DNA Technologies (IDT) (Coralville, USA) and sequencing of primer amplicons was performed by the DNA Sanger Sequencing Facility, Faculty of Natural and Agricultural Sciences, University of Pretoria, Pretoria, South Africa.

4.2.2. Monocerin preparation

Pure monocerin (10 mg) was obtained from Cfm Oskar Tropitzsch GmbH (Marktredwitz, Germany). Methanol (20 ml) was added to the freeze dried monocerin, which upon resuspension, was aliquoted into 1 ml volumes in 20 vials (0.5 mg per vial). The methanol was dried down at room temperature and the vials were stored -20°C until use.

4.2.3. Plant material

Maize plants of the inbred line B73 (susceptible to NLB) (Craven & Fourie, 2011) were grown in plastic seedlings cones containing a soil mixture consisting of one part potting soil (Culterra, Nietgedacht, South Africa) and one part silica sand (Rolfes Silica, Brits, South Africa). The plants were maintained in a growth room with temperatures ranging between 20 to 25°C, with a relative humidity (RH) of between 50 and 100% during the day and night, and a photoperiod

of 16 h. The plants were watered every second day until runoff and were fertilised twice (20 and 30 days after planting) with Nitrosol Organiksol (Fleuron, Johannesburg, South Africa).

4.2.4. Fungal strain, culture condition and inoculum preparation

Exserohilum turcicum isolate 2 (race 23N) was isolated from NLB lesion on maize leaves and identified as isolate 2 by means of a single multiplex polymerase chain reaction (PCR) assay described by Haasbroek *et al.* (2014), whereafter it was maintained and prepared for inoculation of maize plants as described in Chapter 3, Section 3.2.1. The concentration of the conidial suspension was adjusted to 1×10^5 spores/ml prior to inoculation.

4.2.5. Maize inoculation and infiltration

Maize plants (approximately 29 days old) at the V6 growth stage were inoculated by adding 1 ml of a conidial suspension into the whorl of each plant. The inoculated plants were then incubated for 12 h in a growth room at 20°C with 100% RH in the dark. Monocerin was prepared for infiltration by adding pure monocerin to 40% methanol to yield a concentration of 1 mM monocerin. Maize plants at the same growth stage as the inoculation study were infiltrated with 50 µl of a 1 mM monocerin solution. A monocerin solution of 1 mM was used since Cuq *et al.* (1993) reported that the phytotoxic effect of monocerin plateaued at 1 mM monocerin in a maize leaf detached essay. This was performed by nicking the adaxial surface of a fully expanded leaf with a needle and pressure infiltrating the monocerin solution using 1 ml syringe into the wounded surface (Swanson *et al.*, 1988). The infiltration was done on both sides of the midrib, with four infiltration sites per side and thus eight sites per leaf (Figure 4.1). The same procedure was followed for the solvent control (SC) in which the leaf was only infiltrated with 40% methanol and for the wounded control (WC) where the leaves were only nicked. After the inoculation and infiltration, plants were maintained under the same growth conditions as before the treatments. A third control which consisted of uninoculated and non-infiltrated maize leaves, was included.

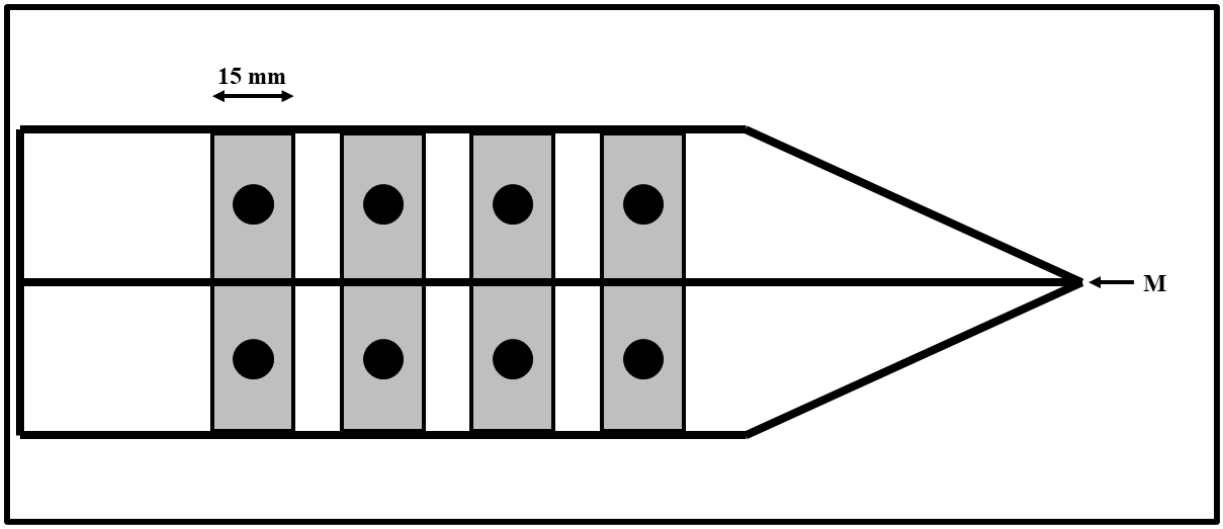

Figure 4.1. Diagrammatic representation of monocerin infiltration sites in a maize leaf. For each treatment or control, there were four infiltration sites on each side of the midrib (M) of the leaf, making a total of eight infiltrated sites, per leaf.

Diseased leaves were harvested at 4, 9 and 14 days post-inoculation (dpi) whereas, for the monocerin treatment, leaves were harvested at 24 and 48 hours post infiltration (hpi). The control tissue was harvested 0 dpi/hpi and the wounded control and solvent control at 24 hai. One diseased or healthy leaf per plant was harvested for the inoculated leaves or the untreated control, respectively. For the monocerin infiltrated leaves, leaf segments were cut into strips of 15 mm wide, which included the lesions (Figure 4.1). All the segments in a biological replicate were pooled together. The same was done for the wounded and solvent controls. Each treatment or control consisted of three biological replicates, with each biological replicate comprised of three plants, which were pooled for downstream analysis. Harvested leaf material was immediately flash-frozen in liquid nitrogen (N_2) and stored at -80°C until used. In total 24 samples were obtained for downstream analysis.

4.2.6. RNA isolation

Total RNA was isolated from all the frozen samples using the InviTrap Spin Plant RNA Mini Kit (Stratec, Berlin, Germany) according to the manufacturer's protocol. Approximately, 100 mg of plant material was ground to a fine powder in liquid nitrogen with the aid of a mortar and pestle and used for the RNA isolations. The RNA was eluted in 30 µl elution Buffer R whereafter the concentration and quality were determined using a Nano Drop 2000 spectrophotometer (Thermo Fisher Scientific, Carlsbad, USA). The integrity of the RNA was assessed by adding 2.5 µl 2X RNA loading dye (New England BioLabs, Ipswich, USA) to 5 µl

RNA, incubated at 65°C for 7 min whereafter the RNA was electrophorized on 2% sodium borate (5.24 mM) agarose gel at 200 V for 30 min.

The RNA samples were treated with deoxyribonuclease (DNase) to remove unwanted genomic DNA. DNase digestion was performed using Turbo DNase (Thermo Fisher Scientific) according to the manufacturer's instructions. A single reaction consisted of 4200 ng RNA, 0.3 µl 10X Turbo DNase buffer and 2 µl Turbo DNase enzyme to obtain a final volume of 35 µl. The samples were then incubated at 37°C for 30 min and the reactions were stopped by, in each case, the addition of 6 µl DNase inactivation reagent, whereafter the samples were incubated for an additional five minutes at 25°C. The samples were then centrifuged at 10 000 g for 90 sec and the supernatant was removed and stored at -80°C until used.

4.2.7. cDNA synthesis

Complementary DNA (cDNA) was synthesised from extracted total mRNA samples, free of DNA, using the Maxima First Strand cDNA Synthesis kit (Thermo Fisher Scientific) following the manufacturer's instructions. A single reaction consisted of 4 µl 5X reaction mix, 2 µl Maxima enzyme mix, 1270 ng RNA and nuclease-free water made up to obtain a final volume of 20 µl. This was done for all 24 samples. The samples were then incubated for 10 min at 25°C and 30 min at 50°C. The reaction was terminated by incubating the samples at 85°C for 5 min. The samples were aliquoted and stored at -80°C until used.

4.2.8. RT-qPCR primer design

Gene-specific primers were selected to test the expression of five PR protein genes which included *PR-1* (Zm00001d018738), *PR-2* (Zm00001d042143), *PR-3* (Zm00001d043988), and *PR-10* (Zm00001d028816) and three references genes *rpol* (Zm00001d012857), *srl* (Zm00001d006480) and *gst3* (Zm00001d042216). When primer sequences were not found from literature, gene-specific primers were designed using IDT's PrimerQuest Tool (https://eu.idtdna.com/Primerquest) and assessed with Net Primer (www.premierbiosoft.com) for internal secondary structures. Primers were designed to adhere to MIQE guidelines (Bustin *et al.*, 2009; Taylor *et al.*, 2010) for RT-qPCR expression studies. Where possible, primers were designed to amplify either a part of a single exon or exon-exon boundary and to the 3' end of the gene. After primers were designed, the Basic Local Alignment Search Tool

(BLAST) was applied to compare the primer sequences against the maize genome (http://ensembl.gramene.org/Tools/Blast) to ensure that the primers were gene-specific and did not target non-specific targets. Primer sequences and associated information are summarised in Table 4.1.

Table 4.1. A summary of the primer sequences and descriptive information of the maize genes analysed with RT-qPCR. All the primer sequences were designed in this study except *srl*. *PR-2* was the only gene whose amplicon differed in size depending on whether it was amplified from cDNA or gDNA and thus could be used to test for gDNA contamination

Gene name (in this study)	Gene target	Synonym name	Reference gene transcript ID	References	Primer sequences 5"-3'	Tm	Amplicon size	
							cDNA	gDNA
rpol	DNA-directed RNA polymerases II IV and V subunit 8B		Zm00001d012857_T001	BG Crampton (pers. Comm)	F: CTCGCAGTGAGCAGTTAGATATG	60°C	111	
					R: CCAAATTCAGAGTAGGCGCTATAA	60°C		
srl	Serine/arginine-rich splicing factor SR45a		Zm00001d006480_T010	BG Crampton (pers. Comm)	F: ACACGCCATTGTTCGAGA	60°C	117	
					R: CAGGTTCGGGTGAACTTTG	60°C		
gst3	Glutathione S-transferase 4	Glutathione S-transferase 3	Zm00001d042216_T001	(Korsman *et al.*, 2011)	F: GGTTGGTCTTTGCATATCCTACTA	60°C	89	
					R: GAAGAAGGGAATTACGGTGAAGA	60°C		
PR-1	Pathogenesis related protein 4	PR-4, PR1-F/R , prp4	Zm00001d018738_T001	(Morris *et al.*, 1998)	F: TGGGTGTCCGAGAAGCAG	60°C	137	
					R: GCGTTGTTGTCGCAGACG	60°C		
PR-2	Glucan endo-13-beta-glucosidase homolog 1	PRm 6b, beta 1,3 glucanase	Zm00001d042143_T001	(Wu *et al.*, 1994; Manghwar *et al.*, 2018)	F: CATTCGCAGCCATTCCTACAG	60°C	120	210
					R: TCAGGTTGATGCCGTTGG	60°C		
PR-3	Chitinase chem5	PRm3, CHEM 5	Zm00001d043988_T001	BG Crampton (pers. Comm)	F: CTGACGGGCACGGTGAT	60°C	120	
					R: TCAGACGCTGCCCTTCAC	60°C		
PR-10	Pathogenesis-related protein 10	PR1, PR10,1, prp6, Pathogenesis-related protein6	Zm00001d028816_T001	(Xie *et al.*, 2010)	F: GTAACAGCAGCCCGATCTT	60°C	141	
					R: GAGGCGATCTCAACAGTCC	60°C		

The cDNA sequences for each gene were obtained from Gramene (http://www.gramene.org/) using their reference gene transcript ID.

4.2.9. Sequencing of cDNA amplicons

Sequencing of each amplicon was done to determine that each primer set was gene-specific and did not bind to non-specific targets. The amplicons to be sequenced were first amplified from maize cDNA through conventional PCR reactions with a gene-specific primer set and subsequently analysed on a 2% sodium borate agarose gel (Brody & Kern, 2004). If these amplicons were specific (single band on the gel) and of the correct size, the PCR reactions were cleaned up with ExoSAP-IT (Thermo Fisher Scientific) according to manufacturer's instructions and used in subsequent sequencing reactions. A single 12 µl sequencing reaction consisted of 1.2 µl BigDye Terminator v3.1 ready reaction mix (Thermo Fisher Scientific), 1.8 µl BigDye Terminator v3.1 5X sequencing buffer (Thermo Fisher Scientific), 1.2 µl of either forward or reverse primer (10 µM) and 7.8 µl clean-up product as template. Cycle conditions consisted of an initial denaturing step of 1 min at 96°C, followed by 25 cycles, each comprising of 96°C for 10 sec, 58°C for 10 sec and 60°C for 4 min. The sequence reactions were cleaned using sodium acetate/ethanol precipitation of DNA. Forward and reverse sequencing reactions for each amplicon were run on an ABI3500xl (Thermo Fisher Scientific) sequencer. Sequenced amplicons were analysed and aligned using CLC Main Workbench 8.0 (Aarhus, Denmark) (Appendix, Table 7.1)

4.2.10. Expression analysis of PR and reference genes

Prior to RT-qPCR analysis of PR proteins, all reactions were optimised using conventional PCR. Reverse transcription-qPCR analysis of the PR protein genes (*PR-1*, *PR-2*, *PR-3*, and *PR-10*) and three reference genes *rpol*, *srl* and *gst3* were performed using the Bio-Rad CFX Connect Real-Time PCR Detection System (Hercules, California, USA). Expression of the genes was measured in three biological repeats with each biological repeat performed in triplicate at all data points as outlined in Section 4.2.5. Each 10 µl reaction comprised of 5 µl RealQ Plus 2x Master Mix Green (Ampliqon, Odense, Denmark), 0.32 µl forward primer (10 µM), 0.32 µl reverse primer (10 µM), 3.36 µl sterile distilled water and 1 µl cDNA (1:25 dilution) or water for the non-template controls. The cycling conditions consisted of an initial denaturing step of 15 min at 95°C, followed by 40 cycles of amplification and quantification, each comprising of 95°C for 10 sec, 60°C for 10 sec and 72°C for 10 sec with a single fluorescence measurement at the end of each elongation step. A melting curve analysis was performed at the end of each run to measure amplification specificity. A standard curve was

set up for each gene tested using seven dilution points ($2x10^{-1}$, $1x10^{-1}$, $2x10^{-2}$, $1x10^{-2}$, $4x10^{-3}$, $2x10^{-3}$, $1x10^{-3}$) containing pooled cDNA of all the samples tested. Gene expression data of all the genes were analysed using Bio-Rad CFX manager and qBASE^{PLUS} with geNorm (Biogazelle, Ghent, Brussels). The relative expression values of the PR protein genes was normalised by means of dividing the relative input cDNA (extrapolated from the respective standard curves) of the PR protein genes by the geomean input reference cDNA of the reference genes *rpol*, *srl* and *gst3* for each sample (Vandesompele *et al.*, 2002; Hellemans *et al.*, 2007).

4.2.11. Statistical analysis

Statistical analysis of all the relative expression data was performed using GraphPad Prism version 4.03 (GraphPad Prism Software, San Diego, California, USA). A one-way analysis of variance (ANOVA) was performed, followed by a Tukey's multiple comparison test with the level statistical significance measured at $p < 0.05$.

4.3. Results

4.3.1. Maize trial (infection and infiltration)

Infection of maize leaves with *E. turcicum* and subsequent disease progression was similar to what was observed in Chapter 3, Section 3.3. The non-infected or control leaves exhibited no visible NLB infection and were healthy overall (Figure 4.2, a). Chlorotic spots were visible at 4 dpi (Figure 4.2, b), turning necrotic at 9 dpi (Figure 4.2, c) whereafter the lesions started to enlarge and elongate forming the distinct cigar shape lesions by which the disease is characterised at 14 dpi (Figure 4.2, d).

Figure 4.2. NLB disease symptoms developed on B73 maize leaves following inoculation with the conidia of *E. turcicum*. (a) Uninoculated leaf (control leaf); (b) Chlorotic spots formed (4 dpi); (c) chlorotic spots turned necrotic (9 dpi); (d) distinct cigar shape lesion was visible and lesions were beginning to coalesce (14 dpi).

Maize leaves were infiltrated with a 1 mM monocerin solution, and further evaluated at 24 and 48 hpi. It was challenging to infiltrate the leaves with the full 1 ml volume of monocerin since the solution did not spread beyond the major vascular bundles which were roughly 5 mm apart but did spread lengthwise since there were no physical obstructions to the solution's movement. At 24 hpi small necrotic lesions that were whitish in colour were observed on the leaves where the leaf surface was nicked and infiltrated with the solution (Figure 4.3, b). After 48 hpi, the lesions were slightly enlarged in size compared to the lesions at 24 hpi (Figure 4.3, b, c). The non-infiltrated control was the same as the infection controls; in other words, healthy tissue that was not mechanically wounded and harvested at 0 dpi/hpi (Figure 4.3, a). For the SC, the leaves were infiltrated with 40% methanol at the same time as the monocerin infiltration. Tissue damage was seen where the leaf was nicked with a syringe needle with a small area around the wound becoming chlorotic (Figure 4.3, d). Tissue damage was only observed where the leaf was wounded with a syringe needle in the WC (Figure 4.3, e).

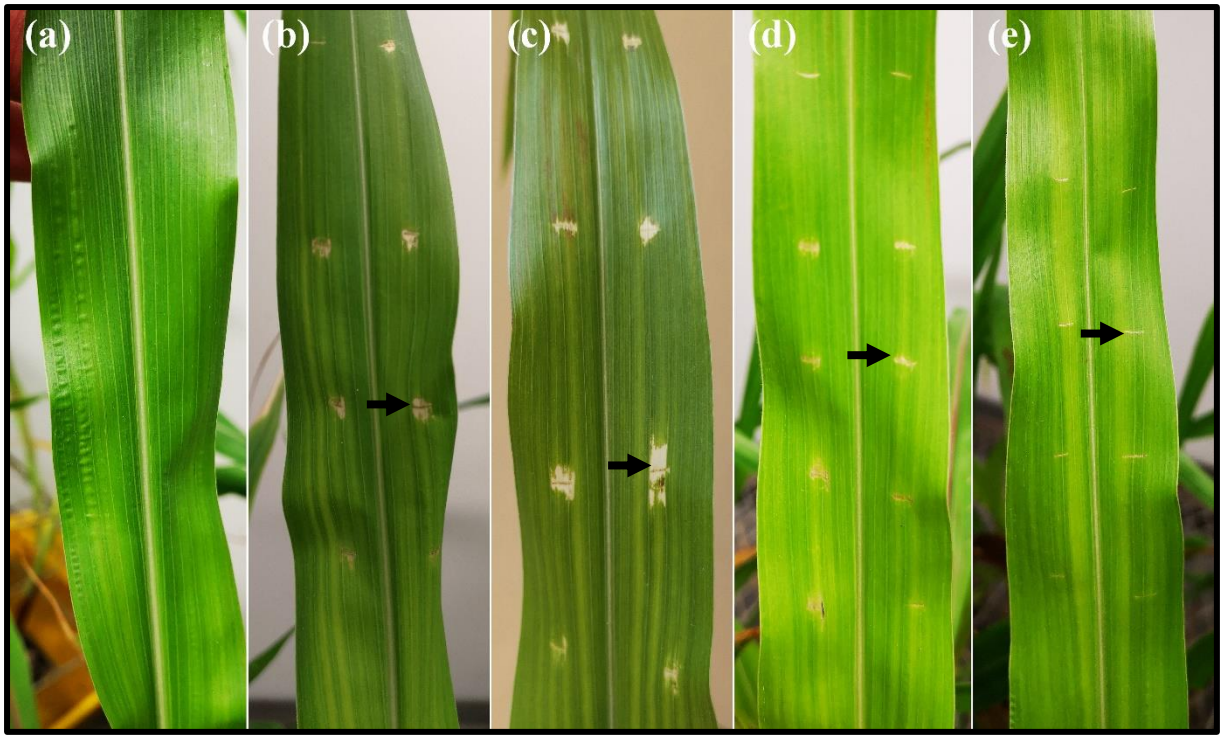

Figure 4.3. Visual progression of lesions forming on maize leaves after infiltration with 1 mM pure monocerin. (a) non-infiltrated leaf (control leaf); (b) necrotic lesions visible 24 hpi with 1 mM monocerin (c) necrotic lesions enlarged in size after 48 hpi with 1 mM monocerin; (d) small necrotic lesions formed as a result of 40% methanol infiltration (SC, 24 hpi); tissue damage as a result of mechanical wounding with a syringe needle (WC; 24 hpi). (Arrows indicate where the lesions/wounding occurred).

4.3.2. RNA isolation and cDNA synthesis

Total RNA was extracted from three biological replicates of each treatment and control during the fungus infection trial and the monocerin infiltration trial. The concentration and quality of all the RNA samples were determined spectrophotometrically. The RNA isolated from all samples ranged from 143.3 to 305.3 ng/µl. The A_{260}/A_{280} and A_{260}/A_{230} absorbance ratios were used as purity indices to determine the quality of the RNA samples. All of the samples had A_{260}/A_{280} ratios between 2.0–2.2 whereas the majority of the samples had A_{260}/A_{230} ratios of between 1.8–2.2. Lower A_{260}/A_{230} values indicated that samples could potentially have carbohydrates or phenolic compounds in them (Kumar *et al.*, 2007). The integrity of the RNA was further analysed through gel electrophoresis on a sodium borate gel. The integrity and quality of the RNA were assessed by inspection of the 28S rRNA and 18S rRNA bands on the agarose gel. Visible and intact bands were seen for all samples and indicated good quality RNA (Figure 4.4). Total RNA was used in cDNA synthesis.

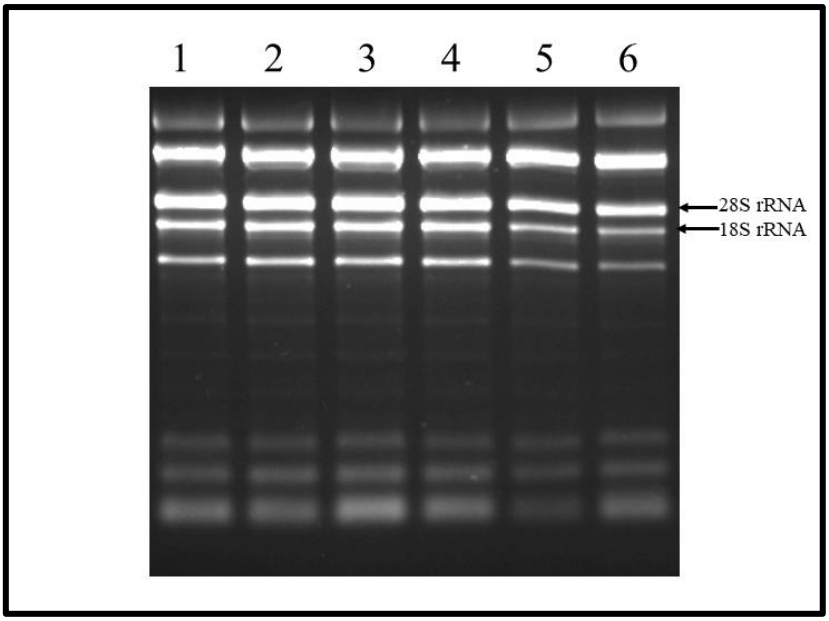

Figure 4.4. The RNA quality was assessed by sodium borate agarose gel electrophoresis of total RNA isolated from maize leaves. Good quality RNA with intact 28S and 18S rRNA bands was seen for all samples. Lanes 1–3 represent the three biological replicates of the solvent control and lanes 4–6 the three biological replicates of the wounded control (only selected samples included in this image).

4.3.3. Choice of pathogenesis related genes for RT-qPCR

The PR proteins selected for this study were all previously shown to be associated with fungal infection in plants and where applicable, also their associated mycotoxins (Wu *et al.*, 1994; Morris *et al.*, 1998; Stone *et al.*, 2000; Xie *et al.*, 2010; Manghwar *et al.*, 2018). Some of the PR proteins have also been classified into new PR groups such as with PR-1 (Table 4.1). With the latest annotation of the maize genome (B73 RefGen_v4), PR-1 has been reclassified as PR-4 (Jiao *et al.*, 2017). The same was seen with the reference gene *gst3* which was reclassified as *gst4*. Although PR-3 was reclassified as Chitinase chem5, it still comprises one of the numerous classes of chitinase of PR-3 (van Loon *et al.*, 2006; Sels *et al.*, 2008). For the ease of comparing and discussing the results in this study the original names have been used.

4.3.4. Expression analysis of PR protein and reference genes

Amplification of the PR protein (*PR-1*, *PR-2*, *PR-3* and *PR-10*) and reference (*rpol*, *srl* and *gst3*) genes by RT-qPCR was undertaken in order to assess whether the expression PR protein genes is induced by *E. turcicum* infection and monocerin infiltration in maize leaves. Reverse transcription-qPCR was performed across all samples, with each sample comprising of three

biological replicates with three technical replicates each. Combined, the three reference genes had an average gene stability value (M) of 0.759 and a pairwise variation value (CV) of 0.304 (Table 4.2). The geomean of the three reference genes for each sample was used to normalise the expression data of the PR genes.

Table 4.2. GeNorm references gene stability analysis of *rpol, srl* and *gst3*. Combined the three genes had an M value of 0.759 and a CV value of 0.304.

Reference target	M	CV
rpol	0.726	0.259
srl	0.807	0.352
gst3	0.743	0.301
Average	**0.759**	**0.304**

Following RT-qPCR amplification of PR and references genes, a melt curve analysis was performed to confirm that only single homogenous cDNA was amplified with each primer set and that primer dimers were absent (Appendix, Figure 7.3). The *PR-2* primer set was designed to amplify from cDNA as well as gDNA, with the gDNA amplicon being bigger in size as compared to the cDNA amplicon size (Table 4.1). This is due to the fact that the forward and reverse primers for *PR-2* span an intron and thus, with gDNA, the intron is not spliced out and hence the bigger amplicon product. Only a single peak was observed for amplification from the *PR-2* primer set thus indicating that the cDNA for all samples was free of gDNA. Standard curves were generated for each PR and reference gene using pooled cDNA of all the samples to determine amplification efficiency (slope of the curve) as well as R^2 (correlation coefficient) values of the RT-qPCR reactions (Appendix, Figure 7.4). The efficiency values ranged between 90% and 110% and an $R^2 > 0.98$ was obtained for all samples and thus data adheres to MIQE requirements (Taylor *et al.*, 2010). The only exception was *PR-3* which had an amplification efficiency of 87% but had an R^2 of 0.9951.

The expression values of *PR-1, PR-2, PR-3* and *PR-10* were determined at each sample point during NLB disease development (Figure 4.5). The expression of each gene was measured at all four sample points during the infection of maize with *E. turcicum*. All four PR genes showed extremely low to almost no expression in the control sample point whereas at 4 dpi and 9 dpi the expression of PR protein genes was induced albeit at a low expression level that was not significantly different to the control expression levels (Figure 4.5). At 14 dpi, all four PR protein genes were highly expressed and were significantly different from the control, 4 dpi

and 9 dpi (Figure 4.5). At 14 dpi the expression of *PR-1*, *PR-2*, *PR-3* and *PR-10* genes were over 1409, 3246, 189 and 33 fold higher, respectively, when compared to each PR gene control gene expression (Figure 4.5). It seems that the fungus is suppressing or evading the plants host defence mechanism by some means, during the initial infection up to 9 dpi, since the expression of all the PR genes was low at 4 and 9 dpi whereas at 14 dpi the PR gene was greatly induced. At 14 dpi the fungus had already caused extensive damage. The expression levels of *PR-10* was substantially lower compared to the other three PR genes indicating that fungal infection does not have a big effect on inducing its gene expression.

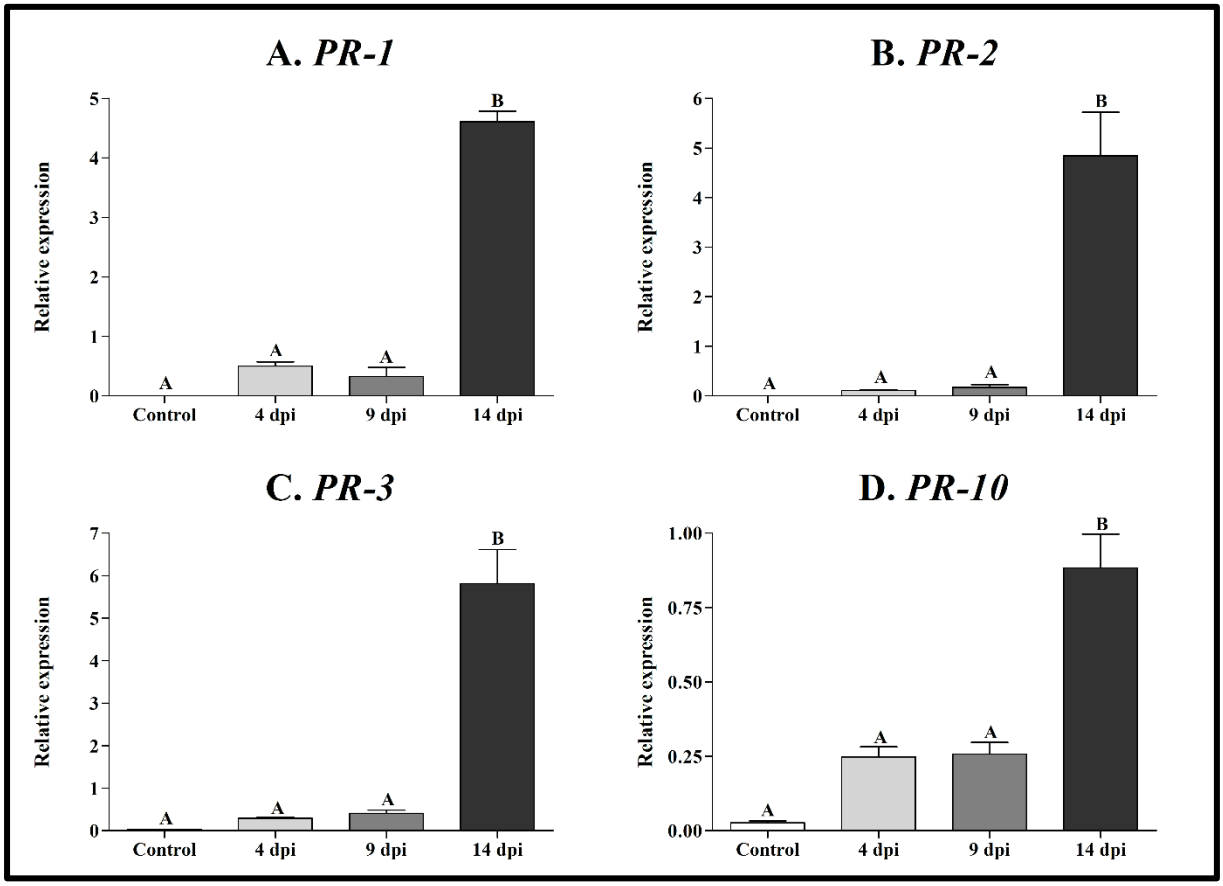

Figure 4.5. Normalised gene expression profiles of *PR-1* (a), *PR-2* (b), *PR-3* (c) and *PR-10* (d) during *E. turcicum* infection in maize leaves. The average relative expression was calculated for each PR protein gene during the infection of maize with *E. turcicum*. Sample points included control (0 dpi), 4 dpi (chlorotic spots), 9 dpi (necrotic spots) and 14 dpi (cigar shape lesions). Each PR protein gene relative expression values were normalised by dividing the relative input cDNA of the PR protein gene by the geomean input reference cDNA of the three reference genes (*rpol, srl* and *gst3*). Statistical analysis of the relative expression data was done using a one-way ANOVA analysis followed Tukey's Multiple Comparison Test. Sample points not designated with the same letter are significantly different (P<0.05). Error bars indicate the standard error of mean.

The same procedure was applied to examine PR gene expression during monocerin infiltration in maize leaves. Since pure monocerin was dissolved in 40% methanol, a solvent control (40% methanol) was included. In addition to the SC, a wounded control was included since mechanical wounding can also have an effect on the expression of certain PR genes (Schweizer *et al.*, 1998; Bravo *et al.*, 2003; Liu *et al.*, 2003). Monocerin and/or the solvent and/or wounding (Figure 4.6) had little effect on inducing the expression of all four PR genes when compared to expression of these genes during fungal infection at 14 dpi except for *PR-10* (Figure 4.5). It appears that the toxin and/or solvent and /or mechanical wounding had a greater effect on inducing the expression of *PR-10* gene than what the fungus had.

The expression levels of all four PR genes of the control in the monocerin infiltration, was negligible as it was the same control used as in the fungal infection. Monocerin induced the expression of all four PR genes at 24 hpi when compared to the control tissue (Figure 4.6). The only exception was *PR-1,* which was induced by monocerin but was not significantly different. The increase at 24 hpi for *PR-1, PR-2, PR-3* and *PR-10* was 115, 344, 24 and 83 fold, respectively, and for 48 hpi 84, 119, 12 and 71 fold, respectively, when both sample points were compared to the control. The effect the toxin had on the expression of all four PR genes was higher at 24 hpi than at 48 hpi. Additionally, the SC also induced the expression level of the PR proteins genes. The expression levels were lower compared to the 24 hpi monocerin treated tissue except for *PR-1* where SC expression values were higher than 24 hpi sample point but were not significantly different. Mechanically wounding the maize leaves did induce the expression of the PR genes but expression was not significantly different compared to the monocerin treated sample points. The low gene expression levels seen in Figure 4.6 suggest that monocerin does not have that great effect on inducing a PR gene host response in maize as compared to the high PR protein gene expression levels observed during fungal infection.

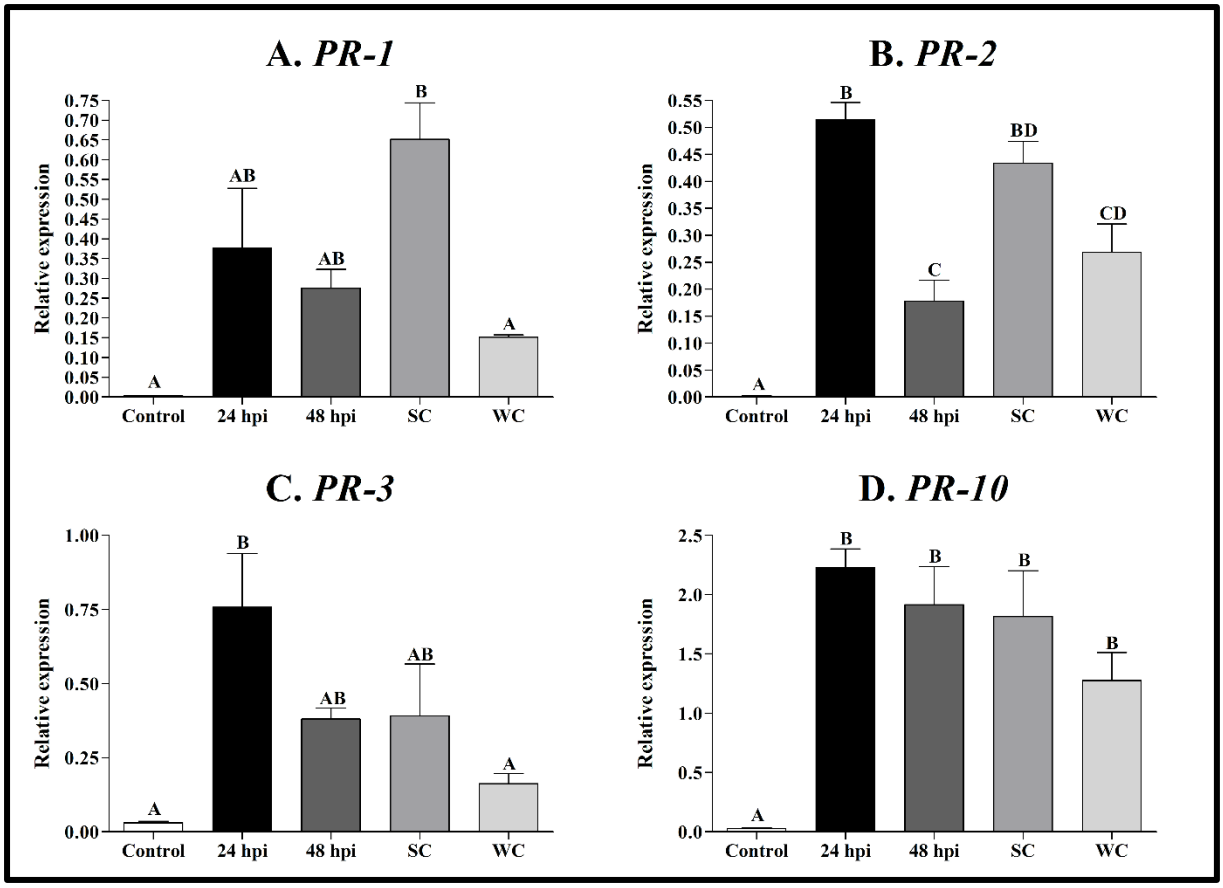

Figure 4.6. Normalised gene expression profiles of *PR-1* (a), *PR-2* (b), *PR-3* (c) and *PR-10* (d) during infiltration of maize leaves with monocerin. The average relative expression was calculated for each PR protein gene during the infiltration of maize leaves with monocerin. Sample points consisted of a control (0 hpi), 24 hpi, 48 hpi, solvent (SC) and wounded control (WC). Each PR protein gene relative expression values were normalised by dividing the relative input cDNA of the PR protein gene by the geomean input reference cDNA of the three reference genes (*rpol*, *srl* and *gst3*). The standard error of mean bars is included in the graphs. Statistical analysis of the relative expression data was done using a one-way ANOVA analysis followed Tukey's Multiple Comparison Test. Sample points not designated with the same letter are significantly different ($P<0.05$). Error bars indicate the standard error of mean.

4.4. Discussion

Once a fungus has established contact with the plant, elicitors are produced and released by the pathogen or the plant itself (Wiesel *et al.*, 2014). This in turns induces further defences such as cell wall reinforcement, phytoalexin production and synthesis of PR proteins. Pathogenesis-related proteins play a major role in defence of plants against these pathogens due to the vast properties of the different PR proteins (Scherer *et al.*, 2005). These PR proteins are found in all parts of the plant including the roots, stems, leaves and floral organs (van Loon *et al.*, 2006). In this study, it was determined whether *E. turcicum* and/or its toxin monocerin elicits a defence

response in maize by inducing the expression of PR proteins, *PR-1, PR-2, PR-3* and *PR-10* genes. The PR proteins chosen in this study have previously been associated with fungal pathogens and/or their associated mycotoxins that they produce (Morris *et al.*, 1998; Xie *et al.*, 2010; Manghwar *et al.*, 2018).

Typical NLB disease progression was observed in maize and correspond to what was observed in previous experiments (Chapter 3, Section 3.3). Maize leaves that were infiltrated with pure monocerin had small necrotic lesions at 24 hpi, which then slightly enlarged after 48 hpi. Cuq *et al.* (1993) reported the same effect on maize leaves when crude monocerin extracts were applied on leaves that had been punctured with a pin. The method of application of monocerin to the leaves used in this study differs to that of Cuq *et al.* (1993). In this study monocerin was infiltrated with a syringe and the leaves were attached whereas in the study by Cuq *et al.* (1993) monocerin was applied as a droplet on the wound and the leaves were detached from the plant. The toxin could have a bleaching effect (removal of chlorophyll) of some kind on the leaf or could kill all the cells in the area surrounding infiltration. The tissue that was treated with methanol (SC) had lesions but these were small and more chlorotic in nature compared to the necrotic lesions caused by monocerin. The mechanical wounding of the leaf surface with a syringe needle did not have any effect on lesion formation except for minimal cell necrosis where the leaf was physically damaged.

From the results presented in this chapter it is clear that the expression of all four PR genes were induced by the *E. turcicum*. All four PR genes were most induced at 14 dpi when the fungus was in its necrotrophic phase and was in the process of completing its life cycle (Kotze *et al.*, 2019). A hemibiotroph (biotrophic phase) initially has to actively suppress the host immune responses, allowing the invasive hyphae to spread throughout infected tissue as well as protecting itself against the plant's defence mechanisms (de Jonge *et al.*, 2011; Koeck *et al.*, 2011). This is followed by the necrotrophic phase during which cell wall degrading enzymes, reactive oxygen species or phytotoxins are released to induce host cell death allowing the fungus to complete its life cycle (Horbach *et al.*, 2011; Koeck *et al.*, 2011). The plant's immune response is actively suppressed or altered by fungal effectors which are secreted into the plant apoplast or cytosol during the biotrophic phase of hemibiotrophs (Koeck *et al.*, 2011). Many fungal effectors have been characterised which include the *Avr* (avirulence) and *Ecp* (extracellular proteins) family of effectors which bind to chitin and thus prevent the plant host defence recognition (Stergiopoulos & de Wit, 2009; Koeck *et al.*, 2011). The overall low

expression of the PR genes at the earlier sample points observed in this study could possibly be due to the fungal effectors that were suppressing the plants host defence. The increase in the expression of PR genes at later sample points (14 dpi) can possonly be contributed to either or both fungal and plant elicitors. Both fungal pathogens and their hosts (plants) have the ability to secrete enzymes (e.g. chitinases, cellulases) that can attack and breakdown each other's cells walls and degrade them into their basic buildings blocks (Wiesel *et al.*, 2014). These building blocks in turn elicit a defence response in the plant. Fungal pathogens such as *Fusarium* spp. produce trichothecenes family phytotoxins that can also elicit a defence response in its host (Nishiuchi *et al.*, 2006).

The function of PR-1 is still poorly understood but it is known to be antifungal in nature or plays a role in host defence signalling and cell death (van Loon *et al.*, 2006). The PR-1 family is a dominant group of PR proteins, is induced by fungal pathogens and SA and is often used as a marker in systemic acquired response (SAR) (van Loon *et al.*, 2006). The expression of *PR-1* is a good indicator of a defence response in maize towards fungal pathogens such as *Bipolaris maydis*¸ *Puccinia sorghi*, *E. turcicum*, *Colletotrichum graminicola* and *Fusarium verticillioides* (Morris *et al.*, 1998; Maschietto *et al.*, 2016; Miranda *et al.*, 2017). It is also one of the most abundantly produced proteins in plants in response to fungal attacks (Breen *et al.*, 2016). Additionally it has been reported that PR-1 could also have a sterol binding activity but the link between sterol binding activity and antimicrobial function remains unclear (Breen *et al.*, 2017). Another PR protein whose functions is relatively unknown is PR-10. It has been reported that PR-10 has antifungal properties but is more known for its ribonuclease activity (Bantignies *et al.*, 2000; Chen *et al.*, 2006). Xie *et al.* (2010) reported that the expression of *PR-10* gene was induced by *Aspergillus flavus* as well as the bacterial pathogen *Erwinia stewartia*. Additionally, *PR-10* was also induced by *B. maydis* (maize pathogen) and the *Colletotrichum sublineola* (sorghum pathogen) (Lo *et al.*, 1999). The expression of *PR-10* gene was induced by *E. turcicum* albeit at a low level compared to the other PR genes. *PR-10* could possibly also be used as indicator of a defence response in plants against fungal pathogens since it is induced by numerous fungal species.

The functions of PR-2 and PR-3 have been well studied in plants in response to fungal pathogens. The PR-*2* family consists of β-1,3-glucanase which hydrolyses β-1,3-linked glucan polymers whereas the PR-3 family consists of endochitinases that catalyses the cleavage β-1,4 bonds in chitin polymers making the fungus more sensitive to osmotic stress (Li *et al.*, 2001;

Laluk & Mengiste, 2010; Ebrahim *et al.*, 2011; Xie *et al.*, 2015). Both β-1,3-glucan and chitin together with mannoproteins are important structural components of fungal cells (Wiesel *et al.*, 2014). The structural components of fungal cell walls can elicit a host defence response in plants but the fungus releases effectors such as *Avr* and *Ecp* (Stergiopoulos & de Wit, 2009). Both *Avr* and *Ecp* can bind to these structural components which suppresses the host defence response or protects the fungus physically due to less chitin and β-1,3-glucan being available to elicit a response (Stergiopoulos & de Wit, 2009; de Jonge *et al.*, 2011). As a result of this the fungus evades the defence response of the host during the biotrophic phase until it has colonised the host and switched over to is necrotrophic phase (de Jonge *et al.*, 2011). The low gene expression of PR proteins during the biotrophic phase could be contributed to fungal effectors and healthy plant cells, which prevents the elucidation of the defence response of the plant. Both PR protein genes' expression was induced at high levels at 14 dpi when the fungus was the most prevalent in the leaf tissue (Kotze *et al.*, 2019). As with fungal cell walls, plant cell walls are composed of cellulose, hemicellulose, pectic polysaccharides and lignin which are broken down by fungal pathogens into β-glucans, xylose, and phenylpropanoid-containing compounds (Wiesel *et al.*, 2014). These break down products can act as plant based elicitors by eliciting a defence response in plants (Wiesel *et al.*, 2014). Fungal cell wall degrading enzymes, phytotoxins and/or fragments formed from cell wall degradation could also elicit a host defence response (Horbach *et al.*, 2011).

In addition, to determine whether the fungus elicits a host response in maize with a focus on PR protein gene expression, the phytotoxic effects of pure monocerin was also investigated. Monocerin indeed induces expression of PR protein genes although at a lower level when compared to the fungus. The only exception was with *PR-10* which was induced at a higher level when compared to fungal infection at the same sample point The SC also induced expression of PR genes and thus a more appropriate solvent should be used in future studies. Nishiuchi *et al.* (2006) reported on the elicitor like activity of trichothecenes in *Arabidopsis thaliana* leaves. The authors indicated that *PR-1* gene expression was induced by trichothecenes between 24 hpi to 72 hpi and was the highest at 48 hpi when compared to the control. In this study *PR-1* gene expression was the highest at 24 hpi whereafter it started to decline and thus the phytotoxic effects of monocerin on PR gene expression were induced faster when compared to trichothecenes. Nishiuchi *et al.* (2006) unfortunately did not indicate the level at which *PR-1* was expressed. These authors used ethanol as a control ethanol which did not have an effect the expression of *PR-1*. Stone *et al.* (2000) studied the effect of different

concentrations of fumonisin B_1 (FB_1) on *Arabidopsis* seedlings on PR proteins. The expression of *PR-1*, *PR-2* and *PR-5* increased with increasing concentrations of FB_1 with 1 mM FB_1 having the greatest effect on the PR proteins. However, Stone *et al.* (2000) did not test the effect of the solvent on the PR proteins. Both of these studies evaluated the effect of the fungal pathogens (which produce these toxins) on the expression of PR protein genes. Both of these mycotoxins (FB_1 & trichothecenes) are comparable to the effects of monocerin seen in this study as they produced similar PR protein gene expression results. Monocerin only induced the expression of PR protein genes at a fraction of the levels that the fungus did. It could be that monocerin is a necrotrophic effector (NE) which could target a specific protein and thus aid the fungus in causing disease.

Hemibiotrophs initially produce effectors such as *Avr4* and *Ecp6* to evade the host defence response by suppressing cell death in the host (Vleeshouwers & Oliver, 2014). At the later stages of infection these genes are downregulated while other NE's are upregulated (Vleeshouwers & Oliver, 2014). It is assumed that NE's usually induce cell death which results in extra nutrients for the fungus but it is possible that cell death results in less anti-fungal radicals or compounds that affect fungal growth as well as being a signal for sporulation (Vleeshouwers & Oliver, 2014). Necrotrophic effectors can be of polyketide, non-ribosomal peptide (NRPS) or protein origin. Vleeshouwers and Oliver (2014) state that the mode of action of NE's involves interaction and not always direct binding with a dominant host gene. T-toxin, which is produced by *B. maydis*, targets the mitochondrial protein t-URF13, which results in alterations to the membrane resulting in the death of the mitochondria (Vleeshouwers & Oliver, 2014). *Didymella maydis* produces PM-toxin which targets the same protein as T-toxin (Stergiopoulos *et al.*, 2013). The mode of action of HC-toxin produced by *Cochliobolus carbonum*, is that it targets histone-deacetylases which results in the repression of gene expression (Stergiopoulos *et al.*, 2013). PtrToxA and PtrToxB produced by *Pyrenophora tritici-repentis* reacts with ToxA binding protein 1 in the chloroplast which results in loss of chlorophyll and the disorganization of thylakoids (Manning *et al.*, 2009). It could be that monocerin does not illicit a host defence response by inducing PR protein gene expression, but rather acts as a NE that targets a specific protein such as ToxA binding protein 1 in the chloroplast or the mitochondrial protein t-URF13.

4.5. Conclusion

The maize host defence response was induced by the *E. turcicum* through an increase in the expression of PR protein genes but was expressed at a much lower level when the leaf tissue was infiltrated with pure monocerin. These genes could then be used as expression markers in breeding studies thus eliminating the use of transgenic plants. It could be that monocerin also exerts its phytotoxic effect on cell organelles such as the mitochondria, chloroplast of plasma membrane, for example. Additionally, monocerin could also be a NE that targets a specific gene as T-toxin does with the mitochondrial protein, t-URF13. Aspects that should be considered in the future studies would include using a different solvent which does not have a toxic effect on maize cells and doing a transcriptomic study to determine what proteins monocerin could possibly target.

4.6. References

Agrios GN, 2005. *Plant Pathology*. San Diego, CA, USA: Elsevier Academic Press.

Aldridge DC, Turner WB, 1970. Metabolites of *Helminthosporium monoceras:* Structures of monocerin and related benzopyrans. *Journal of the Chemical Society C: Organic* **18**, 2598-600.

Bantignies B, Séguin J, Muzac I, Dédaldéchamp F, Gulick P, Ibrahim R, 2000. Direct evidence for ribonucleolytic activity of a PR-10-like protein from white lupin roots. *Plant Molecular Biology* **42**, 871-81.

Bowles DJ, 1990. Defense-related proteins in higher plants. *Annual Review of Biochemistry* **59**, 873-907.

Bravo JM, Campo S, Murillo I, Coca M, San Segundo B, 2003. Fungus- and wound-induced accumulation of mRNA containing a class II chitinase of the pathogenesis-related protein 4 (PR-4) family of maize. *Plant Molecular Biology* **52**, 745-59.

Breen S, Williams SJ, Outram M, Kobe B, Solomon PS, 2017. Emerging Insights into the Functions of Pathogenesis-Related Protein 1. *Trends in Plant Science* **22**, 871-9.

Breen S, Williams SJ, Winterberg B, Kobe B, Solomon PS, 2016. Wheat PR-1 proteins are targeted by necrotrophic pathogen effector proteins. *The Plant Journal* **88**, 13-25.

Brody JR, Kern SE, 2004. Sodium boric acid: a Tris-free, cooler conductive medium for DNA electrophoresis. *Biotechniques* **36**, 214-6.

Bustin SA, Benes V, Garson JA, *et al.*, 2009. The MIQE guidelines: Minimum information for publication of quantitative real-time PCR experiments. *Clinical Chemistry* **55**, 611-22.

Chen ZY, Brown RL, Damann KE, Cleveland TE, 2010. PR10 expression in maize and its effect on host resistance against *Aspergillus flavus* infection and aflatoxin production. *Molecular Plant Pathology* **11**, 69-81.

Chen ZY, Brown RL, Rajasekaran K, Damann KE, Cleveland TE, 2006. Identification of a Maize Kernel Pathogenesis-Related Protein and Evidence for Its Involvement in Resistance to *Aspergillus flavus* Infection and Aflatoxin Production. *Phytopathology* **96**, 87-95.

Craven M, Fourie AP, 2011. Field evaluation of maize inbred lines for resistance to *Exserohilum turcicum*. *South African Journal of Plant and Soil* **28**, 69-74.

Cuq F, Petitprez M, Herrmann-Gorline S, Klaebe A, Rossignol M, 1993. Monocerin in *Exserohilum turcicum* isolates from maize and a study of its phytotoxicity. *Phytochemistry* **34**, 1265-70.

de Jonge R, Bolton MD, Thomma BP, 2011. How filamentous pathogens co-opt plants: the ins and outs of fungal effectors. *Current Opinion in Plant Biology* **14**, 400-6.

Ebrahim S, Usha K, Singh B, 2011. Pathogenesis related (PR) proteins in plant defense mechanism. *Science Against Microbial Pathogens* **2**, 1043-54.

Galeana-Sánchez E, Sánchez-Rangel D, de la Torre-Hernández ME, Nájera-Martínez M, Ramos-Villegas P, Plasencia J, 2017. Fumonisin B_1 produced in planta by *Fusarium verticillioides* is associated with inhibition of maize β-1,3-glucanase activity and increased aggressiveness. *Physiological and Molecular Plant Pathology* **100**, 75-83.

Haasbroek MP, Craven M, Barnes I, Crampton BG, 2014. Microsatellite and mating type primers for the maize and sorghum pathogen, *Exserohilum turcicum*. *Australasian Plant Pathology* **43**, 577-81.

Hellemans J, Mortier G, De Paepe A, Speleman F, Vandesompele J, 2007. qBase relative quantification framework and software for management and automated analysis of real-time quantitative PCR data. *Genome Biology* **8**, R19.

Horbach R, Navarro-Quesada AR, Knogge W, Deising HB, 2011. When and how to kill a plant cell: Infection strategies of plant pathogenic fungi. *Journal of Plant Physiology* **168**, 51-62.

Jiao Y, Peluso P, Shi J, *et al.*, 2017. Improved maize reference genome with single-molecule technologies. *Nature* **546**, 524.

Jondle DJ, Coors JG, Duke SH, 1989. Maize leaf β-1,3-glucanase activity in relation to resistance to *Exserohilum turcicum*. *Canadian Journal of Botany* **67**, 263-6.

Klopper R, Tweer S, 2009. Northern corn leaf blight fact sheet. [http://www.pannar.com/assets/disease_fact_sheets/Northern_Corn_Leaf_Blight.pdf]. Accessed 11 November 2019.

Koeck M, Hardham AR, Dodds PN, 2011. The role of effectors of biotrophic and hemibiotrophic fungi in infection. *Cell Microbiology* **13**, 1849-57.

Korsman J, Meisel B, Kloppers FJ, Crampton BG, Berger DK, 2011. Quantitative phenotyping of grey leaf spot disease in maize using real-time PCR. *European Journal of Plant Pathology* **133**, 461-71.

Kotze RG, van der Merwe CF, Crampton BG, Kritzinger Q, 2019. A histological assessment of the infection strategy of *Exserohilum turcicum* in maize. *Plant Pathology* **68**, 504-12.

Kumar GN, Iyer S, Knowles NR, 2007. Extraction of RNA from fresh, frozen, and lyophilized tuber and root tissues. *Journal of agricultural and food chemistry* **55**, 1674-8.

Laluk K, Mengiste T, 2010. Necrotroph attacks on plants: wanton destruction or covert extortion? *The arabidopsis book* **8**, e0136-e.

Leonard KJ, Suggs EG, 1974. *Setosphaeria prolata*, the ascigerous state of *Exserohilum prolatum*. *Mycologia* **66**, 281-97.

Li WL, Faris JD, Muthukrishnan S, Liu DJ, Chen PD, Gill BS, 2001. Isolation and characterization of novel cDNA clones of acidic chitinases and β-1,3-glucanases from wheat spikes infected by *Fusarium graminearum*. *Theoretical and Applied Genetics* **102**, 353-62.

Liu J-J, Ekramoddoullah AKM, Yu X, 2003. Differential expression of multiple PR10 proteins in western white pine following wounding, fungal infection and cold-hardening. *Physiologia Plantarum* **119**, 544-53.

Lo SC, Hipskind JD, Nicholson RL, 1999. cDNA cloning of a sorghum pathogenesis-related protein (PR-10) and differential expression of defense-related genes following inoculation with

Cochliobolus heterostrophus or *Colletotrichum sublineolum*. *Molecular Plant-Microbe Interactions* **12**, 479-89.

Majumdar R, Rajasekaran K, Sickler C, *et al.*, 2017. The Pathogenesis-Related Maize Seed (*PRms*) Gene Plays a Role in Resistance to *Aspergillus flavus* Infection and Aflatoxin Contamination. *Frontiers in Plant Science* **8**, 1758.

Manghwar H, Hussain A, Ullah A, *et al.*, 2018. Expression analysis of defense related genes in wheat and maize against *Bipolaris sorokiniana*. *Physiological and Molecular Plant Pathology* **103**, 36-46.

Manning VA, Chu AL, Steeves JE, Wolpert TJ, Ciuffetti LM, 2009. A host-selective toxin of Pyrenophora tritici-repentis, Ptr ToxA, induces photosystem changes and reactive oxygen species accumulation in sensitive wheat. *Molecular Plant-Microbe Interactions* **22**, 665-76.

Maschietto V, Lanubile A, Leonardis SD, Marocco A, Paciolla C, 2016. Constitutive expression of pathogenesis-related proteins and antioxydant enzyme activities triggers maize resistance towards *Fusarium verticillioides*. *Journal of Plant Physiology* **200**, 53-61.

Miranda VJ, Porto WF, Fernandes GDR, *et al.*, 2017. Comparative transcriptomic analysis indicates genes associated with local and systemic resistance to *Colletotrichum graminicola* in maize. *Scientific Reports* **7**, 2483.

Miyamoto K, Shimizu T, Lin F, *et al.*, 2012. Identification of an E-box motif responsible for the expression of jasmonic acid-induced chitinase gene *OsChia4a* in rice. *Journal of Plant Physiology* **169**, 621-7.

Morris SW, Vernooij B, Titatarn S, *et al.*, 1998. Induced resistance responses in maize. *Molecular Plant-Microbe Interactions* **11**, 643-58.

Niki T, Mitsuhara I, Seo S, Ohtsubo N, Ohashi Y, 1998. Antagonistic effect of salicylic acid and jasmonic acid on the expression of pathogenesis-related (PR) protein genes in wounded mature tobacco leaves. *Plant and Cell Physiology* **39**, 500-7.

Nishiuchi T, Masuda D, Nakashita H, *et al.*, 2006. Fusarium phytotoxin trichothecenes have an elicitor-like activity in *Arabidopsis thaliana*, but the activity differed significantly among their molecular species. *Molecular Plant-Microbe Interactions* **19**, 512-20.

Robeson DJ, Strobel GA, 1982. Monocerin, a phytotoxin from *Exserohilum turcicum* (= *Drechslera turcica*). *Agricultural and Biological Chemistry* **46**, 2681-3.

Scherer NM, Thompson CE, Freitas LB, Bonatto SL, Salzano FM, 2005. Patterns of molecular evolution in pathogenesis-related proteins. *Genetics and Molecular Biology* **28**, 645-53.

Schweizer P, Buchala A, Dudler R, Métraux JP, 1998. Induced systemic resistance in wounded rice plants. *The Plant Journal* **14**, 475-81.

Sekhon RS, Kuldau G, Mansfield M, Chopra S, 2006. Characterization of *Fusarium*-induced expression of flavonoids and PR genes in maize. *Physiological and Molecular Plant Pathology* **69**, 109-17.

Sels J, Mathys J, De Coninck BM, Cammue BP, De Bolle MF, 2008. Plant pathogenesis-related (PR) proteins: a focus on PR peptides. *Plant Physiology Biochemistry* **46**, 941-50.

Stergiopoulos I, Collemare J, Mehrabi R, De Wit PJ, 2013. Phytotoxic secondary metabolites and peptides produced by plant pathogenic Dothideomycete fungi. *FEMS Microbiology Reviews* **37**, 67-93.

Stergiopoulos I, de Wit PJ, 2009. Fungal effector proteins. *Annual Review of Phytopathology* **47**, 233-63.

Stone JM, Heard JE, Asai T, Ausubel FM, 2000. Simulation of fungal-mediated cell death by fumonisin B1 and selection of fumonisin B1-resistant (*fbr*) *Arabidopsis* mutants. *The Plant Cell Online* **12**, 1811-22.

Swanson J, Kearney B, Dahlbeck D, Staskawicz B, 1988. Cloned avirulence gene of *Xanthomonas campestris* pv. *vesicatoria* complements spontaneous race-change mutants. *Molecular Plant-Microbe Interactions* **1**, 5-9.

Taylor S, Wakem M, Dijkman G, Alsarraj M, Nguyen M, 2010. A practical approach to RT-qPCR-Publishing data that conform to the MIQE guidelines. *Methods* **50**, S1-5.

Uknes S, Mauch-Mani B, Moyer M, *et al.*, 1992. Acquired resistance in *Arabidopsis*. *Plant Cell* **4**, 645-56.

van Loon LC, Rep M, Pieterse CM, 2006. Significance of inducible defense-related proteins in infected plants. *Annual Review of Phytopathology* **44**, 135-62.

van Loon LC, van Strien EA, 1999. The families of pathogenesis-related proteins, their activities, and comparative analysis of PR-1 type proteins. *Physiological and Molecular Plant Pathology* **55**, 85-97.

Vandesompele J, De Preter K, Pattyn F, *et al.*, 2002. Accurate normalization of real-time quantitative RT-PCR data by geometric averaging of multiple internal control genes. *Genome Biology* **3**, RESEARCH0034.1-.11.

Vleeshouwers VG, Oliver RP, 2014. Effectors as tools in disease resistance breeding against biotrophic, hemibiotrophic, and necrotrophic plant pathogens. *Molecular Plant-Microbe Interactions* **27**, 196-206.

Wiesel L, Newton AC, Elliott I, *et al.*, 2014. Molecular effects of resistance elicitors from biological origin and their potential for crop protection. *Frontiers in Plant Science* **5**, 655.

Wise K, 2011. *Diseases of Corn: Northern Corn Leaf Blight*. [https://www.extension.purdue.edu/extmedia/BP/BP-84-W.pdf]. 14 November 2019.

Wu S, Kriz AL, Widholm JM, 1994. Nucleotide sequence of a maize cDNA for a class II, acidic beta-1,3-glucanase. *Plant Physiology* **106**, 1709-10.

Xie YR, Chen ZY, Brown RL, Bhatnagar D, 2010. Expression and functional characterization of two pathogenesis-related protein 10 genes from *Zea mays*. *Journal of Plant Physiology* **167**, 121-30.

Xie YR, Raruang Y, Chen ZY, Brown RL, Cleveland TE, 2015. ZmGns, a maize class I beta-1,3-glucanase, is induced by biotic stresses and possesses strong antimicrobial activity. *Journal of Integrative Plant Biology* **57**, 271-83.

Chapter 5: Evidence of ultrastructural phytotoxicity associated with monocerin, on maize leaves

Abstract

Exserohilum turcicum, the causal agent of northern leaf blight (NLB) of maize, produces a secondary metabolite, monocerin, which is known to be phytotoxic to a wide range of plants. Monocerin could play an important role in disease development. The aims of the study were to determine the phytotoxic effects of monocerin on the ultrastructure of maize leaf cells as well as to investigate whether the expression of genes coding for enzymes involved in starch degradation in the chloroplast are inhibited by the toxin and fungus. For microscopic studies, leaf material infiltrated with 1 and 2 mM monocerin was harvested at 0, 6, 12, 24 and 48 hours post-infiltration (hpi). Samples were prepared according to standard microscopy procedures and analysed using light and transmission electron microscopy. The cytoplasm, vacuole and chloroplast were most affected at both concentrations of monocerin. Chloroplasts appeared to be most sensitive to the toxin which caused disruption of their double-membrane, stroma, thylakoid membranes and an over accumulation of starch granules. In addition, RNA was isolated from monocerin infiltrated and fungus infected leaves whereafter cDNA was synthesised for gene expression studies. The expression of phosphoglucan water dikinase (*pwd*) and α-amylase 3 (*amy3*) (enzymes part of starch degradation) genes was inhibited by the fungus, and *amy3* by monocerin. The fungus and toxin could thus affect the translocation of sugars out of the chloroplast. This study provided a detailed view on the toxic effect of monocerin on the ultrastructure of maize leaf cells. Furthermore, the effect of the toxin and fungus on the expression of genes involved on the degradation of starch granules in the chloroplast was established.

Keywords: *Exserohilum turcicum*, monocerin, northern leaf blight, phytotoxins, starch enzymes, ultrastructure, *Zea mays*.

5.1. Introduction

Many economically important disease-causing phytopathogenic fungi have the ability to produce low molecular weight secondary metabolites or phytotoxins, which could contribute to their survival. For example, metabolites such as pigments could provide protection or pathogenicity whereas toxins could mediate virulence or play a role in infection (Bennett & Klich, 2003; Mobius & Hertweck, 2009). Many phytotoxins that have been described either play a role in the diseases caused by phytopathogenic fungi or are associated with a particular fungus. These phytotoxins can either be host-selective, where they induce pathogenicity in one species or non-host selective where they are phytotoxic towards numerous plant species regardless of whether the species plays host to the fungus (Scheffer & Livingston, 1984; Mobius & Hertweck, 2009). Host-selective phytotoxins includes victorin, HC-toxin, tentoxin, T-toxin and PM-toxin (Scheffer & Livingston, 1984; Collemare & Lebrun, 2011; Stergiopoulos *et al.*, 2013). Non-host selective phytotoxins include the well-known mycotoxins fumonisins, trichothecenes and AAL-toxin as well as cercosporin and elsinochrome (Cutler & Jarvis, 1985; Abbas & Boyette, 1992; Abbas *et al.*, 1995; Collemare & Lebrun, 2011; Kotze *et al.*, 2016). Phytotoxins target numerous cellular components of plants which include the plasma membrane (fumonisins, AAL-toxin), mitochondria (victorin, T-toxin), chloroplast (tentoxin) and ribosomes (trichothecenes) (Mobius & Hertweck, 2009; Collemare & Lebrun, 2011). Disruption of these cellular components leads to chlorosis, necrosis, growth inhibition, wilting and ultimately to the death of the plants (Abbas & Boyette, 1992; Abbas *et al.*, 1995).

Monocerin is a lipophilic, dihydroisocoumarin and polyketide metabolite produced by *Exserohilum turcicum*, which is the causal pathogen for northern leaf blight (NLB) of maize (Aldridge & Turner, 1970; Robeson & Strobel, 1982). It has been reported that monocerin could aid the fungus in causing disease in maize (Aldridge & Turner, 1970; Cuq *et al.*, 1993). Monocerin was first isolated by Aldridge and Turner (1970) from *Exserohilum monoceras* and from *E. turcicum* by Robeson and Strobel (1982). Additionally, Robeson and Strobel (1982) were the first to report on the phytotoxicity of monocerin towards cucumber (*Cucumis sativus* L). and Johnson grass (*Sorghum halepense* Pers.). Monocerin is also phytotoxic towards maize (*Zea mays*), radish (*Raphanus raphanistrum* L.), tomato (*Solanum lycopersicum* L.), ryegrass (*Lolium multiflorum* Lam.) and weeds such as barnyard grass (*Echinochloa crus-galli* (L.) P.Beauv.), bulrush (*Schoenoplectiella juncoides* (Roxb.) Lye) and creeping thistle (*Cirsium arvense* (L.) Scop.) (Cuq *et al.*, 1993; Lim, 1999). Monocerin is considered to be a

non-host specific phytotoxin since it is phytotoxic towards more than one plant species. Not much is known about the mode of action or where the in the plant cell the toxin causes damage. Monocerin could possibly have an effect on the cell division cycle by interfering with the S and G2 stages, and could also disrupt the chloroplast (Gélie *et al.*, 1987; Cuq *et al.*, 1995).

The assimilation of atmospheric carbon dioxide during photosynthesis by leaves yields sucrose and starch as the two end products of the light reaction of photosynthesis (Taiz & Zeiger, 2006). Sucrose can be found in the cytosol and is continuously exported to other non-photosynthetic parts of the plants whereas starch remains in the chloroplast (Taiz & Zeiger, 2006). At the onset of darkness, carbon assimilation stops and the degradation of starch commences in the chloroplast to maintain the export of sucrose (Taiz & Zeiger, 2006; Silver *et al.*, 2014). Starch granules consist mainly of branched polymers of glucose that are highly ordered, semi-crystalline structures (Smith *et al.*, 2005; Silver *et al.*, 2014). The degradation of starch in the chloroplast is initiated with the phosphorylation of the surface of a starch granule by glucan water dikinase (*gwd*) and phosphoglucan, water dikinase (*pwd*) (Smith *et al.*, 2005; Silver *et al.*, 2014). The phosphorylation of the semi-crystalline structure by *gwd* and *pwd* served to solubilise the granule surface for enzymes such as α-amylase (*amy3*), β-amylase (*bam1 & bam3*) and isoamylase (*isa3*) to access the glucan chains (Zeeman *et al.*, 2010). The products of these hydrolyses reactions are then use in downstream reactions with the end product being sucrose (Zeeman *et al.*, 2010).

This study was undertaken to evaluate the phytotoxic effect of monocerin in maize leaves with an emphasis on the cell ultrastructure and starch degradation in the chloroplast. Furthermore, the study was conducted to determine whether monocerin could aid the fungus in causing disease in maize. Additionally, due to the accumulation of starch granules observed in the chloroplast it was determined whether *E. turcicum* and monocerin could inhibit the expression of genes coding for enzymes involved in the degradation of starch in the chloroplast. The results of this study will provide a better understanding at an ultrastructure level as to where the toxin exerts its phytotoxic effects as well as to whether the fungus and toxin are involved in manipulating genes involved in starch degradation in the chloroplast.

5.2. Materials and methods

5.2.1. Materials

All the reagents used in this study were purchased from Merck (Modderfontein, South Africa) unless otherwise stated. Primers were synthesised by Integrated DNA Technologies (IDT) (Coralville, USA) and sequencing of primer amplicons were done by the DNA Sequencing Facility, Faculty of Natural and Agricultural Sciences, University of Pretoria, Pretoria, South Africa.

5.2.2. Preparation of monocerin

Pure monocerin (10 mg) was obtained from Cfm Oskar Tropitzsch GmbH (Marktredwitz, Germany). Monocerin stocks and test concentrations were prepared as described in Chapter 4, Section 4.2.2. In addition to a 1 mM concentration, a 2 mM concentration was also included in this study.

5.2.3. Plant material

Maize plants of the inbred line B73 (susceptible to NLB) (Craven & Fourie, 2011) used in this study were grown as outlined in Chapter 4, Section 4.2.3.

5.2.4. Fungal strain, culture condition and inoculum preparation

Exserohilum turcicum isolate 2 (23N) was isolated from NLB lesion on maize leaves and identified as isolate 2 by means of a single multiplex polymerase chain reaction (PCR) assay described by Haasbroek *et al.* (2014), whereafter it was maintained and prepared for inoculation of maize plants as described in Chapter 3, Section 3.2.1 and Chapter 4, Section 4.2.4.

5.2.5. Maize inoculation and infiltration

Maize plants were either inoculated with *E. turcicum* conidia or infiltrated with 1 and 2 mM monocerin solutions, respectively, as described in Chapter 4, Section 4.2.5 with a few modifications. The control consisted of untreated or healthy tissue and a solvent control (SC)

where tissue was infiltrated with 40% methanol. For the microscopy study, each condition tested consisted of four biological replicates. Leaf samples were harvested at 6, 12, 24 and 48 hours after infiltration (hpi). Control samples were harvested before the infiltration (0 hpi) and the SC samples were harvested at the same sample points as monocerin except for 48 hpi. For RT-qPCR experiments the same biological replicates were used as described in Chapter 4, Section 4.2.5.

5.2.6. Light and transmission electron microscopy preparations

For microscopy only the effect of the toxin on the ultrastructure of maize leaf cells was investigated as the effect of the fungus had already been established in Chapter 3. Control and monocerin infiltrated maize leaf tissue with necrotic lesions, was prepared for light microscopy (LM) and transmission electron microscopy (TEM) as described in Chapter 3, Section 3.2.3. The only modification was that samples prepared for TEM were cut 120 µm thick instead of 100 µm since 100 µm thick monocerin infiltrated samples collapsed when cut with an ultramicrotome.

5.2.7. RNA isolation and cDNA synthesis

For the gene expression studies, the effects of both *E. turcicum* and monocerin were studied. RNA was isolated and cDNA was synthesised as described in Chapter 4, Sections 4.2.6 and 4.2.7, respectively.

5.2.8. RT-qPCR primer design

Gene-specific primers were designed and synthesised as described in Chapter 4, Section 4.2.8 to determine the expression of three genes involved in breaking down starch granules in the chloroplast. These genes included *gwd* (Zm00001d037059), *pwd* (Zm00001d023792) and *amy3* (Zm00001d043662). The same reference genes (*rpol*, *srl* and *gst3*) were used as in Chapter 4. Primer sequences and associated information are summarised in Table 5.1.

Table 5.1. A summary of the primer sequences and descriptive information of the maize genes analysed with RT-qPCR. All the primer sequences were designed in this study except *srl*.

Gene name (in this study)	Gene target	Synonym names	Reference gene transcript ID	References	Primer sequences 5"-3'	Tm	Amplicon size (bp)
rpol	DNA-directed RNA polymerases II IV and V subunit 8B		Zm00001d012857_T001	BG Crampton (pers. Comm)	F: CTCGCAGTGAGCAGTTAGATATG	60°C	111
					R: CCAAATTCAGAGTAGGCGCTATAA	60°C	
srl	Serine/arginine-rich splicing factor SR45a		Zm00001d006480_T010	BG Crampton (pers. Comm)	F: ACACGCCATTGTTCGAGA	60°C	117
					R: CAGGTTCGGGTGAACTTTG	60°C	
gst3	Glutathione S-transferase 4	Glutathione S-transferase 3	Zm00001d042216_T001	(Korsman *et al.*, 2011)	F: GGTTGGTCTTTGCATATCCTACTA	60°C	89
					R: GAAGAAGGGAATTACGGTGAAGA	60°C	
gwd	α-glucan water dikinase 1 chloroplastic		Zm00001d037059_T005	This study	F: CATGAGTACCTTTCGATGGC	60°C	88
					R: CAGACGATGGGTTTGTGG	60°C	
pwd	Phosphoglucan water dikinase chloroplastic		Zm00001d023792_T005	This study	F: CAGAGAGACGCAAAGATGG	60°C	96
					R: GGGATCATGGTCAACTGG	60°C	
amy3	α-amylase 3 chloroplastic		Zm00001d043662_T001	This study	F: GTGAGGAGAGACATTGAAGC	60°C	134
					R: GGTGGATGTGGTTCTGG	60°C	

5.2.9. PCR optimisation, sequencing and expression analysis of genes involved in starch degradation

The specificity of each gene primer set was tested and optimised as outlined in Chapter 4, Section 4.2.9. PCR products were sequenced to confirm that primers did indeed amplify the correct gene (Chapter 4, Section 4.2.10). Sequenced amplicons were analysed and are included in the appendix (Table 7.1). Reverse transcription-qPCR (RT-qPCR) analysis of the genes encoding enzymes involved in starch degradation (*gwd, pwd* and *amy3*) and three reference genes (*rpol, srl* and *gst3*) were performed as described in Chapter 4, Section 4.2.10 whereafter the expression of starch degradation genes was calculated relative to the reference genes for each treatment and sample point tested. Gene expression data was analysed in Bio-Rad CFX manager with the reference genes further analysed in qBASE^{PLUS} with geNorm as explained in Chapter 4, Section 4.3.4.

5.2.10. Statistical analysis

Statistical analysis of the relative expression data was performed using GraphPad Prism version 4.03 (GraphPad Prism Software, San Diego, California, USA). A one-way analysis of variance (ANOVA) was done, followed by a Tukey's multiple comparison test with the level statistical significance measured at $p < 0.05$.

5.3. Results

5.3.1. Monocerin infiltration of maize leaves

Maize leaves were infiltrated with either a 1 or a 2 mM monocerin solution whereafter they were harvested at 6, 12, 24 and 48 hpi. Similar morphological observations were seen in comparison to Chapter 4, Section 4.3.1. The lesions observed in Chapter 4 were small and necrotic after 24 hpi with 1 mM monocerin and enlarged slightly at 48 hpi. The non-infiltrated control (Figure 5.1, a) revealed healthy tissue without any visible lesions whereas with the SC (Figure 5.1, b) damage could be seen, 24 hpi, where the leaf was nicked with a syringe needle with a small area around the wound being necrotic. For both 1 and 2 mM monocerin at 6 and 12 hpi only water-soaked spots were visible and no lesions (images not shown). When leaves were infiltrated with 1 mM monocerin, small necrotic lesions were visible 24 hpi (Figure 5.1, c)

which increased in size after 48 hpi (Figure 5.1, d). It was difficult to infiltrate maize leaves with 2 mM monocerin since the solution did not infiltrate the leaf. This could have been due to the concentration of monocerin being too high to dissolve in 40% methanol and thus the use of an alternative solvent system should be investigated. However, this problem was not seen with 1 mM monocerin. Necrotic tissue was observed 48 hpi, in leaves that were infiltrated with 2 mM monocerin as opposed to 24 hpi where needle damage was only visible (Figure 5.1, e, f). The visual progression of both the toxin and fungus were the same as what was observed in Section 4.3.1 since the same material was used in both this study and Chapter 4 gene expression studies.

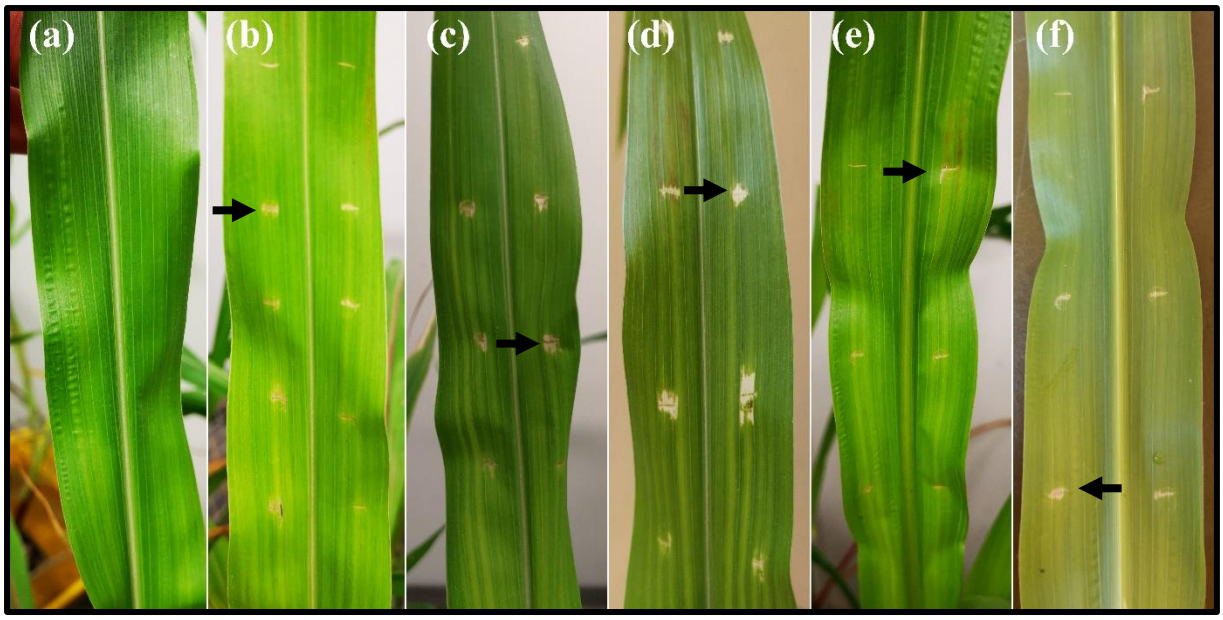

Figure 5.1. Visual progression of lesions forming on maize leaves infiltrated with 1 and 2 mM monocerin. (a) non-infiltrated leaf (control leaf); (b) small necrotic lesions visible after 24 hpi with 40% methanol (SC); (c) small necrotic lesions visible (1 mM monocerin, 24 hpi); (d) necrotic lesion enlarged in size (1 mM monocerin, 48 hpi); (e) only tissue damaged present as a result of mechanical wounding (2 mM monocerin, 24 hpi), (f) necrotic tissue slightly enlarged around area where monocerin was infiltrated (2 mM monocerin, 48 hpi). Arrows indicate where necrotic lesions formed or where the wounding occurred.

5.3.2. The effect of monocerin on the ultrastructure of maize leaf cells

Light and transmission electron micrographs of the non-infiltrated control tissue revealed healthy intact cells with clearly defined chloroplasts in both the bundle sheath and spongy mesophyll cells (Figure 5.2, a, b). Healthy vacuoles were also observed that occupied most of the cell space and caused the contents of the cytoplasm including the chloroplasts to push

against the cellular membrane. Chloroplasts of the bundle sheath cells also had numerous small starch granules within them.

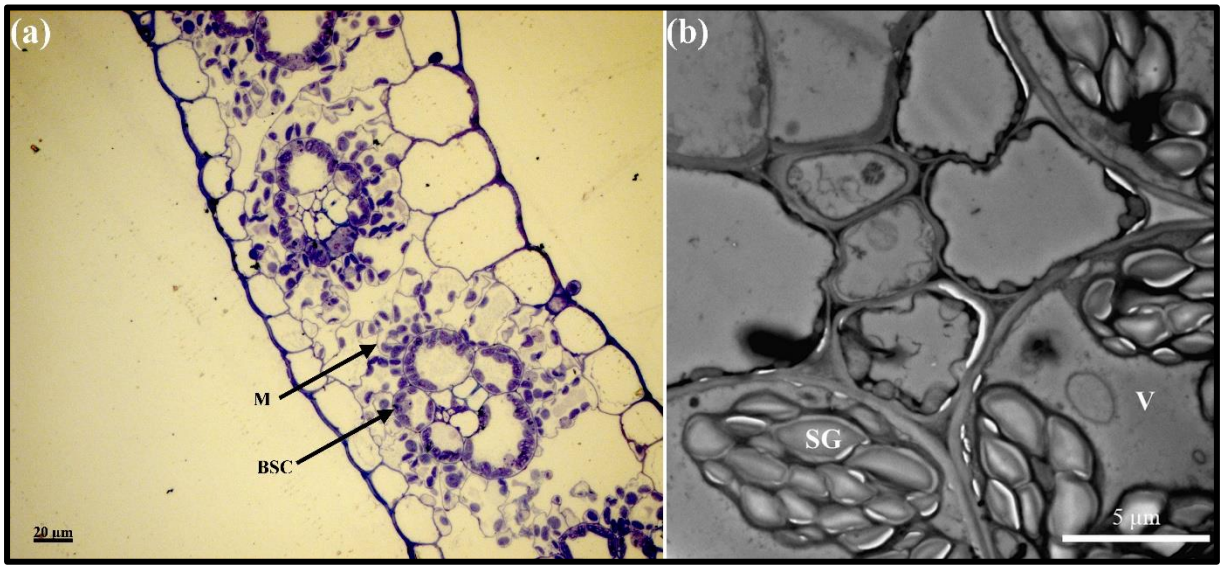

Figure 5.2. Transverse sections of a non-infiltrated (control) B73 maize leaves. (a) light microscopy observations of healthy spongy mesophyll and bundle sheath cells in close proximity to one of the minor veins; (b) transmission electron micrograph of the ultrastructure of control leaf tissue revealed chloroplasts with numerous small starch granules as well as healthy and intact vacuoles. M, spongy mesophyll cells; BSC, bundle sheath cells; SG, starch granule; V, vacuole.

The phytotoxic effects of monocerin were evident at a cellular level at 6 hpi. Light and transmission electron micrographs revealed that starch granules were in the process of enlarging and that spongy mesophyll cells were shrinking and collapsing in tissue treated with 1 mM monocerin (Figure 5.3, a). In addition, chloroplasts could also be seen scattered around in the spongy mesophyll cells. This observation could be a result of the cell losing its turgor pressure due the vacuoles no longer being sufficiently large enough to push the cytoplasm and its contents against the cellular membrane. In Figure 5.3, b, granulation of the cytoplasm as well as vacuoles dissociating into irregular shaped smaller vacuoles could be seen. The stroma of a chloroplast was gradually becoming granulated and grana and stromal thylakoids seemed to loose their integrity (Figure 5.3, c). Spongy mesophyll cells of tissue that were treated with 2 mM monocerin were almost completely collapsed and the bundle sheath cells were full of starch granules (Figure 5.3, d). Severe granulation of the stroma and disruption of the thylakoid membranes were also visible at 2 mM monocerin (Figure 5.3, e). The SC tissue had intact bundle sheath and spongy mesophyll cells with healthy chloroplasts within them (Figure 5.3,

f). Starch granules were also visible in the chloroplast of the bundle sheath cells of the SC tissue.

At 12 hpi the phytotoxic effect of monocerin was more evident than at 6 hpi. Light and transmission electron micrographs revealed that the spongy mesophyll cells had almost completely collapsed and the bundle sheath cells were full of starch granules in tissue treated with 1 mM monocerin (Figure 5.4, a, b). This is almost similar to the effects that 2 mM monocerin had after 6 hpi (Figure 5.3, d, e). In addition, the cytoplasm was completely granulated (Figure 5.4, b). The chloroplast of bundle sheath cells was breaking down as well as being full of starch granules with no thylakoid membranes visible in tissue infiltrated with 2 mM monocerin (Figure 5.4, c). Very little of the cytoplasm remained. In the SC, starch granules could be seen accumulating in the chloroplast and the spongy mesophyll cells were in the early stages of shrinking and collapsing (Figure 5.4, d).

After 24 hpi, similar results were seen in the light and transmission electron micrographs of 1 mM monocerin treated tissue when compared to the same concentration at 12 hpi. The cytoplasm of bundle sheath cells had completely broken down and appeared granulated, and the chloroplast was full of starch granules (Figure 5.5, a). Figure 5.5, b, shows the disintegration of the chloroplast double-membrane and stroma as well as cellular contents pulling away from the cell wall. Starch granules appear larger and the thylakoid membranes have almost complete disintegrated (Figure 5.5, c). In 2 mM monocerin treated tissue, complete tissue collapse could be seen with an over-accumulation of starch granules in the bundle sheath cells (Figure 5.5, d, e). The spongy mesophyll cells completely disappeared with only the remnants of the epidermal cells still visible (Figure 5.5, d). In the SC, the cytoplasm had become granulated and the vacuole dissociated into smaller irregular shapes and was similar to the 1 mM monocerin treated tissue at 6 hpi (Figure 5.5, f).

At 48 hpi, chloroplasts could be seen scattered around in both spongy mesophyll cells as well as the bundle sheath cells of 1 mM monocerin treated tissue (Figure 5.6, a). In the left top part of the micrograph, cells were in the process of dying due to the toxic effect of monocerin whereas in the bottom part healthy cells could still be seen. The plasma membrane had separated from the cell wall and was contracting, and the chloroplast and thylakoid membranes were disintegrating indicating that the cell was in the process of dying (Figure 5.6, b, c). (Van Asch, 1990).

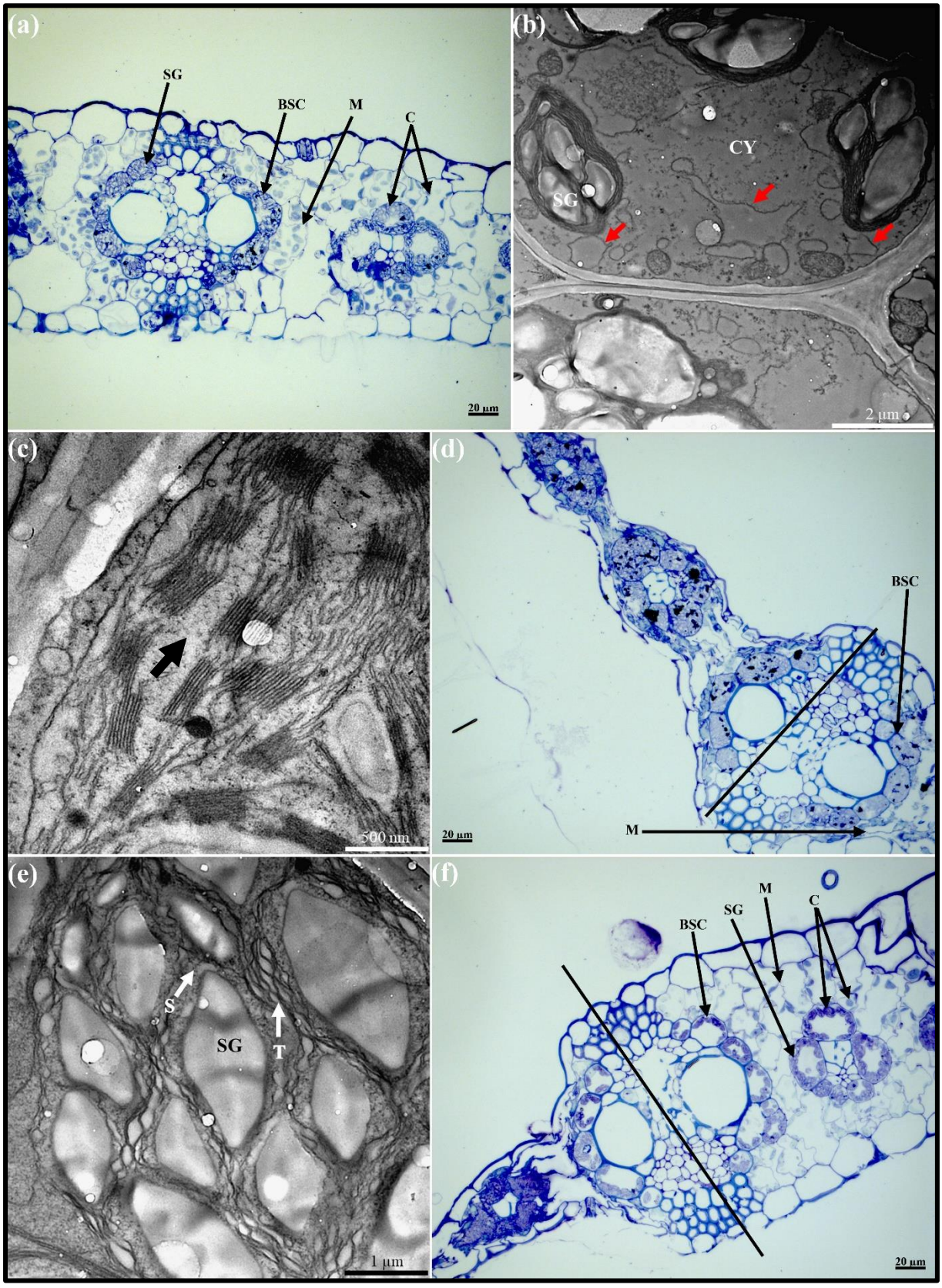
(a)
SG
BSC
M
C
20 µm
(b)
CY
SG
2 µm
(c)
500 nm
(d)
BSC
M
20 µm
(e)
S
SG
T
1 µm
(f)
BSC
SG
M
C
20 µm

Figure 5.3. Transverse sections of maize leaves infiltrated with monocerin 6 hpi. (a) Starch granules in the process of enlarging in bundle sheath cells and spongy mesophyll cells collapsing and shrinking with random distribution of chloroplasts within them; (b) vacuoles dissociating into smaller vacuoles which are irregular in shape and granulation of the cytoplasm is visible; (c) stroma becoming granulated (black arrow); (d) spongy mesophyll cells almost completely collapsed and bundle sheath cells full of starch granules when viewed from right of the black line; (e) granulation of stroma present and disruption of the thylakoid membranes visible; (f) intact chloroplast with starch granules and healthy spongy mesophyll cells can be seen right of the black line. a–c, 1 mM monocerin; d & e, 2 mM monocerin; f, SC. a, d, f, light micrographs; b, c, e, transmission electron micrographs. C, chloroplast; M, spongy mesophyll cells; BSC, bundle sheath cells; CY, cytoplasm; S, stroma; SG, starch granule; red arrows, small vacuoles

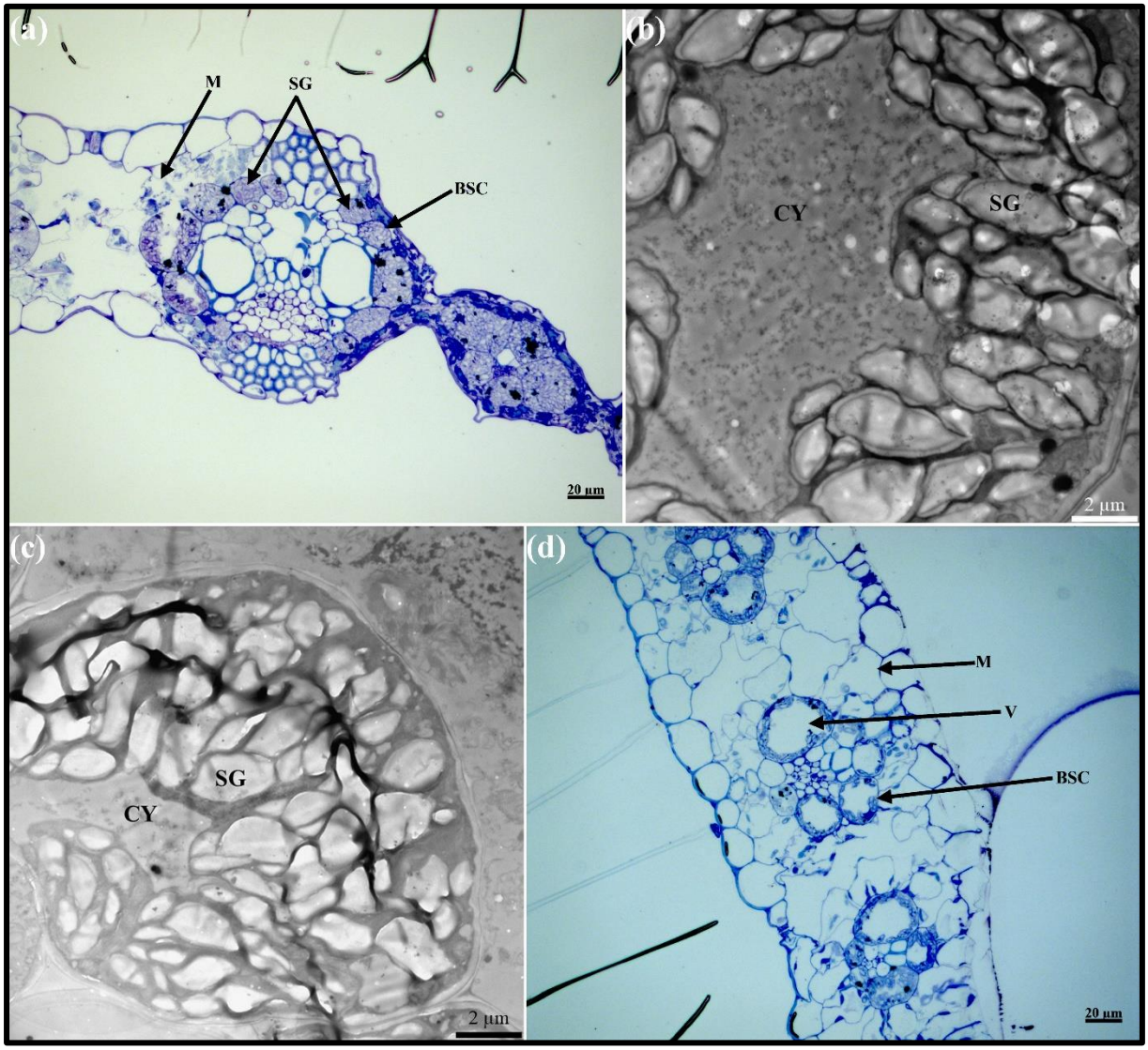

Figure 5.4. Transverse sections of maize leaves infiltrated with monocerin 12 hpi. (a) Spongy mesophyll cells have almost completely collapsed and bundle sheath cells full of starch granules; (b & c) cytoplasm completely granulated and chloroplasts losing their identity and full of starch granules; (d) starch granules in the chloroplast and intact vacuoles still visible in bundle sheath cells, spongy mesophyll cells in the early stages of dying. a & b, 1 mM

monocerin; c, 2 mM monocerin; d, SC. a & d, light micrographs; b & c, transmission electron micrographs. M, spongy mesophyll cells; BSC, bundle sheath cells; CY, cytoplasm; SG, starch granule; V, vacuole.

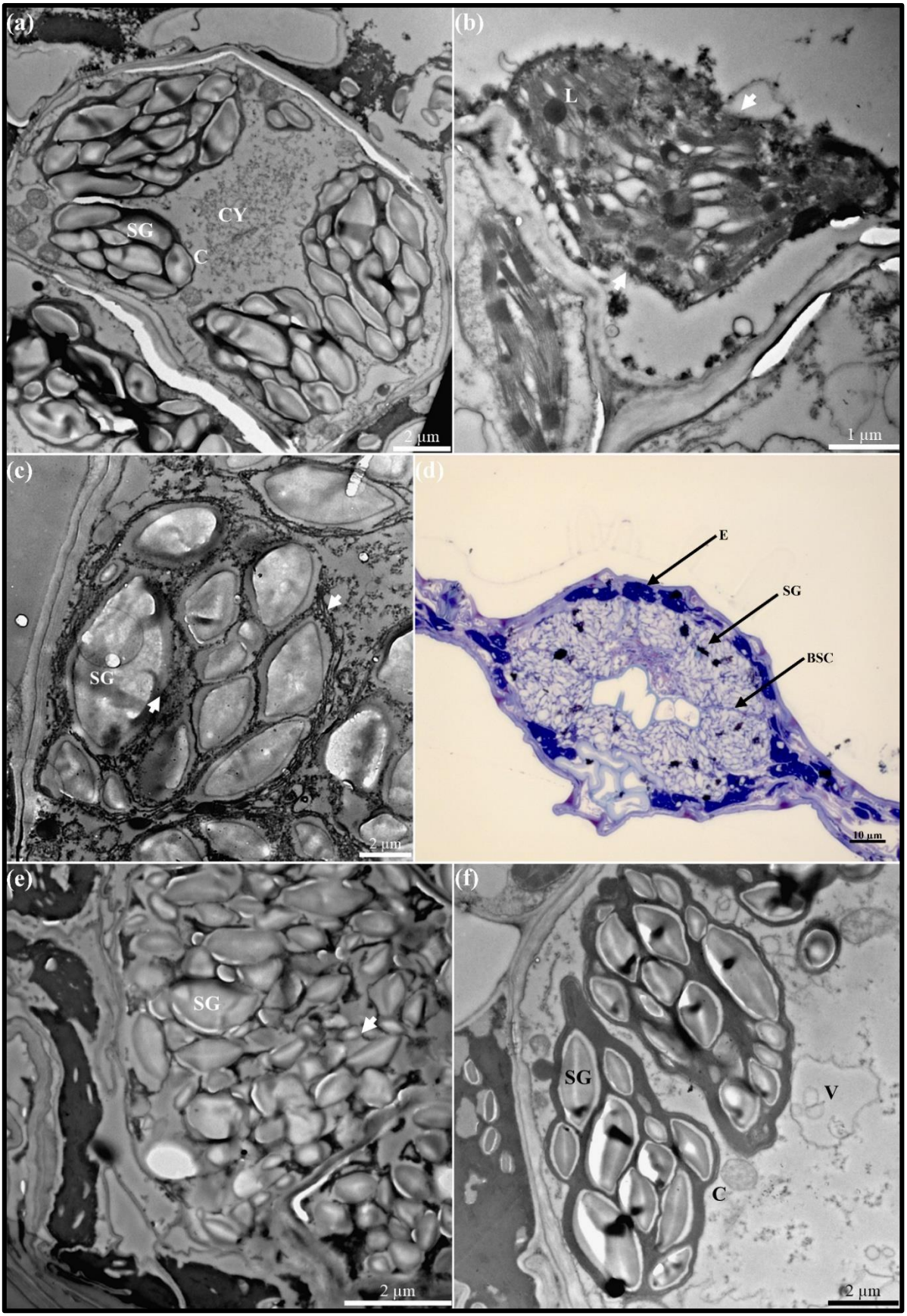

Figure 5.5. Transverse sections of maize leaves infiltrated with monocerin 24 hpi. (a) Cytoplasm completely granulated with chloroplast full of starch granules; (b) chloroplast

double-membrane (white arrows) and the stroma disintegrating; (c) starch granules getting bigger, and thylakoid membranes almost completely disintegrated (white arrows); (d) complete tissue collapse, with an over-accumulation of starch granules in the bundle sheath cells; (e) transmission electron micrograph of one of the bundle sheath cells in image d; (f) cytoplasm becoming granulated as well as the vacuoles dissociating up into smaller vacuoles as well as in the process of disintegrating. a–c, 1 mM monocerin; d & e, 2 mM monocerin; f, SC. d, light micrographs; a–c, e & f, transmission electron micrographs. BSC, bundle sheath cells; C, chloroplast; CY, cytoplasm; SG, starch granule; V, vacuole.

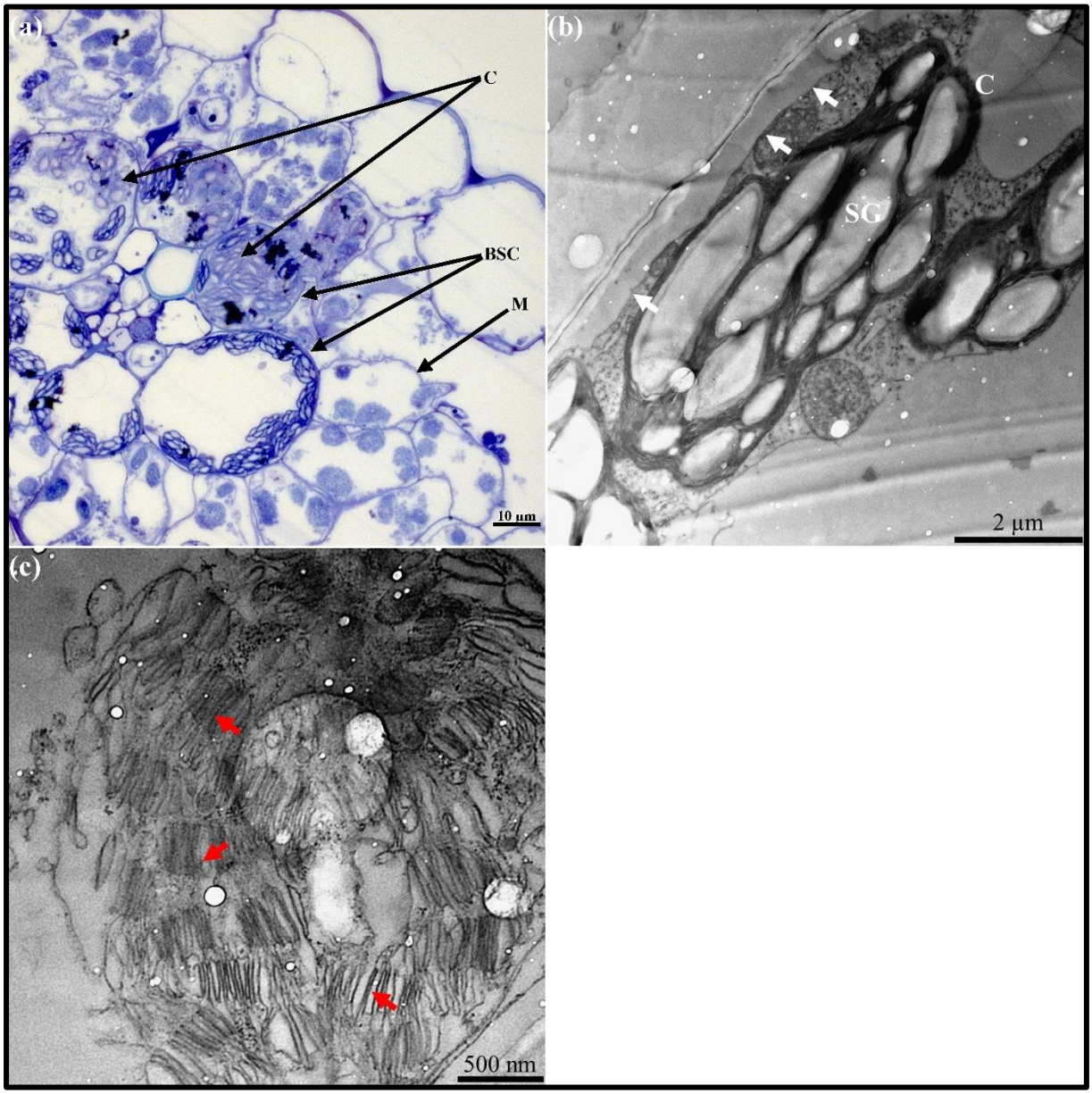

Figure 5.6. Transverse sections of maize leaves infiltrated with monocerin 48 hpi. (a) starch granules increasing in size and quantity in chloroplasts with chloroplasts scattered around in bundle sheath cell. Healthy bundle sheath and mesophyll cells also visible in the micrograph; (b) plasma membrane separated from cell wall (white arrows) with starch granules increasing in size; (c) chloroplast double-membrane and thylakoid membranes (red arrows) busy disintegrating. a–c, 1 mM monocerin. a, light micrographs; b & c, transmission electron

micrographs. BSC, bundle sheath cells; C, chloroplast; M, spongy mesophyll cells; SG, starch granule.

5.3.3. Expression of genes involved in starch degradation

Expression analysis of the three genes (*gwd, pwd* and *amy3*) using RT-qPCR was undertaken to determine if *E. turcicum* and monocerin had an effect on the expression of these genes involved in the breakdown of starch granules in the chloroplast. Reverse transcription-qPCR was performed on *E. turcicum* infected and monocerin treated maize samples as well as nontreated controls, and infiltration and wounding controls (Chapter 4, Section 4.2.5). Each sample consisted of three biological replicates and each biological replicate consisted of three technical replicates. The starch genes were normalised by dividing the expression of the starch genes by the geomean input reference cDNA of the three reference genes (*rpol*, *srl* and *gst3*) for the same sampling point. Following RT-qPCR amplification of the starch degradation and reference genes, a melt-curve analysis was performed to confirm that a single homogenous cDNA amplicon was amplified and that primer dimers were absent (Appendix, Figure 7.3). Standard curves were constructed for each gene of interest as well as reference genes using pooled cDNA of all the samples. The amplification efficiencies were calculated from the slope of the standard curve as well as the R^2 (correlation coefficient) values (Appendix, Figure 7.3 and 7.4). Amplification efficiencies of all the samples ranged between 90% to 110% and a $R^2 > 0.98$ and adhere to MIQE guidelines (Taylor *et al.*, 2010).

The expression values of all three starch enzyme genes were determined at each sample point during NLB disease development (Figure 5.7). With all three starch enzymes, similar trends were noted in that the gene expression was the highest in the control samples, then decreased at 4 and 9 dpi and was the lowest at 14 dpi when the fungus was in its necrotrophic phase and in the process of completing its life cycle (Figure 5.7). The expression of all three starch degradation genes was significantly different between the control and fungal infected tissue (4, 9 and 14 dpi) except for *gwd* (Figure 5.7). The only significant difference seen in *gwd* was between the control tissue and 14 dpi. Both sample points 4 and 9 dpi were lower than the control but not significantly different (Figure 5.7, A). The gene expression of *pwd* at 4 and 9 dpi was the same between the two sample points but was lower and significantly different compared to control samples which indicates that the fungus could have an effect on this gene during the early stages of NLB disease progression (Figure 5.7, B). The same was seen with *amy3* except that the gene expression at 9 dpi was the same as 14 dpi (Figure 5.7, C). With all

three genes, the gene expression at 14 dpi was significantly lower and different when compared to the control samples (Figure 5.7).

The expression of *gwd*, *pwd* and *amy3* was also determined in maize leaves infiltrated with 1 mM monocerin. Two sample points, 24 and 48 hpi monocerin infiltration as well as a control, SC and wounded control (WC) (nicked with syringe needle) were included in the gene expression analysis. Monocerin did not greatly reduce the expression of starch degradation genes in maize leaves (Figure 5.8). With *gwd*, leaves examined at both the 24 and 48 hpi with monocerin as well as the SC and WC were lower but not significantly different compared to the control sample (Figure 5.8, A). This indicated that monocerin did not have an effect on the expression of *gwd*. With *pwd* the same was seen with all the sample points except for the SC which differed significantly from other sample points (Figure 5.8, B). Expression of *amy3* at both 24 and 48 hpi as well as the SC and WC were lower and significantly different when compared to the control samples (Figure 5.8, C).

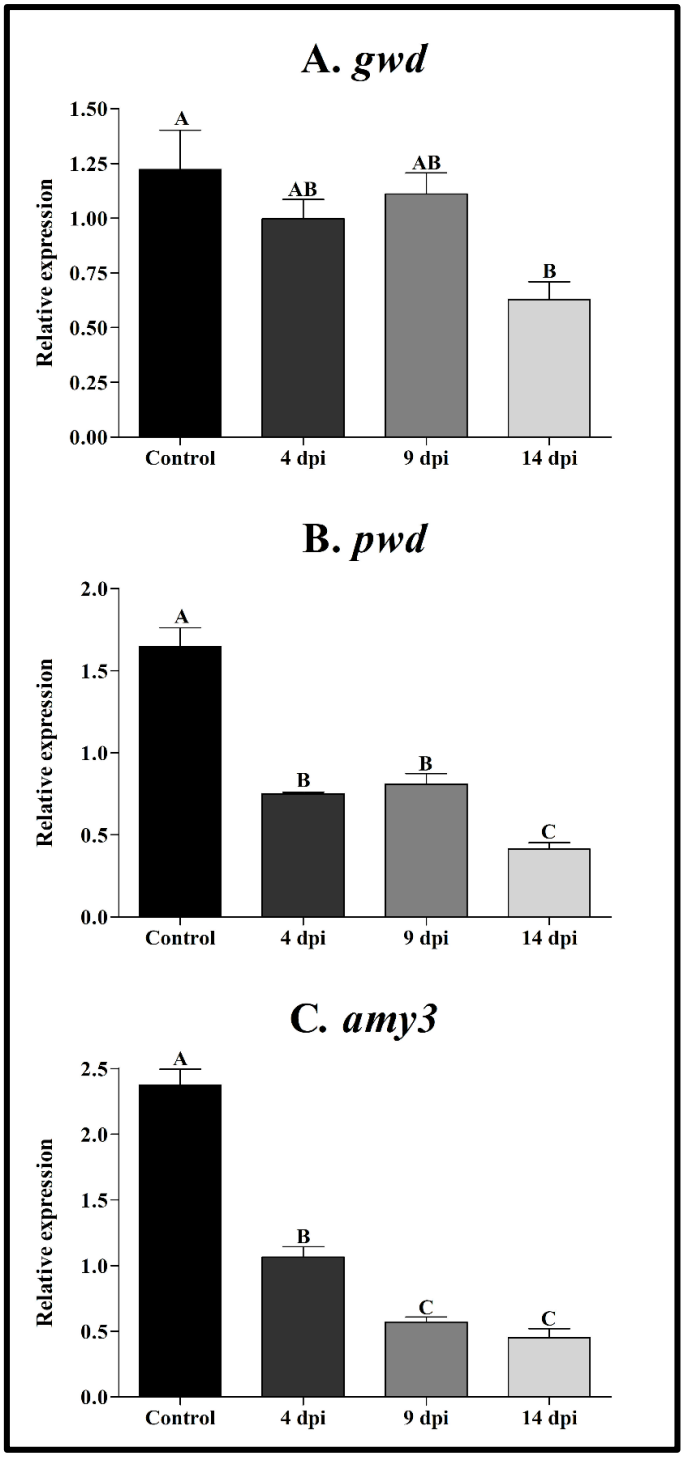

Figure 5.7. Normalised gene expression profiles of the selected genes involved in starch degradation, *gwd* (A), *pwd* (B) and *amy3* (C) during *E. turcicum* infection of maize leaves. The average relative expression was calculated for each gene of interest during the infection of maize with *E. turcicum*. Sample points included control (0 dpi), 4 dpi (chlorotic spots), 9 dpi (necrotic spots) and 14 dpi (cigar shape lesions). Each starch enzyme relative gene expression values were normalised by dividing the relative input cDNA of the gene of interest by the geomean input reference cDNA of the three reference genes (*rpol*, *srl* and *gst3*). Statistical analysis of the relative expression data was done using a one-way ANOVA analysis followed

Tukey's Multiple Comparison Test. Sample points not designated with the same letter are significantly different (P<0.05). Error bars indicate the standard error of mean.

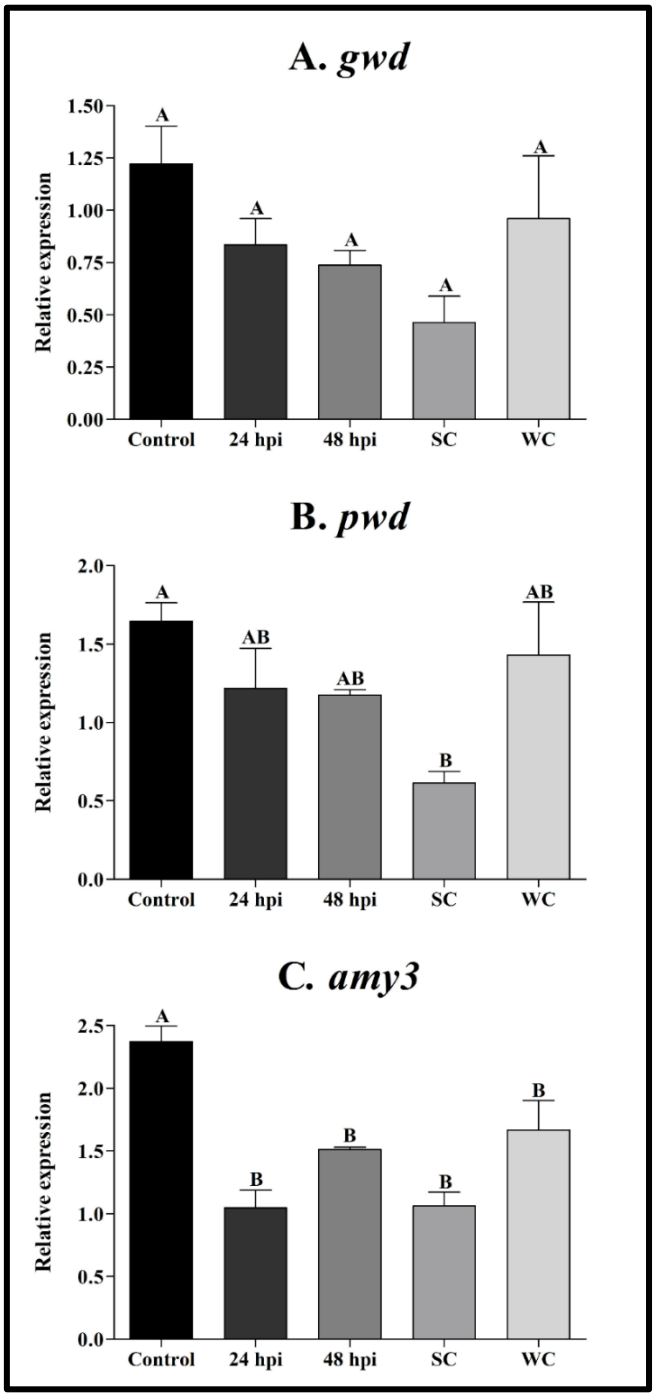

Figure 5.8. Normalised gene expression profiles of the selected genes involved in starch degradation, *gwd* (A), *pwd* (B) and *amy3* (C) during monocerin infiltration of maize leaves. The average relative expression was calculated for each gene of interest during the infiltration of maize leaves with monocerin. Sample points consisted of a control (0 hpi), 24 hpi, 48 hpi, solvent (SC) and wounded control (WC). Each starch enzymes relative gene expression values were normalised by dividing the relative input cDNA of the gene of interest by the geomean input reference cDNA of the three reference genes (*rpol*, *srl* and *gst3*). Statistical analysis of

the relative expression data was done using a one-way ANOVA analysis followed Tukey's Multiple Comparison Test. Sample points not designated with the same letter are significantly different ($P<0.05$). Error bars indicate the standard error of mean.

5.4. Discussion

Studying the effect of monocerin on the cell ultrastructure has provided insight on where the toxin exerts its negative effects. Additionally, the gene expression studies of starch degradation enzymes have answered some questions with regards to the possible mode of action of the toxin. Previous studies only reported on the morphological or growth effects of monocerin in maize and other crops but not on the cell ultrastructure (Aldridge & Turner, 1970; Robeson & Strobel, 1982; Cuq *et al.*, 1993; Lim, 1999). Gélie *et al.* (1987) reported on the toxic effect of the fungus on the maize leaf cell ultrastructure but not by the toxin. To the best of the researcher's knowledge this is the first report on the effect of monocerin on the cell ultrastructure of maize as well as the effect of the fungus and the toxin on the gene expression of enzymes involved in the degradation of starch.

Small whitish necrotic lesions were observed, where the leaf was infiltrated with monocerin after 24 hpi, and the lesions were enlarged slightly after 48 hpi. This concurs with the findings by Cuq *et al.* (1993), who also observed whitish necrotic lesions when the authors treated maize leaves with different concentrations of monocerin. The same was noted by Robeson and Strobel (1982) when creeping thistle was treated with 1 mM monocerin. Additionally, Robeson and Strobel (1982) reported that the phytotoxic effect of monocerin on maize leaves plateaued at concentration of 1 mM monocerin. Although necrosis did occur in the SC as a result of the 40% methanol application, it differed from the monocerin damaged tissue in several ways. The necrotic tissue surrounding the location where the leaf was nicked was smaller when compared to the monocerin treated tissue and the solvent took longer to induce an effect, morphologically and on an ultrastructure level. This indicated 40% methanol could have a minor toxic effect on the cells in the leaves. This was in contrast to what Cuq *et al.* (1993) reported as they did not observe any damage in their SC which was also 40% methanol.

On an ultrastructural level, differences were seen between the control and monocerin treated tissue especially at the later sample points. Control tissue revealed neat and intact cells with clearly defined organelles. Numerous vacuoles as well as chloroplasts with starch granules could be seen. The formation and accumulation of starch granules in the chloroplast together

with sucrose are two end product of carbon assimilation. At the onset of darkness, assimilation of carbon stops, but the degradation of starch granules to maintain the exportation of sucrose out of the chloroplast (Taiz & Zeiger, 2006).

At the earlier sample points, the cytoplasm, vacuole and chloroplast were the most affected by monocerin. Large quantities of granular electron-dense intercellular material were seen in the transmission electron micrographs indicating that the toxin had an effect on the cytoplasm. The vacuoles also started to dissociate into smaller irregular shaped size, which was probably the reason why the chloroplasts were scattered in the cell. In addition, the stroma of the chloroplasts became granulated and the thylakoid membranes were disrupted indicating that the toxin had an effect on the chloroplast. Granulation of the stroma was observed in bean (*Phaseolus vulgaris* L.) leaves treated with systemic fungicide benomyl (Rufner *et al.*, 1975). Abbas *et al.* (1992) also indicated that the primary site of action of fumonisin B_1 (FB_1) in jimsonweed leaves was either the plasma membrane or the tonoplast (membrane surrounding vacuole) followed by disruption of the chloroplast and accumulation of intercellular debris. The swelling of the chloroplast, disruption of the chloroplast double-membrane and subsequent disintegration of the thylakoid membranes could be in response to the stroma of the chloroplast becoming hypertonic due to a mixed combination of cytoplasmic and vacuole contents in the cell (Abbas *et al.*, 1992). Abbas *et al.* (1992) noted that loss of cell wall turgor could be due to the mixed contents of the cytoplasm and vacuole. In this study, the disruption of the chloroplast could have been a direct and/or indirect effect of the toxin since damage was seen early on to both the chloroplast stroma, double membrane and thylakoid membranes as well as the cytoplasm. Damage to the rest of the cellular organelles could have been secondary effect since the cytoplasm was affected as well.

At the later sample points, the more severely affected cells that showed the most degenerative damage were usually in close proximity to where the leaf was infiltrated with monocerin and less damaged cells closer to the edge of the lesion. As time progressed the cytoplasm disintegrated, the spongy mesophyll cells and epidermal cells had collapsed with only the remnants left and the chloroplast double-membrane being in the process of disintegrating. It was only at 48 hpi that the plasma membrane contracted from the cell wall. In spite of the difficulty of infiltrating maize leaves with 2 mM monocerin and the lack of lesions forming, damage to the ultrastructure of maize cells was, nevertheless still seen. Both concentrations of monocerin had similar effects with the only exceptions being that phytotoxic effects of 2 mM

monocerin were seen earlier than 1 mM (e.g. the effects seen at 6 hpi for 2 mM were only seen at 12 hpi for 1 mM monocerin)). As a result of the complete tissue collapse observed after 24 hpi with 2 mM monocerin, it was not further analysed at 48 hpi. Complete tissue collapse would probably have been seen if 1 mM monocerin was analysed at a later time point such as 72 hpi. Similar observations were seen on the ultrastructural level by Steinkamp *et al.* (1979) when the authors treated beetroot (*Beta vulgaris* L.) leaves with cercosporin isolated from *Cercospora beticola*. The observations seen included granulation of the cytoplasm, loss of integrity of cell membranes especially the chloroplast double-membrane and tonoplast and necrotic cells that had collapsed. In addition to these effects the authors also observed starch granules and remnants of the chloroplast membranes in the necrotic cytoplasm (Steinkamp *et al.*, 1979). Steinkamp *et al.* (1979) also indicated that some of these effects were similar to the ultrastructural changes caused by *C. beticola*.

The accumulation of starch granules increased as the time progressed in both monocerin treatments. This could partially be due to sugars not being formed and translocated out of the chloroplast as a result of cells dying, and thus resulting in the overaccumulation of starch granules (Abbas *et al.*, 1992). Alternatively, monocerin could have an effect on the starch genes involved in breaking down starch granules (Smith *et al.*, 2005; Taiz & Zeiger, 2006). In the current study the chloroplasts were more resilient than the other organelles since they were still recognisable even at the later sample points post treatment at both concentrations of monocerin. Similar results were observed when jimsonweed leaves were treated with FB_1 (Abbas *et al.*, 1992). This could be due to the fact that chloroplasts are more protected from oxidative membrane damage compared to other organelles (Halliwell, 1978; Salin, 1988).

When a comparison is made between the phytotoxic effects of monocerin observed in this chapter and the infection of *E. turcicum* in maize (Chapter 3), the only similarities noted between the toxin and fungus treatments included the shrinking and collapsing of the spongy mesophyll cells and accumulation of abundant starch granules in the bundle sheath cells, which ultimately lead to complete tissue collapse. It thus could be that the toxin aids the fungus in causing disease or helps the fungus in establishing itself during its biotrophic phase. . The toxic effects of monocerin were very similar to the toxic effects that *E. turcicum* had on the cell ultrastructure of maize leaves as reported by Gélie *et al.* (1987), who noted that the tonoplast was the first cellular component altered in response to the toxic effect of the fungus towards the leaf cells. This was followed by disorganisation and alteration of organelles which became

scattered throughout the cell. Additionally, they reported that the chloroplast was the most sensitive to the toxic action of the fungus which resulted in disruption of double-membrane as well as the grana (Gélie *et al.*, 1987). Monocerin could partially be responsible in aiding the fungus in establishing itself in maize leaves, but this needs to be supported by additional studies especially involving additional ultrastructure and molecular studies with a monocerin deficient mutant of *E. turcicum*.

The SC initially did not have any effect on cell ultrastructure (Figure 5.3). It is likely that 40% methanol is toxic to maize tissue, but its effects are delayed when compared to monocerin. Due to the toxic effect of 40% methanol another less toxic solvent should be used in further investigations. The challenge with monocerin is that it more readily dissolves in a non-polar solvent. Acetone has been used as a solvent in testing the effect of nonylphenol (endocrine disruptor) on ryegrass, where its effect was no different to the control (Domene *et al.*, 2009). The use of acetone as a solvent, should be considered in future monocerin studies.

Following the microscopic evaluation of the phytotoxic effect of monocerin on maize leaf cells, it was decided to investigate the effect of the toxin on the expression of genes involved in the degradation of starch granules in the chloroplast. This was based on the accumulation of starch granules observed in monocerin infiltrated tissue. Starch is an important storage carbohydrate that is synthesised in the day during photosynthesis and then remobilised (in the form of sugars) during the night when carbon derived from photosynthesis is unavailable (Silver *et al.*, 2014). Reverse transcription-qPCR (RT-qPCR) suggested that the expression of *amy3* was reduced by both *E. turcicum* and monocerin whereas *pwd* was only reduced by the fugus. The fungus and toxin did not have an effect on the expression of *gwd*. Both *gwd* and *pwd* play in important role in starch degradation because the semi-crystalline starch granules need to be phosphorylated for downstream reactions (Smith *et al.*, 2005; Silver *et al.*, 2014). The precise function of *amy3* is still uncertain but it is believed that *amy3* is involved in hydrolysing the internal α-1,4 linkages of linear or branch glucans to release a mixture of linear and branched malto-oligosaccharide (Smith *et al.*, 2005).

Fan *et al.* (2010) reported that starch levels increased in leaves of sweet orange (*Citrus x sinensis* (L.) Osbeck) infected with the bacterial pathogen *Candidatus liberibacter*, which is the causal agent for citrus Huanglongbing (HLB). The authors indicated that the gene expression of the starch degradation enzymes transglucosidase (*dpe2*) and maltose exporter

(*mex1*) was inhibited in response to the pathogen whereas *gwd* was not (Fan *et al.*, 2010). The same was observed in the current study where *gwd* was not inhibited by both *E. turcicum* and monocerin. Both *dpe2* and *mex1* are involved in starch degradation with *dpe2* acting as a transglucosidase by catalysing the release of one glucosyl moiety of maltose and the transfer of another to a glucose acceptor, whereas *mex1* transfers maltose across the chloroplast double-membrane (Smith *et al.*, 2005; Fan *et al.*, 2010). Both maltose and glucose can be exported out of the chloroplast into the cytoplasm at night which increases at the onset of starch degradation but maltose is exported at a higher rate than glucose (Zeeman *et al.*, 2007; Fan *et al.*, 2010). The activity of invertase, which is responsible for hydrolysis of sucrose into fructose and glucose, was also induced in infected leaves (Fan *et al.*, 2010). The decrease in expression levels of *dpe2* and *mex1* resulted in decreased maltose levels and increased sucrose and glucose levels. This resulted in an imbalance of carbohydrate partitioning and thus slowed starch degradation down (Fan *et al.*, 2010).

Similar observations were observed by Gamm *et al.* (2011) who studied the changes in carbohydrate metabolism in grapevine (*Vitis vinifera* L.) leaves in response to the oomycte *Plasmopara viticola* which causes downy mildew. Microarray analysis revealed the gene expression of α-amylase was induced at very high levels whereas β-amylase and *pwd* were not induced (Gamm *et al.*, 2011). The activity of α-amylase was the highest at 7 dpi when lesions were visible on the leaves. This is contrast with what was observed in this study where *pwd* and *amy3* expression was inhibited by *E. turcicum*. Additionally, Gamm *et al.* (2011) reported that invertase activity was induced and that there was an increase in fructose and glucose levels at the later stages of infection just before sporulation. The increase in sugars especially fructose could thus serve as nutrients for the pathogen (Fan *et al.*, 2010; Gamm *et al.*, 2011).

It seems that the effect that fungal pathogens have on starch degradation in the chloroplast is not at the initial starch degradation reactions catalysed by *gwd* and *pwd* but rather downstream. It could thus be possible that *E. turcicum* prefers fructose as nutrient source as opposed to maltose and glucose. *Exserohilum turcicum* could potentially induce the gene expression of invertase and inhibit *dpe2* and *mex1* related enzymes in maize, which would result in an increase in fructose. Furthermore, monocerin could possibly also have an effect on enzymes such as *dpe2* and *mex1* which could result in an increase in fructose as well as an accumulation of starch granules. The increase in fructose aids the fungus since fructose can potentially be a source of carbon for the fungus.

5.5. Conclusion

In this chapter a microscopic study revealed that monocerin exerted a phytotoxic effect on the chloroplast, in particular, but as well as on the cytoplasm and vacuole. Due to the accumulation of starch granules noted in treated cells, expression analysis was performed on three genes coding for enzymes involved in the degradation of these starch granules in the chloroplast of maize leaves. This provided insight on how the fungus could potentially acquire nutrients as well as how monocerin aids the fungus in the infection process. Aspects that should be considered in future studies include conducting an ultrastructure study (with the aid of TEM) of the fungus in the early stages of infection and comparing it to the monocerin to determine if similar effects are seen since monocerin could be a necrotrophic effector. Additionally, the effect of *E. turcicum* and monocerin on the expression of other starch degradation enzymes genes should be investigated

5.6. References

Abbas HK, Boyette C, 1992. Phytotoxicity of fumonisin B_1 on weed and crop species. *Weed Technology*, 548-52.

Abbas HK, Duke SO, Paul RN, Riley RT, Tanaka T, 1995. AAL-toxin, a potent natural herbicide which disrupts sphingolipid metabolism of plants. *Pesticide science* **43**, 181-7.

Abbas HK, Paul RN, Boyette CD, Duke SO, Vesonder RF, 1992. Physiological and ultrastructural effects of fumonisin on jimsonweed leaves. *Canadian Journal of Botany* **70**, 1824-33.

Aldridge DC, Turner WB, 1970. Metabolites of *Helminthosporium monoceras:* Structures of monocerin and related benzopyrans. *Journal of the Chemical Society C: Organic* **18**, 2598-600.

Bennett JW, Klich M, 2003. Mycotoxins. *Clinical Microbiology Reviews* **16**, 497-516.

Collemare J, Lebrun MH, 2011. Fungal secondary metabolites: ancient toxins and novel effectors in plant–microbe interactions. In: Martin F, Kamoun S, eds. *In effectors in plant–microbe interactions.* Oxford, UK: Wiley-Blackwell, 377-400.

Craven M, Fourie AP, 2011. Field evaluation of maize inbred lines for resistance to *Exserohilum turcicum*. *South African Journal of Plant and Soil* **28**, 69-74.

Cuq F, Brown SC, Petitprez M, Alibert G, 1995. Effects of monocerin on cell-cycle progression in maize root-meristems synchronized with aphidicolin. *Plant Cell Reports* **15**, 138-42.

Cuq F, Petitprez M, Herrmann-Gorline S, Klaebe A, Rossignol M, 1993. Monocerin in *Exserohilum turcicum* isolates from maize and a study of its phytotoxicity. *Phytochemistry* **34**, 1265-70.

Cutler HG, Jarvis BB, 1985. Preliminary observations on the effects of macrocyclic trichothecenes on plant growth. *Environmental and Experimental Botany* **25**, 115-28.

Domene X, Ramírez W, Solà L, Alcañiz JM, Andrés P, 2009. Soil pollution by nonylphenol and nonylphenol ethoxylates and their effects to plants and invertebrates. *Journal of Soils and Sediments* **9**, 555.

Fan J, Chen C, Brlansky RH, Gmitter Jr FG, Li ZG, 2010. Changes in carbohydrate metabolism in *Citrus sinensis* infected with '*Candidatus* Liberibacter asiaticus'. *Plant Pathology* **59**, 1037-43.

Gamm M, Heloir MC, Bligny R, *et al.*, 2011. Changes in carbohydrate metabolism in *Plasmopara viticola*-infected grapevine leaves. *Molecular Plant-Microbe Interactions* **24**, 1061-73.

Gélie B, Petitprez M, Souvre A, Albertini L, 1987. Étude ultrastructurale des modifications induites par *Exserohilum turcicum* chez le limbe de *Zea mays*– Effet du gène de résistance Ht-1. *Canadian Journal of Botany* **65**, 2061-6.

Haasbroek MP, Craven M, Barnes I, Crampton BG, 2014. Microsatellite and mating type primers for the maize and sorghum pathogen, *Exserohilum turcicum*. *Australasian Plant Pathology* **43**, 577-81.

Halliwell B, 1978. Biochemical mechanisms accounting for the toxic action of oxygen on living organisms: The key role of superoxide dismutase. *Cell Biology International Reports* **2**, 113-28.

Korsman J, Meisel B, Kloppers FJ, Crampton BG, Berger DK, 2011. Quantitative phenotyping of grey leaf spot disease in maize using real-time PCR. *European Journal of Plant Pathology* **133**, 461-71.

Kotze RG, Crampton BG, Kritzinger Q, 2016. Effect of fumonisin B_1 on the emergence, growth and ceramide synthase gene expression of cowpea (*Vigna unguiculata* (L.) Walp). *European Journal of Plant Pathology* **148**, 295-306.

Lim C-H, 1999. Monocerin and ziganein: phytotoxins from pathogenic fungus *Exserohilum turcicum* Inu-1. *Agricultural Chemistry and Biotechnology* **42**, 45-7.

Mobius N, Hertweck C, 2009. Fungal phytotoxins as mediators of virulence. *Current Opinion in Plant Biology* **12**, 390-8.

Robeson DJ, Strobel GA, 1982. Monocerin, a phytotoxin from *Exserohilum turcicum* (= *Drechslera turcica*). *Agricultural and Biological Chemistry* **46**, 2681-3.

Rufner R, Witham F, Cole Jr H, 1975. Ultrastructure of chloroplasts of Phaseolus vulgaris leaves treated with benomyl and ozone. *Phytopathology* **65**, 345-9.

Salin ML, 1988. Toxic oxygen species and protective systems of the chloroplast. *Physiologia Plantarum* **72**, 681-9.

Scheffer RP, Livingston RS, 1984. Host-selective toxins and their role in plant diseases. *Science* **223**, 17-21.

Silver DM, Kotting O, Moorhead GB, 2014. Phosphoglucan phosphatase function sheds light on starch degradation. *Trends in Plant Science* **19**, 471-8.

Smith AM, Zeeman SC, Smith SM, 2005. Starch degradation. *Annual Review of Plant Biology* **56**, 73-98.

Steinkamp MP, Martin SS, Hoefert LL, Ruppel EG, 1979. Ultrastructure of lesions produced by *Cercospora beticola* in leaves of *Beta vulgaris*. *Physiological Plant Pathology* **15**, 13-26.

Stergiopoulos I, Collemare J, Mehrabi R, De Wit PJ, 2013. Phytotoxic secondary metabolites and peptides produced by plant pathogenic Dothideomycete fungi. *FEMS Microbiology Reviews* **37**, 67-93.

Taiz L, Zeiger E, 2006. *Plant Physiology*. Sunderland, MA, USA: Sinauer Associates.

Taylor S, Wakem M, Dijkman G, Alsarraj M, Nguyen M, 2010. A practical approach to RT-qPCR-Publishing data that conform to the MIQE guidelines. *Methods* **50**, S1-5.

Van Asch MAJ, 1990. *Studies on the resistance of wheat and maize to fungal patogenesis*. Pietermaritzburg, University of Natal, PhD thesis.

Zeeman SC, Kossmann J, Smith AM, 2010. Starch: its metabolism, evolution, and biotechnological modification in plants. *Annual Review of Plant Biology* **61**, 209-34.

Zeeman SC, Smith SM, Smith AM, 2007. The diurnal metabolism of leaf starch. *Biochemical Journal* **401**, 13-28.

Chapter 6: General discussion

Maize (*Zea mays* L.) is a multifunctional crop in the Poaceae family along with other important crops such wheat (*Triticum aestivum* L.), rice (*Oryza sativa* L.), sugar cane (*Saccharum* spp.) and sorghum (*Sorghum bicolor* (L.) Moench). In developing countries, it is an essential source of food and fodder for humans and animals, respectively, whereas in industrialised countries it is a vital source of fodder for animals, is used in ethanol production and is used as a sweetener in high fructose corn syrup to name a few. Over the next 50 years an additional 3.5 billion people will need to be fed, and it is currently estimated that the production of cereal crops alone will need to increase by 70% in order to feed people worldwide by 2050 (Borlaug, 2007; Cairns *et al.*, 2013). However, fungal diseases are one of the many factors that severely hamper maize production (Mueller *et al.*, 2012; Munkvold & White, 2016).

Northern leaf blight (NLB) is one of a plethora of diseases affecting maize production worldwide annually. In South Africa NLB is probably the most widespread foliar disease of maize, with yield losses ranging between 15–30% on average (Klopper & Tweer, 2009). The causal agent for NLB is the hemibiotrophic fungal pathogen *Exserohilum turcicum* (Leonard & Suggs, 1974). Light microscopy studies of *E. turcicum* infection have revealed how the fungus penetrates and colonises the leaf tissue but detailed images of the infection structures and conidiophores are not available. *Exserohilum turcicum* produces monocerin, a secondary metabolite that could aid the fungus in causing disease in maize (Aldridge & Turner, 1970). Monocerin is considered to be a non-host selective toxin as it is phytotoxic towards more than one plant species (Robeson & Strobel, 1982). Phytotoxic effects of monocerin that have been reported include chlorosis and necrosis of leaf tissue, reduced root growth and it could have an impact on cell division (Cuq *et al.*, 1993; Cuq *et al.*, 1995). Not much is known on the mode of action of this toxin as well as how it could be involved in the pathogenicity of *E. turcicum*.

This study thus aimed to elucidate the role that *E. turcicum* infection and monocerin play in the development of NLB in maize. *Exserohilum turcicum* infection and the effect of monocerin on disease development were studied as well as their effect on a molecular level by looking at gene expression of PR proteins and starch enzymes involved in the degradation of starch in the chloroplast.

The infection strategy of *E. turcicum* has previously been characterised by Jennings and Ullstrup (1957), Hilu and Hooker (1964) and Knox-Davies (1974). However, in these earlier works, only light microscopy was used, and the poor reproduction quality of micrographs

rendered interpretation of their findings difficult. This study was thus conceptualised to provide further insight into the infection strategy as well as to confirm the hemibiotrophic lifestyle of the fungus using light microscopy (LM), scanning (SEM) and transmission (TEM) electron microscopy. High-resolution micrographs of how the fungus infected and colonised maize leaf tissue were successfully obtained. Northern leaf blight was characterised by chlorotic spots during the biotrophic phase (0–10 days post inoculation (dpi)) whereafter lesions started forming when the fungus entered its necrotrophic phase (11 dpi). Scanning electron micrographs revealed for the first time *E. turcicum* conidia germinating, forming germination tubes and penetrating the leaf epidermal cells by means of an appressorium. Once the fungus colonised the vascular bundles it switched over to its necrotrophic lifestyle. The fungus completed its life cycle 18 dpi when conidiophores emerged through the stomatal opening. Death of host cells which were not in contact with the fungus during the necrotrophic phase could be due to the fungus releasing a toxic substance such as monocerin and/or cell wall degrading enzymes (CWDE) which are often typical of necrotrophic growth. A question that remains unanswered though, is how the fungus grows between the epidermal cells and the vascular bundle during its biotrophic phase. Future studies should thus involve transforming *E. turcicum* with a fluorescent protein and then characterising fungal growth during the biotrophic phase using confocal microscopy. Ultimately, the work presented in this thesis confirmed the hemibiotrophic lifestyle of this foliar pathogen.

Exserohilum turcicum is continuously evolving resistance against fungicides and resistant maize lines, and thus there is a continuous drive to develop new fungicides as well as new resistant maize lines. This is the case with *E. turcicum* which has the ability to overcome *Ht* resistance genes in maize and thus it is an ongoing process to develop new maize cultivars that are resistant towards this fungus (Leonard *et al.*, 1989). Pathogenesis-related (PR) proteins are one of the many defence mechanisms by which maize protects itself against various stresses such as *E. turcicum* infection. Studies were undertaken to determine whether *E. turcicum* and monocerin elicit a host response in maize with an emphasis on PR protein gene expression. The expression of selected PR protein genes in maize was initially not induced by *E. turcicum* at the early stages of infection (biotrophic phase) but these genes were significantly upregulated at the later stage of infection (necrotrophic phase). During the early stages of infection the fungus was in its biotrophic phase and had to actively suppress the plants immune response to colonise the rest of the tissue as well as to protect itself (de Jonge *et al.*, 2011; Koeck *et al.*, 2011). *Exserohilum turcicum* could possibly release effectors such as *Avr4* (avirulence) and

Ecp6 (extracellular proteins), since these two effectors were expressed in *Cercospora zeina* (causal agent for grey leaf spot) during the infection of maize with *C. zeina* (Langenhoven, 2015). These effectors bind to chitin and thus prevent recognition of the fungus by the plant (Stergiopoulos & de Wit, 2009). The induced expression of PR proteins genes during the necrotrophic phase of the fungus could be due to both plant and fungal elicitors. The effect of monocerin on PR protein gene expression was also evaluated to determine whether the toxin supported the fungus in causing disease. Monocerin as well as the methanol and wounding controls did induce the expression of these proteins genes but at a much lower level when compared to the fungus. Since no significant differences was seen between monocerin and both controls, it could perhaps be due to that either the concentration of monocerin was too low or monocerin could not penetrate the cells when maize leaves were infiltrated with the toxin. Monocerin could be a necrotrophic effector (NE) since it could induce cell death which not only provides nutrients for the fungus but also results in less antifungal compounds being released by the plant (Vleeshouwers & Oliver, 2014). Necrotrophic effectors often target a specific gene such as HC-toxin produced by *Bipolaris zeicola* which targets histone-deacetylase that results in less gene expression (Stergiopoulos & de Wit, 2009). It is possible that monocerin rather affects gene(s) other than the PR genes. Future studies should focus on testing additional PR proteins or different forms of PR proteins against *E. turcicum* as well as monocerin. In additional, monocerin should also be evaluated to determine of it is pathogenicity factor or necrotrophic effector.

In this study the host response of maize toward *E. turcicum* and monocerin was observed through the increase in gene expression of PR proteins. The use of marker-assisted selection is a process by which breeders use DNA markers to select for genes linked to traits of interest (Ribaut & Ragot, 2006). Marker-assisted selection is more economical and efficient when compared to conventional breeding since large field trials are not necessary and with molecular tests the breeding accuracy is improved as well (Ribaut & Ragot, 2006). Pathogenesis-related proteins could thus be used as expression markers to select maize lines with increased resistance against not only *E. turcicum* but other fungal pathogens as well. These expression markers can possibly be used to characterise resistance responses in maize against *E. turcicum*. The upregulation of PR proteins' gene expression circumvents the need to produce transgenic maize lines as well as speeding up conventional breeding in the selection of resistant maize genotypes.

Since death of spongy mesophyll cells not in contact with *E. turcicum* was observed during the histological assessment, the phytotoxic effects of monocerin on the ultrastructure of maize leaf cells was investigated. Higher concentrations of infiltrated monocerin (2 mM) induced phytotoxicity sooner than lower monocerin concentrations (1 mM). It was revealed through light and electron micrographs that the chloroplast was the most sensitive organelle to the phytotoxic effects of monocerin. The degradation and damage of the chloroplast by the fungus as well as monocerin, which ultimately leads to cell death, could be how the fungus accumulates nutrients or it could possibly be a way for the fungus to suppress the plant defence system in order to colonise and infect other parts of the plant. This then prompts the fungus to enter its necrotrophic phase. An over accumulation of starch granules was also observed in TEM micrographs of the monocerin treated tissue. The starch granules kept accumulating and increasing in size following monocerin treatment. It was thus hypothesised that monocerin and *E. turcicum* could possibly play an inhibitory role on the gene expression of enzymes that are directly involved in the degradation of starch granules in the chloroplast. However, monocerin did not have any significant effect on the inhibition of the expression of these genes, whereas *E. turcicum* did. The effect of the fungus and the toxin on additional genes such as invertase should be studied to determine how *E. turcicum* could acquire nutrients during the infection of maize. Invertase is responsible for the hydrolysis of sucrose into fructose and glucose (Fan *et al.*, 2010; Gamm *et al.*, 2011). In addition, the activity of starch enzymes should be determined and as well as quantifying the amount of the different sugars present in the chloroplast. Fructose could be a source of carbon for *E. turcicum* as is the case with other pathogens such as *Plasmopara viticola* and the bacterial pathogen *Candidatus liberibacter* (Fan *et al.*, 2010; Gamm *et al.*, 2011). The toxic effects of monocerin thus could have an effect on other genes involved in the degradation of starch granules or some other cellular effects such as organelle membranes. Additional studies should consider testing the effect of monocerin producing isolates versus monocerin deficient mutants to confirm whether monocerin aids the fungus in causing disease in maize. In addition, transcriptomic studies can be done on maize plants following monocerin treatment to determine which genes are involved in the degradation of starch in the chloroplast are up and/or downregulated. Other phytotoxins produced by *E. turcicum* such as E.t toxin should be studied to determine if they could aid the fungus in causing disease (Bashan *et al.*, 1995).

In conclusion, this study has provided significant insight into the host response of maize towards *E. turcicum* infection and monocerin infiltration. Additionally, a possible explanation

is given on how the fungus could acquire nutrients from starch granules in the host chloroplast in order to survive. The macroscopic observations on the transition of the fungus from a biotrophic phase to a necrotrophic phase will help to address the relationship between fungal colonization, host response, and plant disease. A better understanding about the role that monocerin plays during NLB has been provided but a possible mode of action is yet to be determined. The results of this study will help in developing novel and effective long term strategies in controlling NLB in maize. The histological assessment of the infection strategy of *E. turcicum* can be used to correlate cytological processes with molecular host pathogen studies (fungal quantification, production of effectors) in the laboratory with emphasis on the hemibiotrophic lifestyle of the fungus in maize and sorghum as host. The information gained from the host response of maize against *E. turcicum* infection can be used to identify molecular markers such as induced PR proteins to develop resistant cultivars without producing transgenic lines. An advantage of using PR proteins is that they are induced by multiple fungal and bacterial pathogens and not only *E. turcicum*. Controlling NLB is more feasible when fungicides are applied preventatively as opposed to curatively. The understanding of the disease progression will thus help farmers to apply fungicides at the correct time since they often lack the knowledge about how the disease looks especially during the early stages of infection

6.1. References

Aldridge DC, Turner WB, 1970. Metabolites of *Helminthosporium monoceras:* Structures of monocerin and related benzopyrans. *Journal of the Chemical Society C: Organic* **18**, 2598-600.

Bashan B, Levy RS, Cojocaru M, Levy Y, 1995. Purification and structural determination of a phytotoxic substance from *Exserohilum turcicum*. *Physiological and Molecular Plant Pathology* **47**, 225-35.

Borlaug N, 2007. Feeding a Hungry World. *Science* **318**, 359-.

Cairns JE, Hellin J, Sonder K, *et al.*, 2013. Adapting maize production to climate change in sub-Saharan Africa. *Food Security* **5**, 345-60.

Cuq F, Brown SC, Petitprez M, Alibert G, 1995. Effects of monocerin on cell-cycle progression in maize root-meristems synchronized with aphidicolin. *Plant Cell Reports* **15**, 138-42.

Cuq F, Petitprez M, Herrmann-Gorline S, Klaebe A, Rossignol M, 1993. Monocerin in *Exserohilum turcicum* isolates from maize and a study of its phytotoxicity. *Phytochemistry* **34**, 1265-70.

de Jonge R, Bolton MD, Thomma BP, 2011. How filamentous pathogens co-opt plants: the ins and outs of fungal effectors. *Current Opinion in Plant Biology* **14**, 400-6.

Fan J, Chen C, Brlansky RH, Gmitter Jr FG, Li ZG, 2010. Changes in carbohydrate metabolism in *Citrus sinensis* infected with '*Candidatus* Liberibacter asiaticus'. *Plant Pathology* **59**, 1037-43.

Gamm M, Heloir MC, Bligny R, *et al.*, 2011. Changes in carbohydrate metabolism in *Plasmopara viticola*-infected grapevine leaves. *Molecular Plant-Microbe Interactions* **24**, 1061-73.

Hilu HM, Hooker AL, 1964. Host-pathogen relationship of *Helminthosporium turcicum* in resistant and susceptible corn seedlings. *Phytopathology* **54**, 570-5.

Jennings P, Ullstrup A, 1957. A histological study of 3 *Helminthosporium* leaf blights of corn. *Phytopathology* **47**, 707-14.

Klopper R, Tweer S, 2009. Northern corn leaf blight fact sheet. [http://www.pannar.com/assets/disease_fact_sheets/Northern_Corn_Leaf_Blight.pdf]. Accessed 11 November 2019.

Knox-Davies P, 1974. Penetration of maize leaves by *Helminthosporium turcicum*. *Phytopathology* **64**, 1468-70.

Koeck M, Hardham AR, Dodds PN, 2011. The role of effectors of biotrophic and hemibiotrophic fungi in infection. *Cell Microbiology* **13**, 1849-57.

Langenhoven B, 2015. *Characterisation of three putative effector genes from the maize foliar pathogen Cercospora zeina*. Pretoria, University of Pretoria, MSc dissertation.

Leonard KJ, Levy Y, Smith DR, 1989. Proposed nomenclature for pathogenic races of *Exserohilum turcicum* on corn. *Plant Disease* **73**, 776-7.

Leonard KJ, Suggs EG, 1974. *Setosphaeria prolata*, the ascigerous state of *Exserohilum prolatum*. *Mycologia* **66**, 281-97.

Mueller ND, Gerber JS, Johnston M, Ray DK, Ramankutty N, Foley JA, 2012. Closing yield gaps through nutrient and water management. *Nature* **490**, 254.

Munkvold GP, White DG, 2016. *Compendium of Corn Diseases*. APS press St. Paul, MN.

Ribaut J-M, Ragot M, 2006. Marker-assisted selection to improve drought adaptation in maize: the backcross approach, perspectives, limitations, and alternatives. *Journal of Experimental Botany* **58**, 351-60.

Robeson DJ, Strobel GA, 1982. Monocerin, a phytotoxin from *Exserohilum turcicum* (= *Drechslera turcica*). *Agricultural and Biological Chemistry* **46**, 2681-3.

Stergiopoulos I, de Wit PJ, 2009. Fungal effector proteins. *Annual Review of Phytopathology* **47**, 233-63.

Vleeshouwers VG, Oliver RP, 2014. Effectors as tools in disease resistance breeding against biotrophic, hemibiotrophic, and necrotrophic plant pathogens. *Molecular Plant-Microbe Interactions* **27**, 196-206.

Chapter 7: Appendix

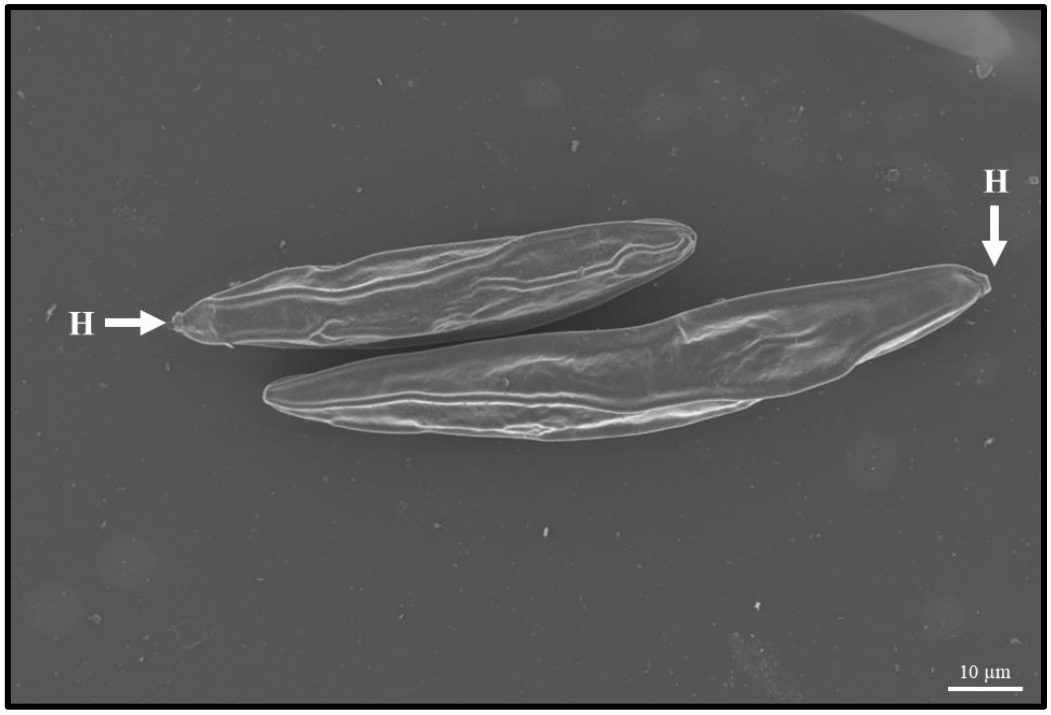

Figure 7.1. Scanning electron micrograph of the conidia of *Exserohilum turcicum* with the protruding hilum (H).

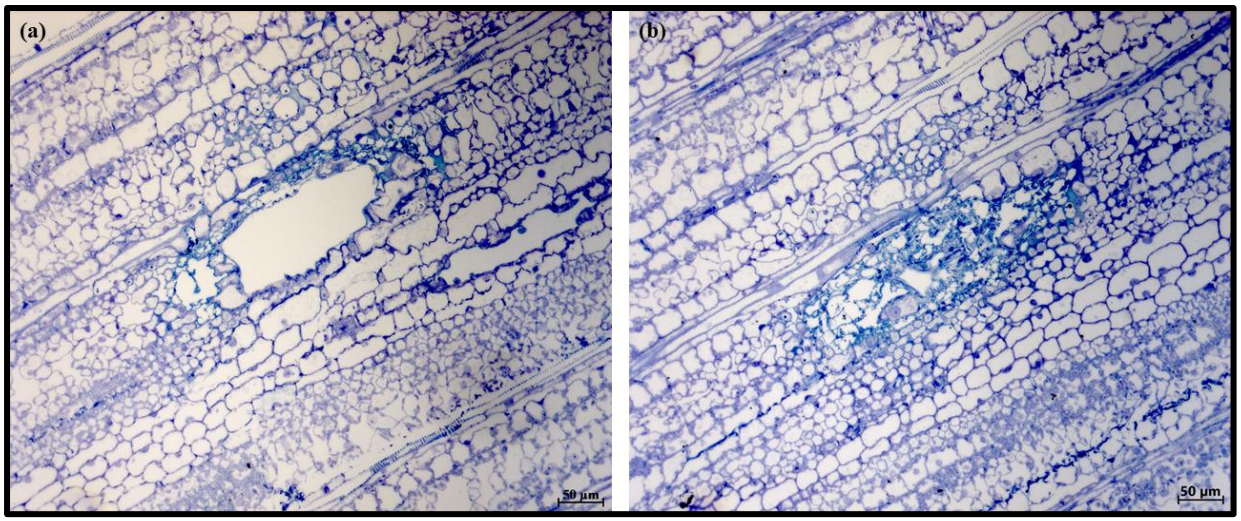

Figure 7.2. Light micrographs of observations of B73 maize leaf paradermal sections after infection by *Exserohilum turcicum* (9 days post-inoculation). (a) Chlorotic spot visible with surrounding healthy tissue; (b) further examinations of the same sample through additional sections revealed necrotic tissue surrounded by the healthy tissue.

Table 7.1. The sequences obtained for the sequencing of each genes amplicon indiciating that the primer set did amplify the correct gene. Included in the table is the gene name, the gene target as well as the rerence gene transcript ID used in the lastes annotation of the maize inbred line B73.

Gene Name	Gene Target	Reference Gene Transcript ID
rpol	DNA-directed RNA polymerases II IV and V subunit 8B	Zm00001d012857_T001
CTCGCAGTGAGCAGTTAGATATGTATATGCAGCTAGATGTTGCCACAGATGTTTATCCTATGCATGCTGGCGAGAAATTTAACATGGTTATAGCGCCTACTCTGAATTTGG		
srl	Serine/arginine-rich splicing factor SR45a	Zm00001d006480_T010
ACACGCCATTGTTCGAGAGGGATTTCATTGCTTCACCTTTCACAGATTTTACCATTCAGAAAAAAAGAAACTACCGGTATGACATACTCGGTACATGTCAAAGTTCACCCGAACCTG		
gst3	Glutathione S-transferase 4	Zm00001d042216_T001
GGTTGGTCTTTGCATATCCTACTAGTGCTGATCTTTTTGTGAAGCTTGGATTGGATGGACGCGTTTTCTTCACCGTAATTCCCTTCTTC		
PR-1	Pathogenesis related protein 4	Zm00001d018738_T001
TGGGTGTCCGAGAAGCAGTACTACGACCACGACACCAACAGCTGCGCGGAGGGGCAGGTGTGCGGCCACTACACGCAGGTGGTGTGGCGCGACTCCACCGCCATCGGCTGTGCCCGCGTCGTCTGCGACAACAACGC		
PR-2	Glucan endo-13-beta-glucosidase homolog 1	Zm00001d042143_T001
CATTCGCAGCCATTCCTACAGGAGTCCAATCCATCGGCGTGTGCTACGGCGTGAACGGCGACAACCTGCCCCCGGCGAGCGACGTGGTGCAGCTGTACCAGTCCAACGGCATCAACCTGA		
PR-3	Chitinase chem5	Zm00001d043988_T001
CTGACGGGCACGGTGATCCCCGCCATCCGAGGCATTGGCAACTACGGCGGCATCATGGTGTGGGACCGCTTTAACGACGTGCAGAACAACTACAGCAGCCAGGTGAAGGGCAGCGTCTGA		
PR-10	Pathogenesis-related protein 10	Zm00001d028816_T001
GTAACAGCAGCCCGATCTTGCATCAGCTAGCTAACTAAGCAAGTAAGCTAAGCTAGCCCTAGGCAACGAGCCGAGCCGTCAAGCTCATCGCAGACCACGAGCCATGGCCTCCACCAACAGCTGGACTGTTGAGATCGCCTC		
gwd	Alpha-glucan water dikinase 1 chloroplastic	Zm00001d037059_T005

CATGAGTACCTTTCGATGGCTGTTCTCGTGCAAGAAGTTGTGAATGCAGATTAT GCTTTTGTCATTCATACCACAAACCCATCGTCTG		
pwd	Phosphoglucan water dikinase chloroplastic	Zm00001d023792_T005
CAGAGAGACGCAAAGATGGCGGTTCTCGTGCAGGAAATGCTGCAGCCAGATC TCTCTTTTGTGCTTCATACAATTAGCCCAGTTGACCATGATCCC		
amy3	Alpha-amylase 3 chloroplastic	Zm00001d043662_T001
GTGAGGAGAGACATTGAAGCGCATAAAAGACTTGTGGAATTTGACACTGATAT TCCTGGAGAAGTTATCATTCATTGGGGAGTTTGCAGAGACAATACTATGACAT GGGAGATCCCACCAGAACCACATCCACC		

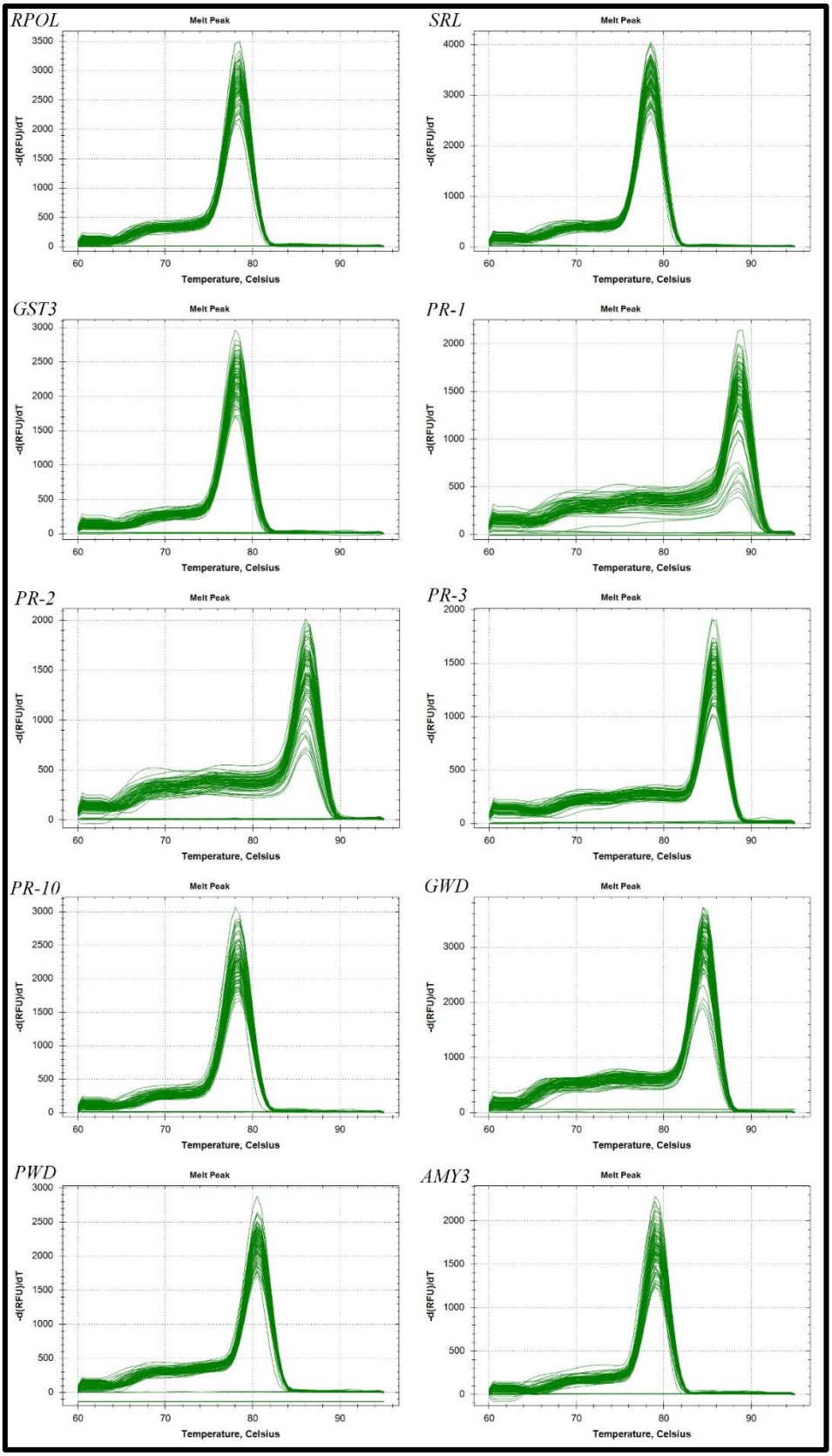

Figure 7.3. Melt-curve analysis of target genes (*PR-1*, *PR-2*, *PR-3*, *PR-10*, *gwd*, *pwd* and *amy3*) and references genes (*rpol*, *srl* and *gst3*). The melting peaks were plotted as the negative rate of change in relative fluorescent units (RFU) against the change in temperature. Melt-curve

analysis of all amplicons analysed revealed single peaks with the absence of primer dimers. Non-template controls had no melt peaks indicating that no contamination was present. The melting points for *PR-1, PR-2, PR-3, PR-10, gwd, pwd, amy3, rpol, srl* and *gst3* were 88.5°C, 86.5°C, 85.5°C, 84.5°C, 78.5°C, 80.5°C, 79°C, 78.5°C, 78.5°C and 78°C, respectively.

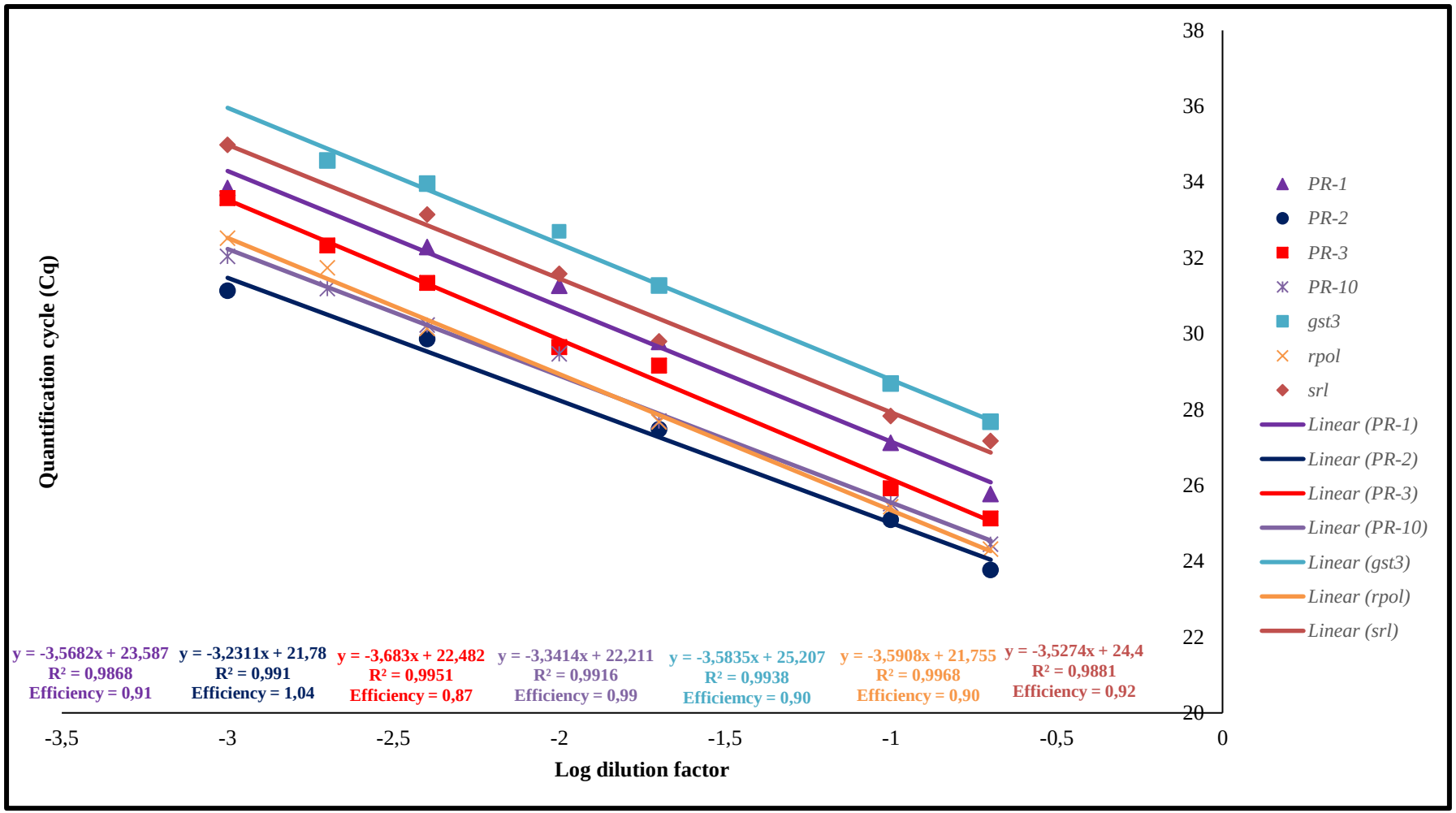

Figure 7.4. Standard curves for generated for each of the PR and reference genes submitted to RT-qPCR analysis. The standard curve of each gene was generated by plotting the quantification cycle (C_q) against the log10 concentration with a linear trend line fitted to the data points of each gene. The equation of each linear trendline, R^2 value as well as the efficiency of each gene is indicated on the graph.

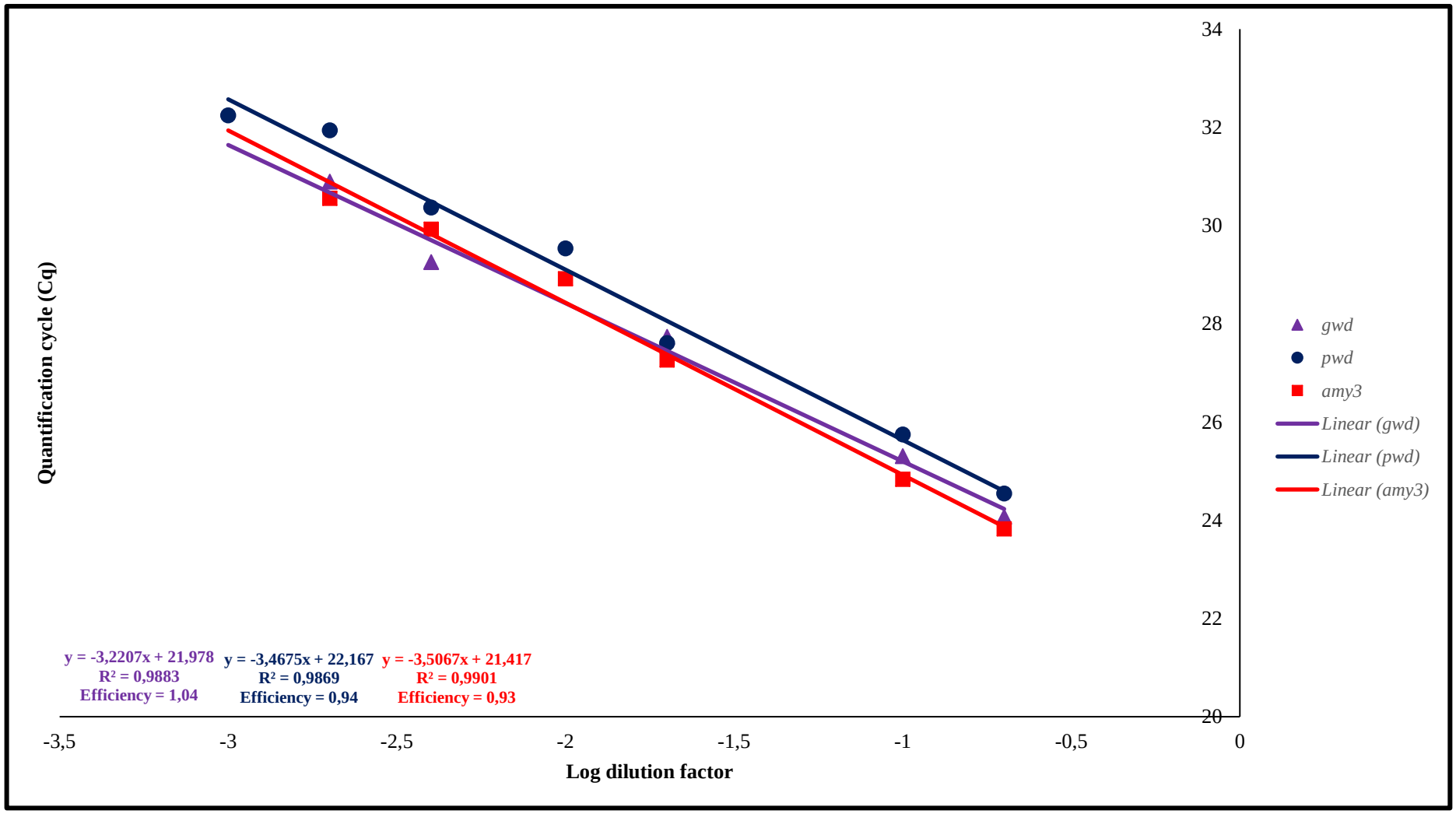

Figure 7.5. Standard curves for generated for each of the starch enzymes genes and reference genes submitted to RT-qPCR analysis. The standard curve of each gene was generated by plotting the quantification cycle (Cq) against the log10 concentration with a linear trend line fitted to the data points of each gene. The equation of each linear trendline, R^2 value as well as the efficiency of each gene is indicated on the graph